Order Number 8820902

Approaches to the study of oxidative stress in the nervous system

Slivka, Adam, Ph.D.

City University of New York, 1988

U·M·I
300 N. Zeeb Rd.
Ann Arbor, MI 48106

PLEASE NOTE:

In all cases this material has been filmed in the best possible way from the available copy. Problems encountered with this document have been identified here with a check mark ✓.

1. Glossy photographs or pages ✓
2. Colored illustrations, paper or print ✓
3. Photographs with dark background ✓
4. Illustrations are poor copy ✓
5. Pages with black marks, not original copy ✓
6. Print shows through as there is text on both sides of page _____
7. Indistinct, broken or small print on several pages ✓
8. Print exceeds margin requirements _____
9. Tightly bound copy with print lost in spine _____
10. Computer printout pages with indistinct print _____
11. Page(s) _____ lacking when material received, and not available from school or author.
12. Page(s) _____ seem to be missing in numbering only as text follows.
13. Two pages numbered _____. Text follows.
14. Curling and wrinkled pages _____
15. Dissertation contains pages with print at a slant, filmed as received _____
16. Other _____

_____

_____

Approaches to the Study of Oxidative Stress in the Nervous System.

by

Adam Slivka

A dissertation submitted to the Graduate Faculty in Biomedical Sciences in partial fulfillment of the requirements for the degree of Doctor of Philosophy, The City University of New York.

1988

This manuscript has been read and accepted for the Graduate Faculty in Biomedical Sciences in satisfaction of the dissertation requirement for the degree of Doctor of Philosophy.

5/28/87
Date

Chair of Examining Committee
Gerald Cohen, Ph.D.

5/28/87
Date

Executive Officer
Terry Krulwich, Ph.D.

Peter Knott, Ph.D.

Sol Berl, M.D.

Catherine Mytilineou, Ph.D.

Richard Heikkila, Ph.D.

Supervisory Committee

The City University of New York

Abstract

Approaches to the Study of Oxidative Stress in the Nervous System

by

Adam Slivka

Adviser: Professor Gerald Cohen

These experiments explore and develop methodology to study the interactions between peroxides, glutathione, and hydroxyl radicals ($^{\cdot}OH$) during oxidative stress in the nervous system.

A biochemical approach was developed to detect $^{\cdot}OH$. The products of $^{\cdot}OH$ attack on dopamine were identified: the products were 2-hydroxydopamine, 5-hydroxydopamine, and 6-hydroxydopamine. Identification of these products provides an investigative approach to study $^{\cdot}OH$ in dopamine neurons.

Other experiments utilized a histochemical method to study the localization of a cellular antioxidant, reduced glutathione (GSH). GSH staining was distributed heterogeneously in brain, with a relative absence in neuronal somata. Low levels of GSH in neuronal somata would make them susceptible to oxidative stress.

The histochemical technique, along with biochemical analyses, were applied to a model of cerebral ischemia (unilateral ligation of the common carotid artery in Mongolian gerbils). Ischemia depleted tissue GSH without a

concommitant rise in oxidized GSH (GSSG); levels of free cysteine were elevated in ischemic tissue. The depletion of GSH in ischemic tissue is most likely due to autolytic breakdown.

The metabolism of catecholamines in ischemic brain may result in oxidative stress. Examination of tissue and extracellular levels of dopamine and metabolites in ischemic striata showed an acute release of dopamine; oxidatve metabolism of dopamine by monoamine oxidase was still supported in ischemic tissue. However, the release and metabolism of dopamine were not causally related to the depletion of GSH, as pretreatment of animals with alpha-methyl-para-tyrosine, to deplete catecholamines, or pargyline, to inhibit monoamine oxidase, failed to protect aginst ischemia-induced GSH depletion. Hydroxylated dopamine products were not found in ischemic tissue.

Biochemical and histochemical techniques were also used to examine glutathione in human and monkey brain. Previous studies indicated that human brain contained primarily GSSG. We demonstrated that levels of GSSG are extremely low when compared to GSH in both human and monkey brain, similar to that seen in tissues from other species.

Lastly, a protocol for repeated administration of a glutathione synthesis inhibitor (buthionine sulfoximine) was found to lower levels of glutathione in the central nervous system of preweanling mice. Previous studies report that brain is resistant to buthionine sulfoximine-induced

depletion of glutathione. This protocol provides an approach to study aspects of glutathione physiology and pharmacology in the nervous system.

Acknowledgements

First and foremost, I would like to thank Dr. Gerald Cohen, in whose lab I received my doctoral training. Dr Cohen's combination of creative scientific approach, meticulous laboratory detail, and rigorous analysis of data provided fertile soil for the intellectual growth of those under his tutelage. Dr. Cohen will remain an excellent role model as well as friend.

Appreciation is extended to the members of Dr. Cohen's laboratory fcr their assistance in performing the experiments described in this thesis. Special mention is reserved for fellow graduate student Mary Beth Spina for her friendship and tireless assistance in many long experiments.

I would also like to thank the Faculty of the Division of Neurobiology and the Department of Neurology; in particular: Drs. Catherine Mytilineou, Timothy Brannan, Jesse Weinberger and Peter Knott for their instruction and collaboration in selected projects.

Special thanks are extended to Dr. Stephen Weiss for initiating and fostering my interest in biomedical research as an undergraduate at the University of Michigan.

Finally, I thank my wife Carrie, and my family and friends for their love and support throughout my studies.

Several publications have resulted from the work described in this dissertation prior to its submission to City University, and appear in abstracted form within the text. A listing of these publications and their location within the dissertation is given below. Releases of copyright are on the proceeding pages.

Publication	Location in text
Slivka, A. and Cohen, G. Hydroxyl radical and attack on dopamine. J. Biol. Chem., 260 (1985) 15466-15472.	Chapter 2.1 Chapter 3
Slivka, A., Spina, M.B., and Cohen, G. Reduced and oxidized glutathione in human and monkey brain. Neurosci. Letts., 74 (1987) 112-118.	Chapter 2.2 Chapter 4
Slivka, A., Mytilineou, C., and Cohen, G. Histochemical evaluation of glutathione in brain. Brain Res. (1987) in press.	Chapter 2.3 Chapter 5
Slivka, A., Kang, J., and Cohen, G. Hydroxyl radicals and the toxicity of oral iron. Biochem. Pharm. 35 (1986) 553-556.	Appendix II
Slivka, A., Kang, J., Cohen, G. Ascorbic acid. Letter to the Editor, N. Engl. J. Med. 315 (1986) 708.	Appendix III

THE MOUNT SINAI MEDICAL CENTER
ONE GUSTAVE L. LEVY PLACE • NEW YORK, N.Y. 10029

Mount Sinai School of Medicine • The Mount Sinai Hospital

Department of Neurology

August 26, 1987

SEP 01 1987

THE EDITOR
JOURNAL OF BIOLOGICAL CHEMISTRY
9650 Rockville Pike
Bethesda, Maryland 20814

Dear sir:

I am writing to request a copyright release for a manuscript entitled "Hydroxyl radical attack on dopamine" by A. Slivka and G. Cohen which appeared in J. Biol. Chem., Vol. 260, No. 29 (1985) pp. 15466-15472. The material will appear in my doctoral dissertation submitted to the City University of New York, in partial fulfillment of the requirements for the degree of Doctor of Philosophy.

I thank you in advance for your assistance.

Sincerely,

Adam Slivka

Adam Slivka
Dept. Neurology
Annenberg 14-72
Mount Sinai School of Medicine
One Gustave Levy Place
New York, N.Y. 10029

PERMISSION GRANTED
contingent upon obtaining that of the author

for the copyright owner
THE AMERICAN SOCIETY OF
BIOLOGICAL CHEMISTS, INC.

please send.

THE MOUNT SINAI MEDICAL CENTER
ONE GUSTAVE L. LEVY PLACE • NEW YORK, N.Y. 10029

Mount Sinai School of Medicine • The Mount Sinai Hospital

Department of Neurology

August 26, 1987

Prof. Alan C. Sartorelli
Yale University School of Medicine
Dept. of Pharmacology
Sterling Hall of Medicine
333 Cedar St.
New Haven, Conn. 06510

Dear Sir:

I am writing to request a copyright release for a manuscript entitled "Hydroxyl radicals and the toxicity of oral iron" by A. Slivka, J.O. Kang, and G. Cohen which appeared in Biochem. Pharmacol. 35, 4 (1986) 553-556. The material will appear in my doctoral dissertation submitted to the City University of New York, in partial fulfillment of the requirements for the degree of Doctor of Philosophy.

I thank you in advance for your assistance.

Sincerely,

Adam Slivka

Adam Slivka
Dept. Neurology
Annenberg 14-72
Mount Sinai School of Medicine
One Gustave Levy Place
New york, N.Y. 10029

Permission granted to reprint if "Reprinted with the permission of the authors and the copyright holder, Pergamon Press, Oxford" appears in the legend. Date: 1 Sep 87
Barbara Z. Renkin:
Regional Managing Editor Barbara Z. Renkin

BIOCHEMICAL PHARMACOLOGY
Department Of Pharmacology
Yale University School Of Medicine
333 Cedar Street P.O. Box 3333
New Haven, CT 06510 U.S.A.
Tel: (203) 785-4291

PERGAMON PRESS

September 28, 1987

Adam Slivka
Dept. of Neurology
Annenberg 14-72
Mount Sinai School of Medicine
One Gustave Levy Place
New York, NY 10029

Dear Mr. Slivka:

With reference to your attached request to reprint/reproduce material from a Pergamon journal, we herewith grant permission to do so, provided:

1. The material to be reproduced has appeared in our publication without credit or acknowledgement to another source.

2. Suitable acknowledgement to the source be given, preferably as follows:

   Reprinted with permission from [Journal Title, Volume Number, Author(s), Title of Article], Copyright [Year], Pergamon Journals, Ltd.

3. The author's approval in writing be obtained (the address or affiliation that appears in the journal is the most current available).

4. A copy of your work is submitted upon publication to the Journal Permissions Department.

This permission is for one-time use and for use in editions for the handicapped.

We only grant non-exclusive world English rights. If an individual wants rights for all languages, it would have to be applied separately.

Sincerely,
Cherie Burak
Ms. Cherie Burak
Journals Permissions

MATERIAL TO BE REPRINTED/REPRODUCED AND TO BE USED IN:

As per your attached letter(s).

Enclosure: original request(s) for permission

PERGAMON JOURNALS, INC.
Maxwell House, Fairview Park, Elmsford, NY 10523 (914) 592-7700 Fax: (914) 592-3625 Telex: 13-7328 Cable: PERGAPRES EMFD
A member of the BPCC PLC Group of companies

The New England Journal of Medicine

Rights and Permissions Department

September 3rd, 1987

Mr. Adam Slivka
Mt. Sinai Medical Ctr.
Dept. of Neurology
Annenberg 14-72
One Gustave Levy Place
New York, NY 10029

Dear Mr. Slivka:

Thank you for your letter of August 26th, 1987 requesting permission to use Journal material.

You may have permission to use the material referenced in your letter provided it is properly credited. Any reference should include the author(s), title, source, volume, pages, and year.

Also, this permission is granted for the specific purpose outlined in your letter. If material is to be used in any other way, permission must be requested from this office on a case-by-case basis prior to publication.

Also, please forward a copy of your publication to this office so that we may have it on file should you request again.

Again, thank you for requesting permission.

Sincerely,

C. D. Pattison

Cynthia D. Pattison
Rights & Permissions Assistant

1440 Main Street, Waltham, Massachusetts 02254-0803 • (617) 893-3800

(2) 413

THE MOUNT SINAI MEDICAL CENTER
ONE GUSTAVE L. LEVY PLACE • NEW YORK, N.Y. 10029

Mount Sinai School of Medicine • The Mount Sinai Hospital

Department of Neurology

August 26, 1987

Dr. D.J. Reis
Laboratory of Neurobiology
Dept. of Neurology
Cornell University Medical College
411 East 69th St. Rm KB 410
New York, N.Y. 10021

Dear Sir:

I am writing to request a copyright release for a manuscript entitled "Reduced and oxidized glutathione in human and monkey brain" by A. Slivka, M.B. Spina, and G. Cohen which appeared in Neurosci. Letts., 74 (1987) 112-118. The material will appear in my doctoral dissertation submitted to the City University of New York, in partial fulfillment of the requirements for the degree of Doctor of Philosophy.

I thank you in advance for your assistance.

Sincerely,

Adam Slivka

Adam Slivka
Dept. Neurology
Annenberg 14-72
Mount Sinai School of Medicine
One Gustave Levy Place
New york, N.Y. 10029

NSL 04381
74/1 pp. 112-118.

Elsevier Science Publishers B.V.
(Biomedical Division) Amsterdam,
date: 11-9-87
Permission granted subject to
permission from the author(s)
and to full acknowledgement
of the source J Greenars

THE MOUNT SINAI MEDICAL CENTER
ONE GUSTAVE L. LEVY PLACE • NEW YORK, N.Y. 10029

Mount Sinai School of Medicine • The Mount Sinai Hospital

Department of Neurology

August 26, 1987

Professor Dr. D.P. Purpura
Brain Research
Office of the Dean
Albert Einstein College of Medicine
1300 Morris Park Avenue
Bronx, N.Y. 10461

Dear Dr. Purpura:

I am writing to request a copyright release for a manuscript entitled "Histochemical evaluation of glutathione in brain" by A. Slivka, C. Mytilineou, and G. Cohen which appeared in Brain Research, 409, (1987) 275-284. The material will appear in my doctoral dissertation submitted to the City University of New York, in partial fulfillment of the requirements for the degree of Doctor of Philosophy.

I thank you in advance for your assistance.

Sincerely,

Adam Slivka

Adam Slivka
Dept. Neurology
Annenberg 14-72
Mount Sinai School of Medicine
One Gustave Levy Place
New york, N.Y. 10029

Elsevier Science Publishers B.V.
(Biomedical Division) Amsterdam,
date: 11-9-87
Permission granted subject to
permission from the author(s)
and to full acknowledgement
of the source J. Greenaway

TABLE OF CONTENTS

LIST OF FIGURES

LIST OF TABLES

OVERVIEW

Redox reactions in which molecular oxygen (O_2) participates as the oxidant are commonly encountered in an aerobic environment. Products of these reactions include highly reactive forms of reduced oxygen, such as superoxide, hydrogen peroxide, and the hydroxyl radical. A considerable literature exists on the generation of these reactive species in biochemical systems in vitro, and by isolated organelles (e.g., mitochondria, microsomes) and activated leukocytes. Published reports also deal with the generation of hydrogen peroxide or the presumptive formation of superoxide or hydroxyl radicals in organs or tissues in vitro and in vivo. Reactions of superoxide, hydrogen peroxide, and hydroxyl radicals can result in oxidative changes, such as loss of glutathione, ascorbate, and alpha-tocopherol, formation of lipid peroxides, and hydroxylation or oxidation of a variety of biomolecules.

The evolution of life in an aerobic environment necessitated the acquisition of antioxidant mechanisms. Oxidative stress may be defined as a state in which cellular antioxidant defenses are unable to effectively eliminate pro-oxidant molecules or radicals. Pro-oxidant species include organic hydroperoxides and quinones, as well as related free radicals, such as semiquinones and alkoxyl, peroxyl, and alkyl radicals. Oxidative stress can occur either through reductions of antioxidant mechanisms or increased production of endogenous pro-oxidants or exposure

to exogenous pro-oxidants. There is growing experimental evidence which links oxidative stress to a variety of pathologic events.

The high reactivity and short life span of oxy-radicals has made their measurement in vivo extremely challenging. In particular, the hydroxyl radical is so difficult to detect that some investigators question its existence in biologic systems. Investigators who choose to study oxidative stress in the nervous system encounter additional problems. Compared to other tissues, such as liver, heart, or muscle, the brain is extremely heterogeneous with a large number of different cell types and extensive morphologic differentiation and biochemical compartmentalization within a given cell. In view of the importance and complexity of brain, approaches to the cellular localization of oxy-radicals and antioxidant defenses in brain become especially challenging.

The experiments described in this thesis were initiated to explore and develop methodology that could be used to study oxidative stress in the nervous system. Two approaches were used: In one, a biochemical approach was employed to study the most reactive of the oxidant radicals, namely, the hydroxyl radical ($^{\bullet}OH$). The identification of unusual products of $^{\bullet}OH$ attack on endogenous neurotransmitters might serve to detect $^{\bullet}OH$ and to specify the neuronal cell type. The products of $^{\bullet}OH$ attack on

dopamine were identified and characterized by high performance liquid chromatography; the main products were ring-hydroxylated forms, namely, 2-hydroxy- , 5-hydroxy- , and 6-hydroxydopamine. The formation of 6-hydroxydopamine had been reported previously in a model system consisting of iron-EDTA, ascorbate, and dopamine. It is now known, however, that iron-EDTA and ascorbate, with or without added hydrogen peroxide, is a model $^{\cdot}$OH-generating system. Reinvestigation of this system showed that small amounts of 6-hydroxydopamine were indeed formed, but that the major products were 2-hydroxydopamine and 5-hydroxydopamine.

The second approach utilized a histochemical method to study the localization of a major cellular antioxidant, reduced glutathione (GSH), in brain. This technique, permits visualization of the distribution of GSH under the fluorescence microscope. An interesting and unexpected finding was a relative absence of GSH from neuronal cell bodies in rodent and primate brain. The histochemical method along with standard biochemical analyses, was applied to a rodent model of ischemia; oxidative stress has been implicated as a factor in tissue damage produced by ischemia. Loss of GSH without accumulation of oxidized glutathione was observed in the striatum and hippocampus, regions that are susceptible to ischemic damage in the model system studied. The histochemical method showed that loss of GSH was particularly prominent in fiber bundles that course through the striatum. Changes in dopamine and its

oxidative metabolites in the striatum were also monitored during brain ischemia. In separate studies, a reinvestigation of levels of GSH and GSSG in monkey and human brain clarified an error in the literature concerning human brain. Lastly, an approach to lowering brain GSH through administration of buthionine sulfoximine, a GSH synthesis inhibitor, was investigated.

CHAPTER 1: REVIEW OF THE LITERATURE

1.1 Production of oxygen radicals and peroxides in brain.

1.1.1 Basic biochemistry.

Molecular oxygen (O_2) is ubiquitous in aerobic organisms and participates in many enzymatic and non-enzymatic biochemical reactions. The univalent reduction of O_2 to water generates two oxygen-centered free radicals and proceeds as follows:

$$O_2 \text{ ----> } O_2^{\cdot -} \text{ ----> } H_2O_2 \text{ ----> } {}^{\cdot}OH \text{ ----> } H_2O \quad \text{(eq. 1)}$$

$O_2^{\cdot -}$ is the superoxide anion radical, H_2O_2 is hydrogen peroxide, and $^{\cdot}OH$ is the hydroxyl radical. Electrons can be donated to O_2 through the actions of enzymes (viz., a variety of oxidases) or through the autoxidation of reduced metals (e.g., Fe^{2+}, Cu^{+}, or certain chelates) and organic compounds such as ascorbate, glutathione, and polyphenols (e.g., catecholamines). A review of some of the potential mechanisms for the generation of peroxides and oxy-radicals in brain will follow. Emphasis is placed on those mechanisms that may be relevant to the studies described in this thesis.

1.1.2 Enzymatic generation of oxy-radicals and hydrogen peroxide.

a) Monoamine Oxidase

There are a variety of enzymes which generate H_2O_2 as a reaction product. One enzyme that serves a major role in

the metabolism of amine neurotransmitters in the brain is monoamine oxidase (MAO). MAO is a flavoprotein that catalyzes a two-electron oxidation of monoamines, linked to the two-electron reduction of O_2 to yield the corresponding aldehyde, ammonia, and H_2O_2 in the following reaction:

$$RCH_2NH_2 + O_2 + H_2O \text{ -------> } RCHO + NH_3 + H_2O_2 \quad \text{(eq. 2)}$$

MAO is widely distributed in brain and is localized to the outer mitochondrial membrane of neuronal and non-neuronal cells. This enzyme is responsible for the intracellular metabolism of brain monoamines such as dopamine, norepinephrine, and serotonin.

b) Xanthine Oxidase

Xanthine Oxidase is an enzyme involved in the metabolism of purines (see Figure 1). This enzyme exists mainly in the dehydrogenase (Type D) form and catalyzes the conversion of hypoxanthine to xanthine and xanthine to uric acid. In this process, electrons are transferred from the substrate to the cofactor, NAD^+ (Eq. 3).

$$NAD^+ \text{ -----> } NADH \text{ (Type D)} \quad \text{(Eq. 3)}$$

When the enzyme is isolated in vitro without special precautions, the dehydrogenase converts to an oxidase (Type O). Conversion from Type D to Type O takes place by either limited proteolytic cleavage or sulfhydryl oxidation of the D form (Stripe and Della Corte, 1969). The reactions catalyzed by type O are the same as type D, however, the oxidase reaction transfers electrons from the substrate to

O_2. Both one-electron and two-electron transfers occur, generating $O_2^{\cdot -}$ and H_2O_2 respectively (Eqs. 4 and 5)

$$O_2 \text{ -----> } O_2^{\cdot -} \quad \text{(Type O)} \qquad \text{(Eq. 4)}$$

$$O_2 \text{ -----> } H_2O_2 \quad \text{(Type O)} \qquad \text{(Eq. 5)}$$

Evidence exists for the in vivo conversion of Type D enzyme to Type O in ischemic tissue (see section 1.1.6 a).

The activity of xanthine oxidase in brain parenchyma is relatively low while substantial enzyme activity has been reported in brain capillaries (Betz, 1985).

Figure 1. The conversion of xanthine dehydrogenase (Type D) to xanthine oxidase (Type O) during ischemia.

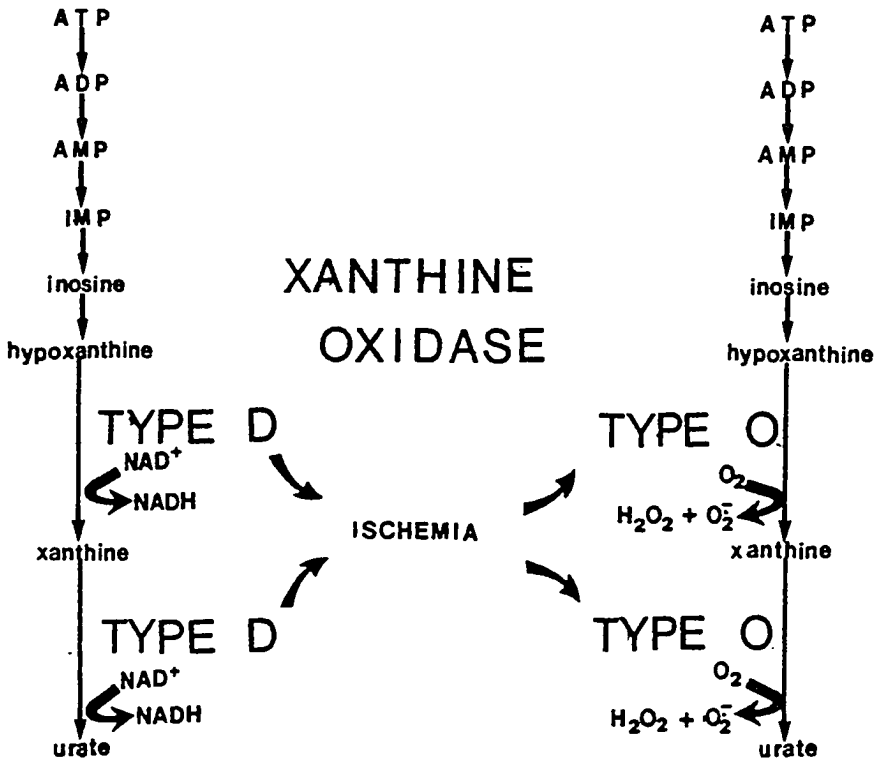

1.1.3 $O_2^{\cdot -}$ and H_2O_2 from mitochondria.

Under normal conditions, the vast majority of O_2 consumption by mitochondria proceeds via the four-electron reduction of O_2 to H_2O, a reaction catalyzed by mitochondrial cytochrome oxidase. Boveris (1977) demonstrated that up to 4% of the O_2 consumed by mitochondria results from univalent and divalent reduction of O_2, with subsequent formation of $O_2^{\cdot -}$ and H_2O_2. He identified ubiquinol and ubisemiquinone as sources of the electron "leak" for O_2 reduction. The production of $O_2^{\cdot -}$ and H_2O_2 by mitochondria was shown to be dependent on respiratory state, and, in perfused liver, was estimated to be close to 2% of the total organ uptake of O_2 .

1.1.4 Generation of hydroxyl radicals

A classical source of $^{\cdot}OH$ is from the homolytic scission of water during x-irradiation (Stein and Weiss, 1949). Another source is from the univalent reduction of hydrogen peroxide by metal ions (Walling et al., 1975), first reported by H.J.H. Fenton (1894). The Fenton reaction between a ferrous salt or ferrous chelate and H_2O_2 is given in equation 6:

$$Fe^{2+} + H_2O_2 \text{ -----> } Fe^{3+} + OH^- + {}^{\cdot}OH \qquad \text{(Eq. 6)}$$

In biochemical or cellular systems, variants of the Fenton reaction exist in which the ferric ions (or chelates) that are generated in equation 1 are subsequently recycled by suitable reducing agents. Two examples of recycling

systems for iron-EDTA are the presence of either enzyme-generated superoxide radicals (Eq. 7, i.e., the "metal-catalyzed Haber-Weiss reaction" sequence) (Beauchamp and Fridovich, 1970; McCord and Day, 1975; Cohen, 1985) or ascorbate (Eq. 8) (Cohen and Cederbaum, 1980; Fee, 1980):

$$Fe^{3+} + O_2^- \text{-----> } Fe^{2+} + O_2 \qquad \text{(Eq. 7)}$$

$$2Fe^{3+} + AH_2 \text{-----> } 2Fe^{2+} + A \qquad \text{(Eq. 8)}$$

Iron-EDTA and ascorbate (with or without added hydrogen peroxide) is a well-known model hydroxylating system (Udenfriend et al., 1954; Breslow and Lukens, 1960).

1.1.5 Oxy-radicals and H_2O_2 from autoxidation reactions.

a) Iron

The reactions of transition metals with O_2 or H_2O_2 have been well studied. The principal transition metals that have been identified as biologically relevant are iron, and to a lesser extent copper. The role of iron as a catalyst in the generation of $^{\cdot}OH$ from H_2O_2 was discussed in section 1.1.4. The autoxidation of ferrous ions in solution at neutral pH proceeds as follows:

$$Fe^{2+} + O_2 \text{-----> } Fe^{3+} + O_2^{\cdot -} \qquad \text{(eq. 9)}$$

$$O_2^{\cdot -} + O_2^{\cdot -} + 2H^+ \text{-----> } H_2O_2 + O_2 \qquad \text{(eq. 10)}$$

$$Fe^{2+} + H_2O_2 \text{-----> } Fe^{3+} + OH^- + {}^{\cdot}OH \qquad \text{(Eq. 6)}$$

$O_2^{\cdot -}$ is a strong reducing agent and a weak oxidant, and will reduce Fe^{3+} to Fe^{2+} (Eq. 7). The protonated form of $O_2^{\cdot -}$ is the perhydroxyl radical ($HOO^{\cdot}$, Eq. 11). This compound is a strong oxidant and will oxidize Fe^{2+} to Fe^{3+} (Eq. 12).

$$O_2^{\cdot -} + H^+ \text{-----> } HOO^{\cdot} \quad \text{(Eq. 11)}$$

$$HOO^{\cdot} + Fe^{2+} + H^+ \text{-----> } Fe^{3+} + H_2O_2 \quad \text{(Eq. 12)}$$

The rate of autoxidation of Fe^{2+} in aqueous solutions is dependent on the pH as well as the presence and characteristics of additional compounds which can interact with or chelate ferrous ions. In "physiologic" media (i.e. phosphate buffer at neutral pH), these reactions proceed extremely rapidly (Cohen, 1985). The identification of physiologic metal chelators is a topic of intense current interest.

Iron in brain, as well as in other tissues, is comprised of heme iron and non-heme iron. Non-heme iron is unevenly distributed in brain. Studies with human brain indicate that regions with relatively high concentrations (100-200 ug/gm wet weight) include globus pallidus, red nucleus, substantia nigra, caudate, and putamen (Cummings, 1948; Hallgren and Sourander, 1958; Harrison et al., 1968). A similar distribution of non-heme iron has been described in rat brain (Hill and Switzer, 1984). Sub-cellular localization studies indicate that non-heme iron is enriched in microsomes, mitochondria, and myelin (Hallgren and Sourander, 1958; Youdim and Green, 1977; Youdim et al., 1980). In one study, synaptosomes were also enriched in non-heme iron (Rajan et al., 1976).

b) 6-Hydroxydopamine (6-OHDA)

6-OHDA is a well characterized neurotoxin that selectively accumulates in and destroys catecholaminergic neurons (Kostrzewa and Jacobowitz, 1974). The molecular mechanisms of 6-OHDA-mediated neurotoxicity are attributed to the products of the autoxidation of 6-OHDA (Figure 2), primarily, the formation of $O_2^{\cdot -}$, H_2O_2, and $^{\cdot}OH$ (Cohen et al., 1976; Graham et al., 1978; Cohen and Heikkila, 1974). These observations are supported by the following experimental observations: 1) 6-OHDA-mediated toxicity is increased by the addition of ascorbate (Heikkila and Cohen, 1972), a reducing agent that will cycle the quinone back to the polyphenol and drive oxy-radical-generating reactions, 2) 6-OHDA-mediated toxicity is diminished by norepinephrine (Sachs et al., 1975), a compound which scavanges $O_2^{\cdot -}$ and thus limits its catalytic effect on 6-OHDA autoxidation as well as its participation in the generation of $^{\cdot}OH$ via a Haber-Weiss type reaction, and 3) 6-OHDA-mediated destruction of sympathetic neurons is attenuated by potent scavangers of $^{\cdot}OH$ (Cohen et al., 1976).

Figure 2. Mechanisms of toxicity of 6-OHDA and 6-OHDOPA

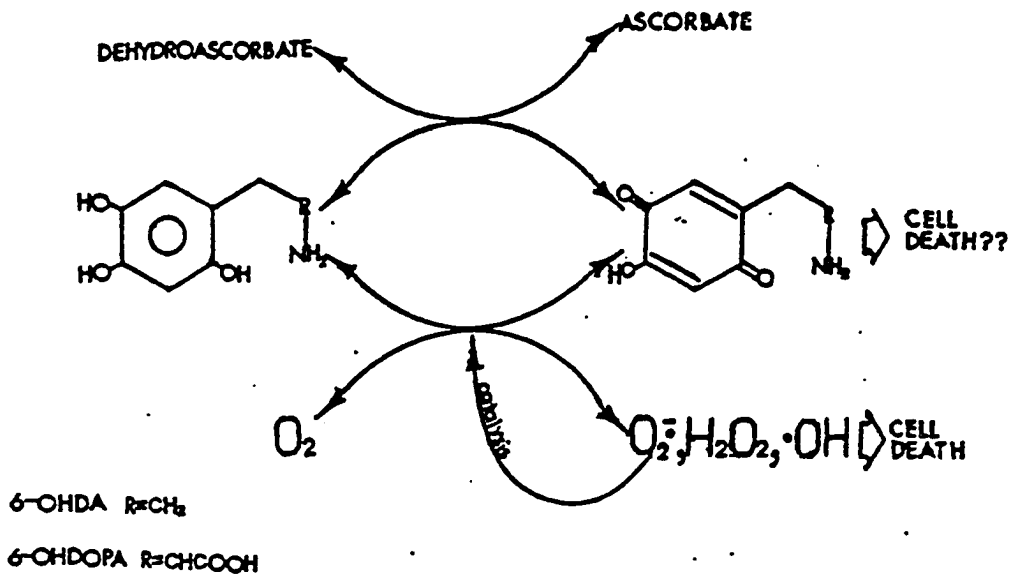

c) Other catecholamines

Endogenous catecholamines (i.e., DA, NE) may undergo autoxidation reactions to generate $O_2^{\cdot -}$, H_2O_2, and the respective quinones. Each of these products has been postulated to be toxic (Graham et al., 1978; Cohen, 1983). Dopamine has been shown to be toxic to cells in culture in several studies (Prasad and Kollmorgan, 1969; Graham et al., 1978). Graham et al. (1978) compared the rate of autoxidation of dopamine to norepinephrine and epinephrine; they found that the latter two catecholamines, which are less toxic than dopamine, undergo autoxidation less readily than dopamine. In addition, these investigators provided evidence that the mechanism of dopamine-mediated cytotoxicity is dependent upon the formation of both oxy-radicals and quinones.

1.1.6 Production of oxy-radicals and H_2O_2 during ischemia.

Ischemia results when blood flow to tissue is interrupted. Although ischemia, per se, will cause tissue damage if it proceeds uninterrupted, spontaneous reperfusion can suddenly reintroduce blood flow to the O_2-deprived tissues. Mechanisms involved in spontaneous reperfusion include: resolution of thrombi and emboli, development of collateral circulation, and deaggregation of platelets. Ischemia is not anoxia, and tissue pO_2, as well as blood flow in an ischemic region, are never zero. Several lines of experimental evidence suggest that biochemical changes

that occur in ischemic tissue may predispose this tissue to damage mediated by O_2, through the generation of oxy-radicals and peroxides by mechanisms that have been described above. This damage can become evident during recirculation, and has been referred to as "reperfusion injury". A brief description of these biochemical changes, with special reference to cerebral ischemia, will follow.

a) Perturbations in ion flux.

Reduction of cerebral blood flow below a threshold range, will result in a massive efflux of potassium ions from brain cells with a corresponding influx of sodium ions (Harris and Simon, 1984). This results in membrane depolarization and a consequent increase in cytoplasmic calcium ions. Potassium induced depolarization of neurons is associated with release of neurotransmitters. A massive release of neurotransmitters may be associated with toxic sequelae. As noted earlier (section 1.1.5 c) extracellular dopamine can be toxic to neurons due to autoxidation. This is particularly true in extracellular space, which is devoid of natural protective mechanisms. Alternatively, metabolism of large amounts of catecholamine by MAO can generate fluxes of H_2O_2 (section 1.1.2 a). In addition, excitatory amino acids (e.g. glutamate) can be neurotoxic (reviewed by Olney, 1983), and their release may contribute to ischemic cell death. It has been demonstrated that hypoxia can induce massive release of dopamine in striatum, as well as glutamate and aspartate in hippocampus of experimental

animals (Benveniste et al., 1984; Hagberg et al., 1985; Brannan et al., 1986).

An influx of calcium can lead to activation of proteases through the action of second messenger systems (i.e. calmodulin). This is the proposed mechanism for the conversion of xanthine dehydrogenase (Type D) to xanthine oxidase (Type O) during ischemia (McCord and Roy, 1982; see section 1.1.2 b). In studies with intestine, inhibition of proteases protected tissue from reperfusion injury (Parks and Granger, 1983; Parks et al., 1985). Ischemia also leads to decreases in high energy phosphates, and increases in nucleotide monophosphates and free purines. Metabolism of purines will provide increased substrates for xanthine oxidase. In the presence of O_2, which is provided during reperfusion, increased xanthine oxidase activity will generate fluxes of $O_2^{\cdot -}$ and H_2O_2 (see Figure 1). In studies of intestine and heart, inhibition of xanthine oxidase with allopurinol, or pretreatment of tissue with enzymes that detoxify $O_2^{\cdot -}$ and H_2O_2 (superoxide dismutase or catalase; see sections 1.2.1 and 1.2.2) protected against reperfusion damage (De Wall et al., 1971; Dalsing et al., 1983; Parks and Granger, 1983).

b) Changes in tissue pH.

The endogenous intracellular and extracellular buffers in brain may be overcome by increases in organic acids that occur during ischemia (Kraig et al., 1985). Lactic acid

formed from anaerobic glycolysis is thought to be the main contributor to the increased acidity (Rehncrona et al., 1981). It has been shown that lactate can be elevated 40-fold during ischemia; the extracellular pH can fall to approximately 6.2, while intracellular pH can fall as low as 5.5 (Kraig et al., 1986). These low pH values may be directly toxic, or may lead to further toxic events (i.e., protonation of superoxide to form the oxidant species, $^{\bullet}OOH$; Eq. 11). Iron salts exhibit increased solubility in acidic solutions. Ischemia has been shown to mobilize stored iron in brain, increasing cytoplasmic low molecular weight iron (Komara et al., 1986). The role of iron as a catalyst in the formation of oxy-radicals and peroxides was discussed in sections 1.1.4 and 1.1.5 a. It has been suggested that the availability of free iron is rate limiting for the occurrence of these radical producing reactions in vivo, and even small increases in free iron during ischemia may have profound effects on the production of toxic species.

c) Alteration in mitochondrial redox state.

Fridovich (1979) has suggested that hypoxia may lead to increased ratios of reduced to oxidized intermediates in the mitochondrial electron transport chain. Such a shift in the redox state would increase the occurrence of spontaneous autoxidation reactions of components which have been shown to generate $O_2^{\bullet -}$ and H_2O_2 (see section 1.1.3), particularly during tissue reoxygenation.

d) Reduction of antioxidants.

Levels of several endogenous antioxidants (described in section 1.2) are reduced during ischemia. In rodent brain, reduced glutathione (GSH) and ascorbate are significantly lowered in several different models of ischemia (Folbergrova et al., 1979; Rehncrona et al., 1980; Cooper et al., 1980). Lowered levels of antioxidant can render tissue more vulnerable to oxidative stress during reperfusion.

1.2. Antioxidant defenses.

Oxy-radicals and H_2O_2 are highly reactive and have been shown to participate in reactions which induce cellular damage (Del Maestro, 1980; Freeman and Crapo, 1982). Damage may occur through a direct interaction between the reactive forms of reduced oxygen and essential cellular constituents, or through initiation of toxic chain reactions that lead to disruption of cellular integrity.

Lipid peroxidation is an example of the latter process (Eqs. 13-16).

$$^{\bullet}OH + RH \longrightarrow H_2O + R^{\bullet} \quad \text{(Eq. 13)}$$

$$^{\bullet}OOH + RH \longrightarrow H_2O_2 + R^{\bullet} \quad \text{(Eq. 14)}$$

$$R^{\bullet} + O_2 \longrightarrow ROO^{\bullet} \quad \text{(Eq. 15)}$$

$$RH + ROO^{\bullet} \longrightarrow R^{\bullet} + ROOH \quad \text{(Eq. 16)}$$

Oxygen-derived radicals can abstract hydrogen atoms from fatty acid moieties of cell membranes to generate carbon-centered lipid radicals ($R^{\bullet}$, Eqs. 13, 14). In the presence of O_2, the carbon-centered radicals form peroxyl radicals

(ROO$^{\bullet}$, Eq. 15), which can abstract hydrogen atoms from neighboring fatty acids to generate cytotoxic lipid hydroperoxides (ROOH) and additional lipid radicals (R$^{\bullet}$, Eq. 16). Alkoxyl radicals (RO$^{\bullet}$) formed from lipid hydroperoxides (ROOH) also participate in the process. Lipid peroxidation results in disruption of cellular membranes.

Cellular mechanisms that detoxify oxy-radicals and peroxides have evolved to protect organisms from these toxic species.

1.2.1 Detoxification of $O_2^{\bullet -}$.

The detoxification of $O_2^{\bullet -}$ occurs mainly through the enzymatic actions of the superoxide dismutases (SOD; Fridovich, 1978). SOD catalyzes the dismutation of 2 moles of $O_2^{\bullet -}$ to yield one mole of O_2 and one mole of H_2O_2 (Klug et al., 1972):

$$O_2^{\bullet -} + O_2^{\bullet -} \text{------>} O_2 + H_2O_2 \quad \text{(eq. 11)}$$

Previous studies with rat brain indicate substantial SOD activity (Fried and Mandel, 1975) with a relatively homogeneous gross distribution and mainly cytosolic subcellular localization (Thomas et al., 1976).

1.2.2 Detoxification of peroxides.

H_2O_2 is detoxified by two enzymatic systems, catalase and glutathione peroxidase (GSH-peroxidase).

a) Catalase

Catalase is a heme enzyme that catalyzes the

disproportionation of 2 moles of H_2O_2 to yield one mole of O_2 and two moles of H_2O:

$$H_2O_2 + H_2O_2 \text{ -------> } O_2 + 2H_2O \quad \text{(Eq. 17)}$$

During this reaction, a stable intermediate is formed [catalase-H_2O_2 (compound I)] that can be identified spectrophotometrically (Chance, 1947). The appearance of compound I has been used to detect H_2O_2 (Oshino and Chance, 1977). Catalase is localized subcellularly to peroxisomes ("microperoxisomes" in brain; DeDuve and Baudhuin, 1966). Levels of enzyme activity in the brain are low (Gaunt and DeDuve, 1976; Sinet et al., 1980; Brannan et al., 1981), but appear most concentrated in catecholaminergic neuronal cell bodies in several nuclei (McKenna et al., 1976).

b) GSH-Peroxidase.

GSH peroxidase is a selenium containing enzyme that couples the reduction of H_2O_2 or organic peroxides to the oxidation of GSH (Mills, 1957; Little and O'Brien, 1968) in the following reaction:

$$ROOH + 2\ GSH \text{ -----> } GSSG + ROH + H_2O \quad \text{(Eq. 18)}$$

GSSG can then be reduced by the flavo-enzyme GSSG reductase, with the concomitant oxidation of NADPH as follows:

$$GSSG + NADPH + H^+ \text{ -----> } 2\ GSH + NADP^+ \quad \text{(Eq. 19)}$$

Like catalase, the activity of GSH peroxidase in brain is low (DeMarchena et al., 1974; Lawrence et al., 1974). Cellular localization studies indicate that in rat brain, both GSH peroxidase and GSSG reductase exhibit highest activity in the striatum (Brannan et. al., 1980a and

1980b).

Using perfused rat liver and benzylamine as a substrate, Oshino and Chance (1977) showed that MAO-generated H_2O_2 was coupled to oxidation of GSH to GSSG, and not to formation of compound I. This was followed by the studies of Maker et al. (1980) in which the addition of serotonin and dopamine to brain homogenates resulted in oxidation of GSH to GSSG. Sinet et. al. (1980) measured H_2O_2 production in rat brain in vivo by following the rate of reaction of compound I with 3-amino-1,2,4-triazole, which was administered systemically. They found that neither increasing MAO activity (supplying substrate for neuronal MAO by inducing turnover of dopamine with reserpine) nor decreasing MAO activity (administration of the MAO-inhibitor pargyline) had any effect on the measured H_2O_2. It seems probable that the H_2O_2 generated by MAO is preferentially detoxified by GSH peroxidase and does not reach the catalase contained in the microperoxisomes (Oshino and Chance, 1977; Sinet et al., 1980; Maker et al., 1981; Jones et al., 1981).

Several reports have suggested that the H_2O_2 generated during the metabolism of monoamines by MAO may be toxic (Cohen et al., 1976; Graham et al., 1978; Sinet et al., 1980; Cohen, 1983). Allis and Cohen (1977) administered the neurotoxin 5,7-dihydroxytryptamine to mice and inhibited the destruction of noradrenergic terminals in the left atrium with either an MAO inhibitor or hydroxyl radical scavengers.

This report provides the first and only evidence suggesting toxicity of MAO-generated H_2O_2 via $^{\cdot}OH$ formation.

1.2.3 Detoxification of $^{\cdot}OH$.

There are no antioxidant defenses which are specific for hydroxyl radicals. The hydroxyl radical is an extremely reactive species that oxidizes cellular constituents or added agents via direct addition (e.g., ring hydroxylation), hydrogen atom abstraction, and electron transfer. In cellular systems, it is expected that $^{\cdot}OH$ will react with a variety of molecules at the site of its generation. A great many biologically relevant compounds exhibit second order reaction rate constants of 10^9-$10^{10} M^{-1}s^{-1}$, which constitute essentially diffusion-limited reactivity (Anbar and Neta, 1967; Dorfman and Adams, 1973). GSH and ascorbic acid are two such compounds that are present in most cells in high (mM) concentrations and are believed to be particularly important in protecting cells from $^{\cdot}OH$-mediated toxicity. It is generally believed that an indiscriminate attack by $^{\cdot}OH$ on membranes, proteins, essential sulfhydryl groups, and other tissue constituents, is a major reason for tissue damage during x-irradiation (Bielski and Gebieki, 1977), during exposure in vivo to $^{\cdot}OH$-generating cellular toxins (Cohen, 1978), or in the presence of $^{\cdot}OH$-generating biochemical systems in vitro (Beauchamp and Fridovich, 1970).

CHAPTER 2: INTRODUCTION TO EXPERIMENTS.

2.1 Identification of the products of $^{\cdot}OH$ attack on dopamine.

Evidence for the existence of $^{\cdot}OH$ in biochemical systems in vitro has been based on the identification of products formed when $^{\cdot}OH$ attacks an exogenous compound added in relatively high concentration. For application to unperturbed cellular systems, an endogenous scavenger must be present naturally in relatively high concentration, it must have a relatively high rate constant for reacting with $^{\cdot}OH$, and the product(s) formed must be identified and quantified. We wished to develop a probe for application to the study of catecholamine-secreting neurons.

Previous studies have shown that $^{\cdot}OH$ will engage in the ring-hydroxylation of a variety of aromatic compounds including phenol and substituted phenols such as tyrosine (Land and Ebert, 1967; Richmond et al., 1981; Ingleman-Sundberg and Ekstrom, 1982). Dopamine, an endogenous catecholamine, is present in high concentration in specific neurons in the central nervous system. The rate constant for the reaction of $^{\cdot}OH$ with dopamine is $5.9 \times 10^{9} M^{-1} s^{-1}$ at pH 4.7 (Richter and Waddell, 1983). In 1959, Senoh et al. used an Fe^{2+}-EDTA/ascorbate system at pH 5.5 to oxidize dopamine, and reported ring hydroxylation to form a product that appeared to be 6-OHDA, as well as side-chain hydroxylation to form norepinephrine.

In studies described in this thesis (Ch. 3), $^{\bullet}OH$ was generated in the presence of dopamine at neutral pH by either Fe^{2+}-DTPA/H_2O_2 (a standard Fenton-type system with a ferrous-chelate, Eq. 6), or by Fe^{2+}-EDTA/ascorbate (Eqs. 6, 8-10; a recycling system), and the products of the ring-hydroxylation of dopamine were identified. Ion-pair HPLC with electrochemical detection was used to separate and identify the products.

Figure 3 illustrates the three possible ring-monohydroxylated products of dopamine (DA): 2-OHDA, 5-OHDA, and 6-OHDA. We observed formation of all three hydroxylated products. The effect of the addition of $^{\bullet}OH$ scavangers on product formation was also studied.

Figure 3. Ring monohydroxylation of dopamine (DA; 3,4-dihydroxyphenylethylamine) by the hydroxyl radical (·OH). The products are 2-OHDA, 5-OHDA and 6-OHDA.

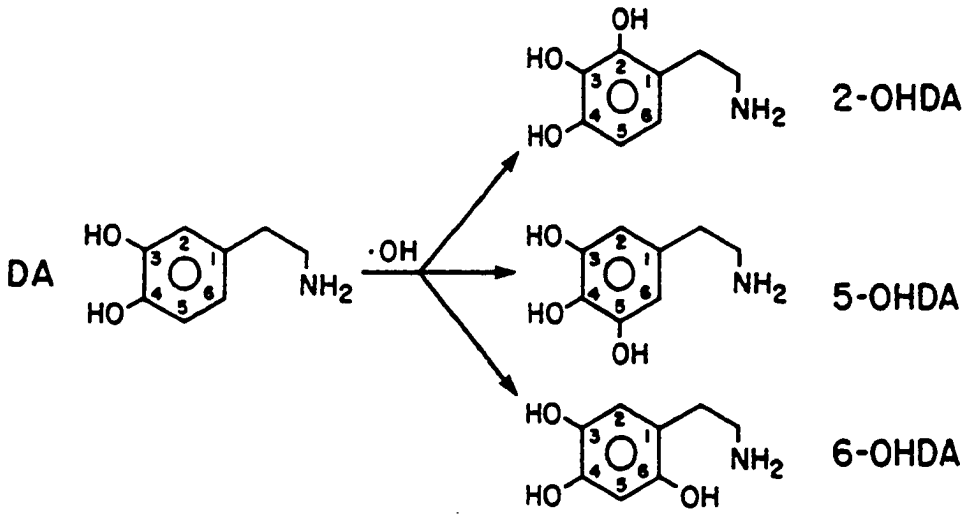

2.2 Reduced and oxidized glutathione in brain.

Reduced glutathione (GSH, gamma-glutamylcyteinylglycine) plays an essential role in protecting cells from oxidative stress (Haugaard, 1968; Aebi and Suter, 1974; Sies, 1983; Wellner et al. 1984). GSH is relatively ubiquitously distributed. It is present at levels of 1-2 mM in brain, and as high as 10 mM in liver. Identified protective functions for GSH include its role as substrate for GSH peroxidase in the elimination of hydrogen peroxide and organic peroxides as follows:

2 GSH + ROOH -----> GSSG + ROH + H_2O (Eq. 18)

where R is either hydrogen (viz., hydrogen peroxide; Mills, 1960; Cohen and Hochstein, 1963) or an alkyl group (viz., an organic peroxide; Sies, 1983), GSSG is glutathione disulfide, and ROH is either water or an alcohol. GSH also maintains essential sulfhydryl groups of enzymes and structural proteins in the reduced state (Jocelyn, 1962). In addition, GSH forms addition products with quinones, such as those derived from catecholamines (Agrup et al., 1975), and it may react directly with reactive free radicals, including semiquinone radicals ($SQ^{\cdot}$). Other properties of GSH, not related to oxidant stress, include its role in transporting amino acids via the gamma-glutamyl cycle, as cofactor for glyoxylase, and as cofactor for glutathione-S-transferases (Orlowski and Karkowski, 1976).

GSSG in brain and other tissues is normally rapidly

reduced (to 2 GSH) by GSSG reductase, an enzyme that utilizes NADPH as cofactor (Orlowski and Karkowski, 1976). An elevated level of GSSG can serve as an indicator of oxidative stress (Rehncrona et al., 1980; White et al., 1986), while the redox couple GSSG/GSH may provide an index of the redox state of the tissue. Levels of GSSG and GSH measured in rodent tissues generally show that amounts of GSSG constitute only several %, or less, of the total glutathione (Table 2, Chapt. 4). An exception appears in reports concerning human brain (Table 3A, Chapt. 4), where very high levels of GSSG, constituting 41-100% of the total glutathione, have been indicated (Perry et al., 1971; Perry et al., 1982a). In this current report, we have looked anew at human and also monkey brain to assess the levels of GSSG and GSH, and the apparent redox state of the tissue. In our hands, primate brain shows characteristics that are similar to rodent brain (Table 3B, Chapt. 4).

2.3 Histochemical evaluation of GSH in brain.

In order to study the cellular distribution of GSH, Asghar et al. (1975) developed a histochemical procedure based on the sulfhydryl reagent Mercury orange [1-(4-chloromercuriphenylazo)-naphthol-2], which was first introduced by Bennett (1951) for the visualization of total tissue sulfhydryl groups. Mercury orange has been used previously either to visualize total tissue sulfhydryls (Bennett, 1951) or as a selective stain for protein

sulfhydryls (Bennett, 1951; Barka and Anderson, 1965), depending upon the method of tissue preparation. The method cannot be applied to study GSH in fixed tissue because small soluble compounds, such as GSH, are lost or modified during fixation. The main application of the Mercury orange method has been to study protein sulfhydryl groups in fixed tissue (Barka and Anderson, 1965).

Mercury orange reacts with sulfhydryl groups to form fluorescent orange precipitates that can be visualized either by bright field microscopy or by fluorescence microscopy. The reaction with small soluble sulfhydryl compounds, such as GSH and cysteine, takes place in minutes ($T^1/_2$ = 3-4 min), whereas the reaction with protein sulfhydryls requires several hours (Asghar et al., 1975). Asghar et al. (1975) used short staining periods in order to apply Mercury orange as a selective agent for visualization of GSH in freshly-thawed tissue sections; GSH is the major soluble cellular sulfhydryl constituent (Orlowski and Karkowski, 1976). Fresh frozen tissues were used in order to prevent the loss of GSH that takes place during tissue fixation and to limit oxidation of GSH to the disulfide. The diffusion of GSH from the tissue sections during staining was prevented by dissolving the Mercury orange in toluene; neither GSH nor the GSH-Mercury orange complex is soluble in toluene. The GSH-Mercury orange complex is also insoluble in water, so that aqueous media can be used for

subsequent fixation and counterstaining.

Asghar et al. (1975) surveyed several tissues of the rat. These investigators found a uniform distribution of reaction product within hepatocytes throughout the liver, a localization of product to particular cell types in the kidney, lung, and testis, and increased stain intensity in the periphery of the lens as compared to its center. The brain was not studied. Several investigators have used the Mercury orange staining technique to study alterations in GSH content in liver during treatment with various hepatotoxins (Deml and Osterle, 1980; Harisch and Meyer, 1985).

This study describes the utilization of Mercury orange for the histochemical localization of GSH in rodent and monkey brain. The brain is an extremely heterogeneous organ with a large number of different neuronal and non-neuronal cell types, and extensive morphological differentiation and biochemical compartmentalization within a given cell. For example, neurons can vary in chemical composition at the soma, dendrites, axons, and terminals. The histochemical analysis of GSH in brain has not been described heretofore, and may provide important qualitative information on regional or cellular variations in GSH content.

2.4 Depletion of brain GSH in preweanling mice with buthionine sulfoximine.

Buthionine sulfoximine (BSO) [S-(n-butyl) homocysteine sulfoximine] is an inhibitor of gamma-glutamylcysteine synthetase, the enzyme catalyzing the first step in the synthesis of reduced glutathione (GSH). BSO was introduced by Griffith et al. (1979) as an agent which could deplete cellular levels of GSH. Treatment of cells in culture with BSO results in loss of over 90 % of GSH (Dethmers and Meister 1981). Administration of BSO to rats by subcutaneous injection or orally in drinking water, lowers levels of GSH in many tissues including liver, kidney, pancreas, lung and muscle (Giffith and Meister 1979), without causing gross pathologic abnormalities; the brain is resistant to systemically administered BSO. This resistance may be due either to an inability to attain sufficiently high concentrations of BSO in brain, or to the slow turnover of GSH in brain (Griffith and Meister 1979).

In contrast to adults, preweanling mice are extremely sensitive to repeated subcutaneous injections of BSO, responding with greater depletions of GSH in several organs and developing generalized symptoms of lethargy, emaciation, and fur abnormalities (Calvin et al. 1986). Mice receiving injections during 9-12 days of age developed cataracts; mice receiving injections during 14-17 days of age did not exhibit cataracts, but 6 of 28 animals developed hind limb paralysis. These observations prompted the present study,

which examines the effects of repeated subcutaneous injections of BSO on brain levels of GSH in 14-17 day preweanling mice.

2.5 Ischemia and oxidative stress in brain.

a) GSH and GSSG in ischemic brain.

It has been proposed that free radicals and peroxides are involved in initiating the process of ischemic brain damage (see section 1.1.6). GSH has been shown to be important in the detoxification of peroxides through its enzymatic conversion to GSSG (see section 1.2.2 b), and in the scavanging of intracellular free radicals as well. The ratio of GSH to GSSG reflects the redox state of a tissue, and can be altered during oxidative stress. Few studies have examined the influence of ischemia or hypoxia on the GSH-GSSG status in brain.

Folbergrova et al. (1979) failed to demonstrate any alterations in GSH or GSSG in cortical tissue or cisternal cerebrospinal fluid of rats made hypoxic with mechanical ventilation. Rehncrona et al. (1980) induced both complete reversible ischemia (momentarily increasing intracranial pressure as described by Ljunggren et al. 1974 and Nordstrom et al. 1978) and incomplete reversible ischemia (temporary clamping of both carotid arteries) in rats. They found similar decreases in GSH in both models. However, there was no concomitant increase in GSSG. This study was followed by the work of Cooper et al. (1980) who studied glutathione and

ascorbate during total cerebral ischemia (decapitation), and reversible, bilateral hemispheric ischemia (four-vessel occlusion model of Pulsinelli and Brierley, 1979) in rats. Thirty minutes of complete ischemia lowered total glutathione (GSH + GSSG) by 7%, but had no effect on GSSG or reduced and total ascorbate in forebrain. In the reversible ischemia model, there was no change in glutathione or ascorbate during the 30 min. of ischemia; after 24 hr. of recirculation, total brain glutathione fell by 25%, with no change in GSSG, total ascorbate, or reduced ascorbate.

Another experimental model of ischemia utilizes unilateral carotid ligation in the Mongolian gerbil, and was first described by Levine and Payan (1966). Approximately 40% of adult gerbils have an incomplete circle of Willis without connecting arteries between basilar or carotid systems. Unilateral carotid ligation in these animals produces a stroke model that shares similar characteristics to cerebral infarction seen in humans following occlusion of one carotid artery. This model has been widely used. It is experimentally convenient in that the half of the brain contralateral to ligation serves as a control for comparison to the ipsilateral ischemic half.

Previous studies have demonstrated that irreversible damage to neuronal metabolism may not occur until as late as 24 hours after ligation, although behavioral signs of stroke are apparent within 1 hour. Tissue damage is not

homogeneous; there are regional and cellular differences in susceptibility (affected regions include ipsilateral striatum, hippocampus, cortex overlying hippocampus, and diencephalon; Levine and Payan, 1966). A study examining the effects of unilateral carotid ligation on GSH and GSSG in gerbils has not been performed to date.

In this study, brains from gerbils exhibiting behavioral signs of stroke following unilateral (left) common carotid ligation, were analyzed for GSH and GSSG at various time periods. A histochemical technique for visualization of soluble sulfhydryl compounds was utilized to obtain qualitative information on regional and cellular effects of ischemia on GSH. Biochemical assays on dissected regions of control and ischemic hemispheres were utilized for quantitative analyses of GSH and GSSG.

The levels and metabolism of monoamines have been shown to be altered during ischemia, and may disturb the GSSG:GSH ratio in brain (see section 1.1.6). The effects of pretreatment of gerbils with alpha-methyl-para-tyrosine methyl ester (AMPT, which depletes brain catecholamines by inhibition of catecholamine synthesis) or treatment with pargyline (which inhibits metabolism of catecholamines by MAO) on ischemia-mediated alterations of GSH were also studied.

Finally, alterations in the levels of peptides and free amino acids have been shown to occur in brain post-mortem (Perry et al., 1980) and during ischemia (see section

1.1.6). Dissected regions of control and ischemic hemispheres from gerbils subjected to unilateral carotid ligation were analyzed for free amino acids and peptides.

b) Dopamine and its metabolites in ischemic brain.

Several investigators have demonstrated altered levels of brain neurotransmitters in ischemic hemispheres following unilateral carotid ligation in gerbils. Lust et al. (1975) found that dopamine and norepinephrine levels fell while gamma-aminobutyric acid levels rose in the ischemic cortex 6 hours after carotid ligation; serotonin and glutamate were not affected in this study. Zervas et al. (1977) showed decreases in dopamine, but not norepinephrine in ischemic hemispheres, as well as in isolated dopamine-rich regions. Lavyne et al. (1975) and Mrsulja et al. (1976) demonstrated decreases in dopamine and norepinephrine in the ischemic hemispheres at 24 hours post-ligation. Studies by Weinberger and Cohen (1982 and 1983) in gerbils demonstrated that catecholamine nerve terminals in ischemic regions are more sensitive to damage produced by unilateral carotid ligation when compared to GABA, glutamate, or serotonin nerve terminals. It has been suggested that catecholamine levels fall in ischemic tissue following their release from neurons, elicited by ischemia-induced membrane depolarization (section 1.1.6 a). A recent study by Brannan et al. (1987) used in vivo electrochemical detection to provide evidence for a significant increase in extracellular

dopamine in the ischemic striatum of gerbils exhibiting behavioral signs of stroke following unilateral carotid ligation. A potential role for released catecholamines in tissue damage produced by ischemia has been previously described (section 1.1.6 a), and is supported by the observations of Weinberger et al. (1985) who found that depletion of catecholamines by pre-treatment of gerbils with alpha-methyl-para-tyrosine protected dopamine, serotonin, and glutamate nerve terminals from ischemia-induced injury.

In order to further investigate the effects of ischemia on tissue levels of dopamine and its metabolites, levels of dopamine, DOPAC, and HVA were measured by HPLC in control and ischemic striata of gerbils exhibiting signs of stroke. Analyses were conducted at 2 hr., 4hr., and 8 hr. after left common carotid ligation. In addition, these compounds were measured bilaterally in striata of sham-operated animals. Ischemic tissue was also examined for the presence of hydroxylated isomers of dopamine in an effort detect $^{\bullet}OH$.

In separate experiments, extracellular dopamine, DOPAC, and HVA were measured by an in vivo intracerebral dialysis (ICD) technique in the ipsilateral striata of anesthetized gerbils after left carotid ligation. In some experiments, in vivo electrochemical recordings were obtained simultaneously and correlated with ICD analyses of dopamine, DOPAC, HVA, and ascorbate.

METHODS, RESULTS AND DISCUSSION

CHAPTER 3: HYDROXYL RADICAL ATTACK ON DOPAMINE.

Materials and Methods:

Reagents were obtained from the following sources: $Fe(NH_4)_2(SO_4)_2 \cdot 6H_2O$, hydrogen peroxide (30% reagent), dimethyl sulfoxide, disodium EDTA, and L-ascorbic acid (Fisher Scientific), DTPA (Sigma), ethanol (190 proof, Pharmaco), mannitol (Malinckrodt), catalase (crystalline aqueous suspension, Worthington Biochemicals), thymol (Amend Drug & Chem.), 3,4-dihydroxyphenylethylamine hydrochloride (dopamine, Calbiochem), 2,4,5-trihydroxyphenylethylamine hydrobromide (6-OHDA) and 3,4,5-trihydroxyphenylethylamine hydrochloride (5-OHDA, Regis), and 2,3,4-trihydroxyphenylethylamine (2-OHDA, gift from by Dr. Cyrus Creveling, National Institutes of Health). The water used in all experiments was purified by ion exchange (Continental Water Corp.), distilled in an all glass still (Corning), and polished by passage through a Millipore Q system (Millipore Corp.). Separate stock solutions were prepared at the following concentrations: 2 mM ferrous salt, 2.4 mM EDTA, 2.4 mM DTPA, 10 mM dopamine, 10 mM and 100 mM ascorbate, 8.8 mM hydrogen peroxide, and 0.2 M phosphate buffer at pH 7.2.

Two model $^{\cdot}OH$-generating systems in 50 mM phosphate buffer (pH 7.2) were used: Fe^{2+}-DTPA/H_2O_2 and Fe^{2+}-EDTA/ascorbate. Fe^{2+}-EDTA/ascorbate system at neutral pH is a model hydroxylating system (Udenfriend et al., 1954),

commonly referred to as the "Udenfriend system" (Breslow and Lukens, 1960). Reagent H_2O_2 need not be added in the latter system because it is generated during the autoxidation reactions of ferrous-EDTA and ascorbate.

The sequence of addition of reagents is important in Fenton-type oxidations (Cohen, 1985). Ferrous ions are oxidized rapidly by molecular oxygen in phosphate buffer at neutral pH (Cohen et al., 1981). Subsequent addition of hydrogen peroxide will not yield a Fenton reaction (equation 3) after iron has been transformed to the ferric state. However, the ferrous-DTPA chelate in neutral phosphate buffer is relatively stable to autoxidation (Cohen et al., 1981), and it will donate an electron to H_2O_2 and generate $^{\cdot}OH$ in a Fenton-type reaction (Cohen and Sinet, 1982). The ferric-DTPA chelate is not readily reduced by either superoxide or ascorbate. The ferric-EDTA chelate, on the other hand, is readily reduced, and ferrous-EDTA will engage in a Fenton-type reaction. The sequence of additions and final concentrations of reagents for the Fe^{2+}-DTPA/H_2O_2 system (10 mL final volume) were as follows: water, phosphate buffer (final concentration 50 mM, pH 7.2), dopamine (1 mM), DTPA (240 uM), ferrous salt (200 uM), and lastly, hydrogen peroxide (44 uM). In some experiments, catalase (100 units/mL), heat-inactivated catalase (placed in a vigorously boiling water bath for 10 min. followed by resuspension of the denatured protein by trituration through a 27 gauge needle), or thymol (15 uM) was added to the

reaction mixture prior to the addition of dopamine. For the Fe^{2+}-EDTA/ascorbate system (10 mL final volume), the additions and final concentrations were as follows: water, phosphate buffer (final concentration 50 mM, pH 7.2), dopamine (1 mM), ascorbate (1 mM), EDTA (240 uM), and ferrous salt (200 uM).

Reaction mixtures were incubated at room temperature with intermittent stirring. At various time periods, aliquots (0.1 mL) were removed and quenched by dilution to 1.0 mL in ice-cold 0.4 M perchloric acid, with and without added ascorbate, such that the final concentration of ascorbate was either 0.1 mM or 1.0 mM (see text). In some experiments, mannitol, ethanol, or dimethyl sulfoxide was added at various concentrations before the addition of dopamine.

Standard dilutions (1 ug/mL) of 2-OHDA, 5-OHDA, and 6-OHDA were prepared daily as chromatographic standards by diluting cold stock solutions (1.0 mg/mL in 0.4 M perchloric acid containing 1.0 mM ascorbate as antioxidant) into ice-cold 0.4 M perchloric acid containing 1.0 mM ascorbate; these dilutions were resistant to oxidative loss during the course of the experiment. In some experiments, dilutions were made into ice-cold 0.4 M perchloric acid containing 0.1 mM ascorbate; in that event, a substantial fraction of the 6-OHDA was lost (see text).

Analyses were performed by HPLC with an electrochemical

detector equipped with a glassy-carbon electrode (Bioanalytical Systems) set at an oxidizing potential of either +0.2 volts or +0.8 volts (see text) versus a Ag/AgCl reference electrode. In some experiments, the potential was varied between +0.2 volts and +0.8 volts. The sensitivity of the detector was set at 20 nAmps for full scale deflection on the chart recorder. At set time intervals, the output from the recorder was changed from 1.0 volt to 100 mvolts full scale in order to instantaneously increase the sensitivity 10-fold (2 nAmps full scale). The mobile phase consisted of an aqueous solution of citric acid (125 mM), sodium phosphate (125 mM), EDTA (100 mg/liter), and sodium octylsulfate (30 mg/liter) as the paired ion; the pH was adjusted to 2.5 with concentrated phosphoric acid (Seiden and Vosmer, 1984). The flow rate was 1.0 ml/min. Samples (20 uL) of quenched reaction mixtures were injected over a C-18 reverse-phase column (Bioanalytical Systems, 5 um beads, 25 cm length).

Results:

Figure 4 is a series of chromatograms showing the separation of mixtures of standard solutions of 2-OHDA, 5-OHDA, and 6-OHDA by HPLC and electrochemistry. Although 5-OHDA and 6-OHDA appeared as a merged peak, they could be separately identified by their electrochemical oxidation properties. The electrochemical detector was set at +0.8 volts in panels A-C and +0.2 volts in panels D-F. Panel A

shows the separation of a mixture of 6-OHDA and 2-OHDA; panel B shows the separation of 5-OHDA and 2-OHDA. In panel C, all three monohydroxylated forms of dopamine were injected together; 5-OHDA and 6-OHDA did not separate from one another, but they did separate from 2-OHDA. Panels D-F are repeat injections of the mixtures shown in panels A-C, with the electrochemical detector set at +0.2 volts. Only 6-OHDA was seen at +0.2 volts. Thus, by altering the voltage of the electrochemical detector, effective separation of 5-OHDA and 6-OHDA could be achieved.

The peak height of 6-OHDA varied directly with the amount of ascorbate present in the perchloric acid diluent. 6-OHDA is much more easily oxidized by molecular oxygen than is either 5-OHDA or 2-OHDA. Ascorbate is required to maintain the 6-OHDA in the reduced state. When standard solutions of 2-OHDA, 5-OHDA, and 6-OHDA were prepared in 0.4 M perchloric acid containing 0.1 mM ascorbate, a 5-fold increase in concentration of 6-OHDA was required in order to obtain equivalent peak heights for 2-OHDA, 5-OHDA, and 6-OHDA (Figure 4, see legend). Increasing the ascorbate concentration to 1 mM increased the peak height of 6-OHDA without affecting 5-OHDA or 2-OHDA. At +0.8 volts, the markedly increased size of the ascorbate peak interfered with the chromatographic detection of the hydroxylated dopamine isomers. At +0.2 volts, however, the electrode response to the ascorbate was diminished sufficiently to allow for a clean analysis of the 6-OHDA peak; at +0.2

volts, 5-OHDA was barely visible (Cf. Fig 4). The requirement for high concentrations of ascorbate (viz., 1 mM) to prevent autoxidation of 6-OHDA is a second way to differentiate between 5-OHDA and 6-OHDA. Therefore, in all subsequent studies, analyses for 6-OHDA were performed by quenching the reaction mixtures in perchloric acid containing 1.0 mM ascorbate and analyzing at +0.2 volts. Analyses for 5-OHDA and 2-OHDA were carried out by quenching the reaction samples in perchloric acid containing 0.1 mM ascorbate and analyzing at +0.8 volts. Reaction-generated peaks were compared to appropriate standards. The standards were diluted into reaction medium (with H_2O_2 and/or Fe^{2+} omitted), allowed to stand for 10 minutes, and then diluted further into cold 0.4 M perchloric acid containing ascorbate, such that the final concentration was 0.1 mM for analyses of 2-OHDA and 5-OHDA, and 1.0 mM for analyses of 6-OHDA.

Figure 4: Separation of 2-OHDA, 5-OHDA, and 6-OHDA by HPLC and electrochemical oxidation.

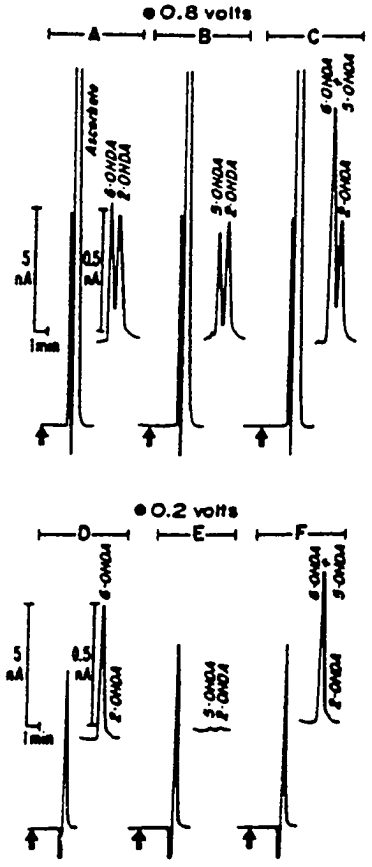

Standard solutions were prepared in 0.4 M perchloric acid containing 0.1 mM ascorbate. Mixtures of standards contained 0.4 ng 2-OHDA, 0.4 ng 5-OHDA , and 2.0 ng 6-OHDA, in a 20 uL injection volume; these amounts produced roughly equivalent peak heights under the described conditions. The points of sample injection are marked by arrows. All three compounds showed electrochemical responses (peaks) when the detector was set at +0.8 volts (panels A-C): 2-OHDA separated chromatographically from either 6-OHDA (panel A) or 5-OHDA (panel B), but 5-OHDA and 6-OHDA chromatographed as a merged peak (panel C). Only 6-OHDA was visible when the electrochemical detector set at +0.2 volts (panels D-F). The HPLC conditions are described in the Materials and Methods section.

Figure 5 shows the 2-OHDA and 5-OHDA formed from dopamine after 10 minutes of incubation with the Fe^{2+}-EDTA/ascorbate system. The electrochemical detector was set at +0.8 volts and the final concentration of ascorbate in quenched aliquots of reaction mixture was 0.1 mM. In panel A, iron was omitted and no products were observed. In the complete system (with iron, panel B), two peaks appeared (x and y), the first of which co-chromatographed with added authentic 5-OHDA (panel C), while the second co-chromatographed with added authentic 2-OHDA (panel D). When samples were reanalyzed with the detector set at +0.2 volts, the two peaks were essentially absent (not shown). In order to verify the identity of the peaks, reaction samples were rechromatographed repeatedly with the electrochemical detector set at various voltages between +0.2 volts and +0.8 volts.

Figure 6A shows that the first peak (peak x) generated by the Fe^{2+}-EDTA/ascorbate system had electrochemical oxidation properties that were indistinguishable from authentic 5-OHDA standard. The electrochemical properties were, however, clearly different from 6-OHDA, which gave a substantial response at lower oxidizing voltages. Panel B compares the electrochemical oxidation properties of the second peak (peak y) with authentic 2-OHDA. The electrochemical oxidation properties could not be distinguished from 2-OHDA, but were substantially different from 6-OHDA.

Figure 5. Generation of 5-OHDA and 2-OHDA in the Fe^{2+}-EDTA/ascorbate system.

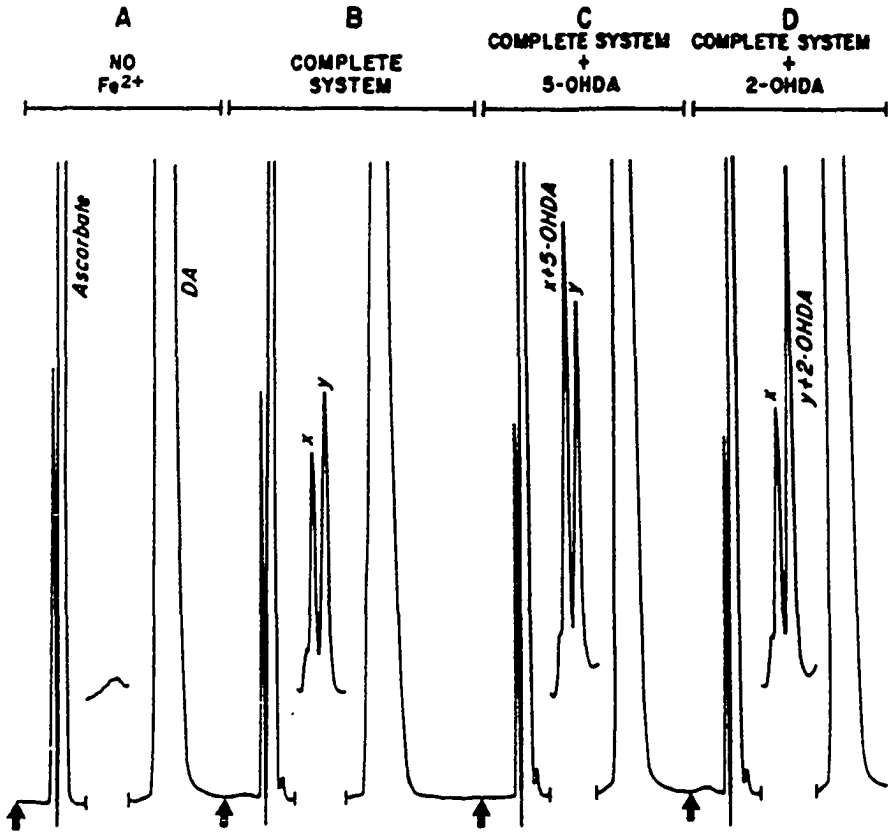

The reaction medium consisted of 1 mM dopamine (DA), 1 mM ascorbate, 240 uM EDTA, 200 uM ferrous ammonium sulfate (Fe^{2+}), and 50 mM phosphate buffer at pH 7.2. Samples were incubated at room temperature for 10 min. Aliquots (100 uL) were removed and diluted to 1 mL in cold 0.4 M perchloric acid at a final ascorbate concentration of 0.1 mM. HPLC analyses (20 uL injection) were conducted with the electrochemical detector set at + 0.8 volts. The points of sample injection are marked by arrows. The sensitivity of the recorder was increased 10-fold, where indicated between the ascorbate and DA peaks. Panel A is a control without added ferrous salt. Panel B shows products formed in the complete system. Panels C and D show co-chromatography of authentic 5-OHDA and 2-OHDA (0.4 ng) with products x and y, respectively.

Figure 6. Electrochemical oxidation properties of authentic standards and reaction-generated peaks in the Fe^{2+}-EDTA/ascorbate system.

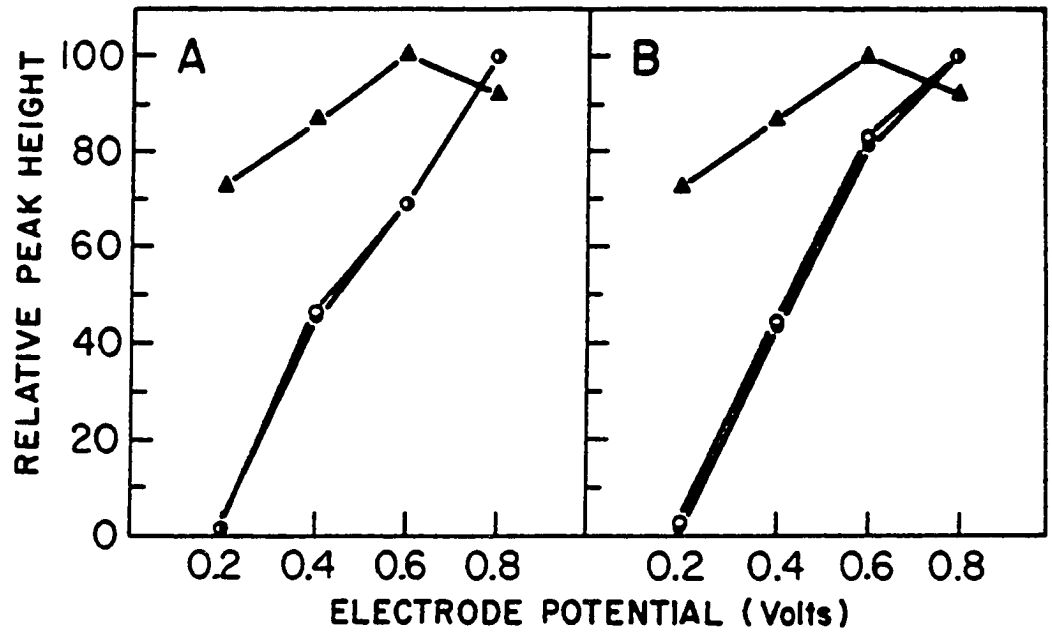

Samples were processed as described in the legend to Figure 5. Panel A shows the relative peak heights of authentic 5-OHDA (open circles, 100 = 0.90 nA), reaction-generated 5-OHDA (closed circles, 100 = 1.02 nA), and authentic 6-OHDA (closed triangles, 100 = 0.35 nA) at several electrode potentials, with the detector sensitivity set at 2 nA for full scale deflection of the recorder. Similarly, panel B shows the relative peak heights of authentic 2-OHDA (open circles, 100 = 0.94 nA), reaction-generated 2-OHDA (closed circles, 100 = 1.28 nA), and authentic 6-OHDA (closed triangles, 100 = 0.35 nA) at different electrode potentials. Results are from a single experiment. Similar results were obtained in replicate experiments.

Similar results were obtained upon analysis of the products formed in the Fe^{2+}-DTPA/H_2O_2 system. Panel A of Figure 7 shows the absence of product when ferrous ions and H_2O_2 were omitted from the reaction. Panel B shows product formation upon the addition of ferrous ions and H_2O_2, while panels C and D show that the reaction products co-chromatographed with co-injected authentic standards of 5-OHDA and 2-OHDA, respectively. When the reaction mixture was analyzed with the detector set at +0.2 volts, the two peaks were essentially absent (not shown).

Figure 8 demonstrates that when the reaction was quenched by dilution into 0.4 M perchloric acid in the presence of 1.0 mM ascorbate, and analyzed at +0.2 volts, a peak with chromatographic and electrochemical properties indistinguishable from 6-OHDA was present (panel B for the Fe^{2+}-EDTA/ascorbate system and panel D for the Fe^{2+}-DTPA/H_2O_2 system). However, when aliquots of reaction mixture were quenched in the presence of only 0.1 mM ascorbate, the 6-OHDA peak was essentially absent (panels A and C). Standard solutions of 6-OHDA behaved similarly when diluted to similar concentrations into 0.4M perchloric acid with either 1 mM or 0.1 mM ascorbate. Direct analyses at +0.2 volts of samples of the Fe^{2+}-EDTA/ascorbate (1 mM) reaction mixture without prior dilution into perchloric acid confirmed the presence and amount of 6-OHDA in the reaction mixture.

Figure 7. Generation of 5-OHDA and 2-OHDA in the Fe^{2+}-DTPA/H_2O_2 system.

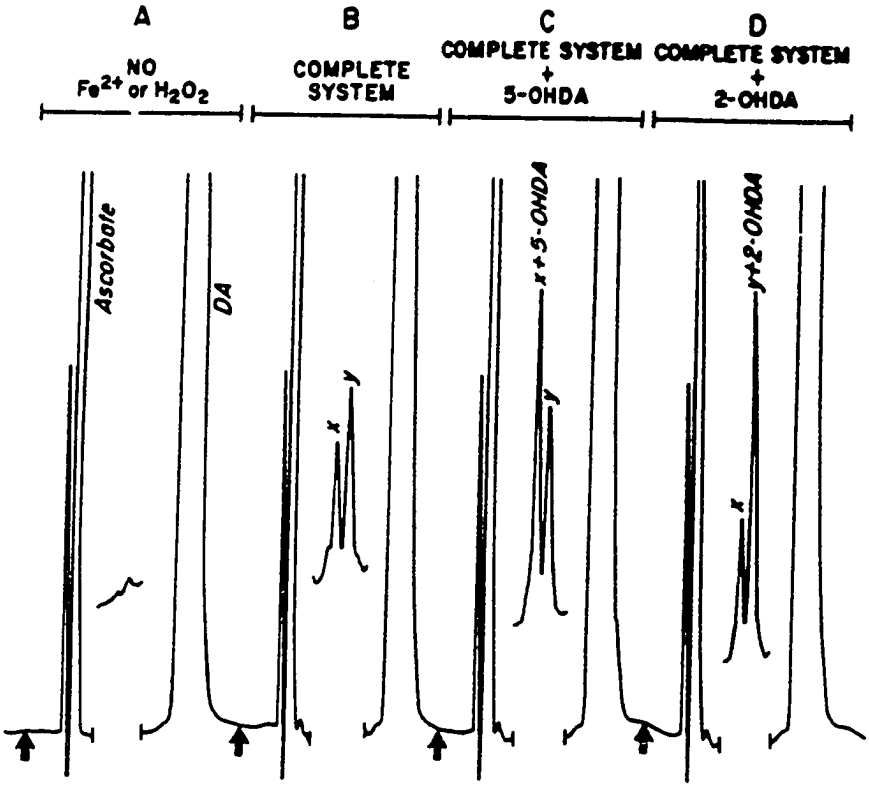

The reaction medium consisted of 1 mM dopamine (DA), 240 uM DTPA, 200 uM ferrous ammonium sulfate (Fe^{2+}), 44 uM hydrogen peroxide, and 50 mM phosphate buffer at pH 7.2. Samples were incubated at room temperature for 10 min. and then they were processed as indicated in the legend to Figure 5. Panel A is a control in which the ferrous salt and H_2O_2 were omitted. Panel B shows products formed in the complete system. Panels C and D show co-chromatography of authentic 5-OHDA and 2-OHDA (0.4 ng) with products x and y, respectively.

Figure 8. The effect of ascorbate concentration on the stability and detection of 6-OHDA.

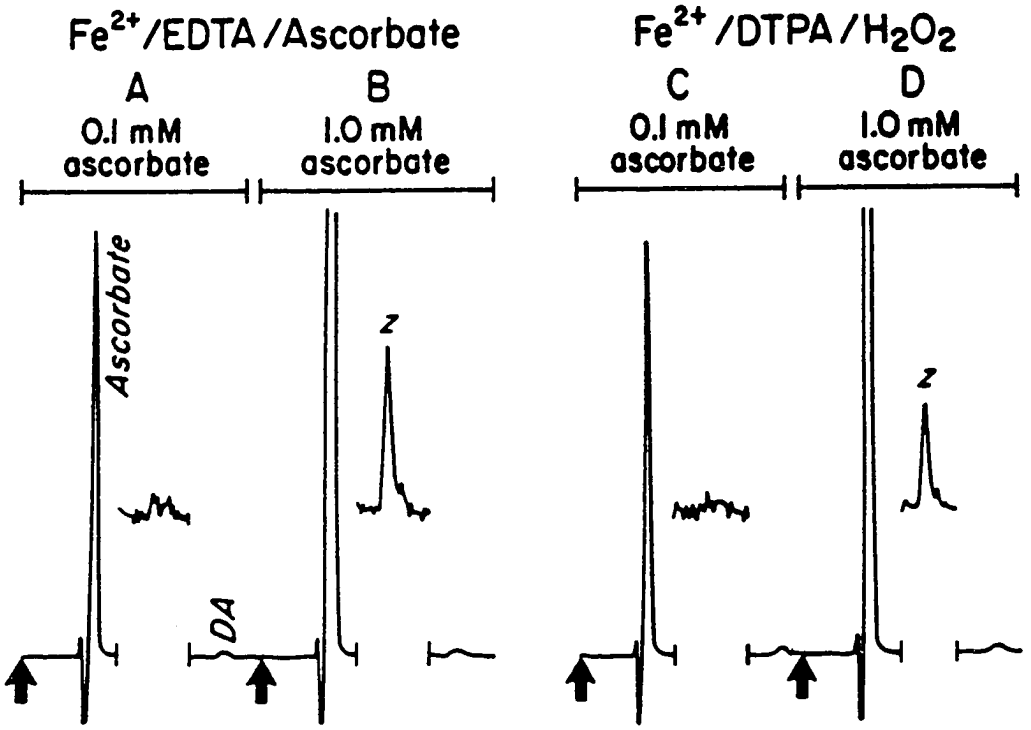

Reaction mixtures were processed as described in the legends to Figures 5 and 7 for the Fe^{2+}-EDTA/ascorbate system and the Fe^{2+}-DTPA/H_2O_2 system, respectively (complete systems), except that dilutions into cold 0.4 M perchloric acid were made so that the final ascorbate concentration was either 0.1 mM or 1.0 mM. HPLC analyses (20 uL injection) were conducted with the electrochemical detector set at + 0.2 volts. A reaction-generated product (peak z) is seen in either system when the ascorbate concentration is 1.0 mM (panels B and D), but not when the ascorbate concentration is 0.1 mM (panels A and C).

Figure 9 shows product formation with time in the Fe^{2+}-EDTA/ascorbate system and the Fe^{2+}-DTPA/H_2O_2 system. Product formation in the Fe^{2+}-EDTA/ascorbate system (panel A) was continuous, but fell off with time. Product formation in the Fe^{2+}-DTPA/H_2O_2 system (panel B) was greater than 70% complete by 2 minutes and reached a plateau. In both systems, at all time points tested, 2-OHDA was formed in greater amounts than 5-OHDA, which was formed in greater amounts than 6-OHDA. The relative amounts of products at all time points were approximately 2-OHDA:5-OHDA:6-OHDA = 3:2:1.

When Fe^{2+}-DTPA was incubated with dopamine in the absence of added H_2O_2, small amounts of products were formed: 0.28 $\pm$ 0.07 ug 5-OHDA/10 ml and 0.58 $\pm$ 0.15 ug 2-OHDA/10 ml at 10 min (mean $\pm$ S.D., N=3) (compare to amount in Fig. 9). Addition of catalase (100 units/ml) inhibited product formation under these conditions (0.04 $\pm$ 0.05 ug 5-OHDA/10 ml and 0.07 $\pm$ 0.09 ug 2-OHDA/10 ml). Heat-inactivated catalase or addition of 15 uM thymol (an amount 10-fold in excess of that present as a preservative in the catalase) did not give significant inhibition of product formation. These results indicate that some H_2O_2 was generated in the system, probably from the autoxidation reactions of dopamine and Fe^{2+}-DTPA.

Figure 9. Product formation with time in the Fe^{2+}-EDTA/ascorbate system (panel A) and the Fe^{2+}-DTPA/H_2O_2 system (panel B).

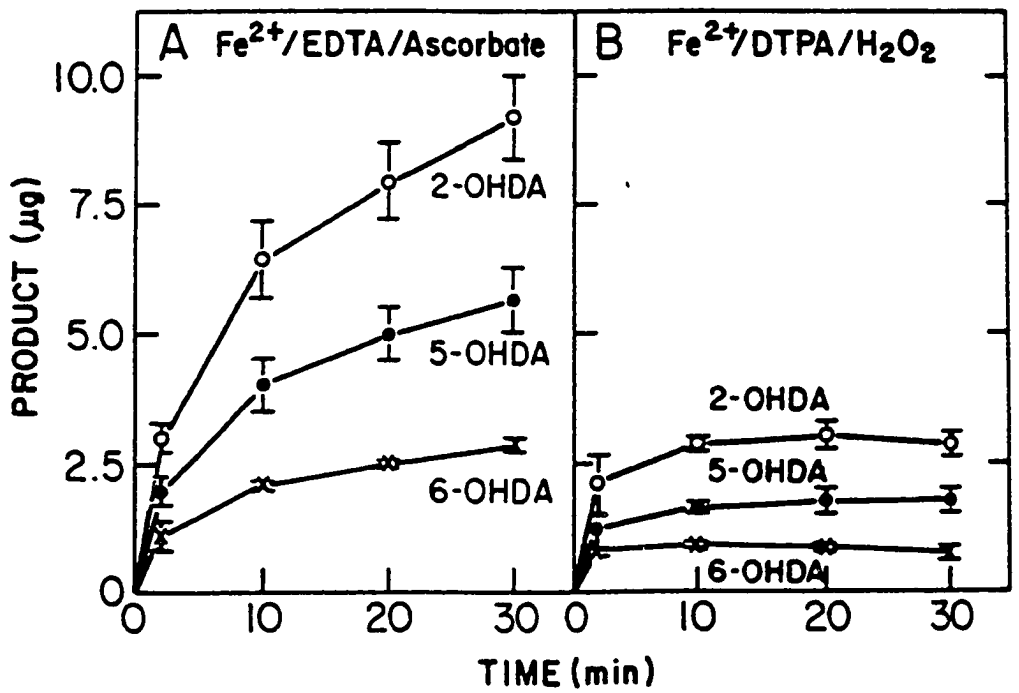

Conditions are given in the legends to Figures 5 and 7, respectively. Aliquots (100 uL) of reaction medium were removed at the indicated times and quenched by dilution to 1.0 ml in 0.4 M perchloric acid containing either 0.1 mM ascorbate (for analysis of 5-OHDA and 2-OHDA) or 1.0 mM ascorbate (for analysis of 6-OHDA). The electrochemical detector was set at +0.8 volts for analysis of 5-OHDA and 2-OHDA, and at +0.2 volts for analysis of 6-OHDA. Product formation was calculated by comparison of reaction-generated peak heights with those of authentic standards. Each point represents the mean ± S.D. (N=3).

Senoh et al. (1959) had reported formation of norepinephrine when Fe^{2+}-EDTA/ascorbate and dopamine were incubated together. Small amounts of norepinephrine were detected in our experiments: 0.33 ± 0.09 ug/10 ml in the Fe^{2+}-EDTA/ascorbate system and 0.22 ± 0.02 ug/10 ml in the Fe^{2+}-DTPA/H_2O_2 (mean ± S.D. at 10 min, N=3). The norepinephrine is visible in Figs. 5 and 7 (panels B) as a small peak which follows the ascorbate peak. The lower yield of norepinephrine compared to ring-hydroxylated dopamine analogs is in accord with lower rate constants for reaction of aliphatic compared to aromatic moieties (Dorfman and Adams, 1973).

The effect of addition of $^{\cdot}OH$ scavengers on the yield of products in the Fe^{2+}-EDTA/ascorbate system is shown in Table 1. Dimethyl sulfoxide, mannitol and ethanol were tested. All three scavengers inhibited the formation of 5-OHDA and 2-OHDA in a dose-dependent manner. Dimethyl sulfoxide was the most potent, while mannitol and ethanol exhibited lesser potencies, in accord with known second order rate constants (Dorfman and Adams, 1973; Goldstein and Czapski, 1984) for the reactions with $^{\cdot}OH$: dimethyl sulfoxide = 7.1 x $10^9 M^{-1}s^{-1}$ and mannitol or ethanol = 1.8 x $10^9 M^{-1}s^{-1}$. Scavengers at a concentration of 10 mM inhibited the formation of 6-OHDA to a similar extent as 2-OHDA and 5-OHDA formation. Studies conducted with the Fe^{2+}-DTPA/H_2O_2 system gave comparable results: The yields of products in the presence of 10 mM mannitol, 10 mM ethanol and 10 mM

dimethyl sulfoxide, respectively, were (% control, N=3 per group) 37.6%, 32.7% and 10.3% for 5-OHDA, and 36.1%, 29.8% and 12.6% for 2-OHDA.

Table 1. Suppression of yields of 2-hydroxydopamine, 5-hydroxydopamine, and 6-hydroxydopamine in the iron-EDTA/ascorbate system with hydroxyl radical scavenging agents. Dopamine was present at 1 mM. Values are the mean ± S.D. for N = 3 per group.

Scavenger (mM)	2-OHDA (ug/10 ml)	(% Control)	5-OHDA (ug/10 ml)	(% Control)	6-OHDA (ug/10ml)	(% Control)
None (control)	5.77 ± 0.04	(100)	3.59 ± 0.56	(100)	2.89 ± 0.38	(100)
Dimethylsulfoxide						
0.1	5.62 ± 0.66	(97.4)	3.47 ± 0.40	(96.7)		
1.0	3.59 ± 0.27	(62.2)	2.32 ± 0.09	(64.6)		
10	0.77 ± 0.17	(13.3)	0.47 ± 0.11	(13.1)	0.47 ± 0.05	(16.3)
100	0.14 ± 0.00	(2.4)	0.08 ± 0.02	(2.2)		
Mannitol						
0.1	5.96 ± 0.99	(103.1)	3.69 ± 0.57	(102.8)		
1.0	5.12 ± 0.47	(88.7)	3.17 ± 0.30	(88.3)		
10	2.54 ± 0.39	(44.0)	1.61 ± 0.26	(44.8)	1.28 ± 0.05	(44.3)
100	0.48 ± 0.16	(8.3)	0.29 ± 0.10	(8.1)		
Ethanol						
0.1	5.45 ± 0.61	(94.4)	3.37 ± 0.22	(93.9)		
1.0	4.79 ± 0.80	(83.0)	2.85 ± 0.40	(79.4)		
10	2.35 ± 0.58	(40.7)	1.37 ± 0.23	(38.2)	1.25 ± 0.17	(43.3)
100	0.58 ± 0.21	(10.1)	0.22 ± 0.04	(6.1)		

Discussion:

The hydroxylation of aromatic compounds has been used by others as an indicator of the generation of $^{\cdot}OH$ by model enzymatic and non-enzymatic systems (McCord and Day, 1978; Halliwell, 1978; Raghavan and Steenken, 1980; Rowley and Halliwell, 1982). Radzik et al. (1983) exploited the advantages of HPLC with electrochemical detection to analyze for hydroxylated aniline and phenol derivatives that were generated by the hypoxanthine/xanthine oxidase system (a metal-catalyzed Haber-Weiss system). Similarly, we used HPLC with electrochemical detection to study the products of the ring-hydroxylation of dopamine, a naturally-occurring neurotransmitter agent, by two well-characterized $^{\cdot}OH$-generating systems.

The ring hydroxylation of dopamine by Fe^{2+}-EDTA/ascorbate (recycling system) or by Fe^{2+}-DTPA/H_2O_2 (direct Fenton system) results in three distinct products: 2-OHDA, 5-OHDA and 6-OHDA (Fig. 3). Analyses for the monohydroxylated products were based on their differing chromatographic and oxidation properties: 2-OHDA was separated from 5-OHDA and 6-OHDA by HPLC (Fig. 4), while 5- and 6-OHDA were distinguished from one another by their respective oxidative properties at +0.2 and +0.8 volts (Fig. 4) and by the requirement for added reductant (1 mM ascorbate) to maintain 6-OHDA in the reduced state (Fig. 8). The identities of the products were verified by co-chromatography with added standards (e.g., Figs. 5 and 7)

and by fuller examination of their respective electrochemical oxidation properties (e.g., Fig. 6).

Richter and Waddell (1983) studied the interaction of dopamine with $^{\bullet}OH$ generated by pulse radiolysis. They reported that addition of $^{\bullet}OH$ to each of the ring positions was equiprobable. Their studies were conducted in the absence of oxygen or ferric ions which can oxidize the transient trihydroxycyclohexadienyl radical intermediates to stable products. Under these conditions, the intermediates eliminated water to give the semiquinone(s) of dopamine. In phosphate-buffered medium at neutral pH, the dehydration reaction for the 6-OH intermediate was faster than that for the 2-OH and 5-OH intermediates, which could not be differentiated from each other. The reaction rate constants were $2.2 \times 10^{8} M^{-1}s^{-1}$ and $0.65 \times 10^{8} M^{-1}s^{-1}$, respectively. The ratio of 2-OHDA:5-OHDA:6-OHDA formed in our studies was approximately 3:2:1 in either system. The lower yield of 6-OHDA can probably be attributed to the more-rapid water elimination reaction of the 6-hydroxylated radical intermediate.

Analysis of the Fe^{2+}-DTPA/H_2O_2 system revealed that product formation was essentially complete after 2 min. (Fig. 9B), reflecting a rapid Fenton reaction. Formation of trace amounts of products in the absence of added H_2O_2 (but in the presence of added Fe^{2+}) was due to the formation of trace amounts of H_2O_2 via the autoxidation of the added

dopamine and/or Fe^{2+}-DTPA, and could be blocked by the addition of catalase (see Results). In the Fe^{2+}-EDTA/ascorbate system, product formation was dependent on the addition of iron, and was continuous in time (Fig 9A), reflecting the redox cycling of iron and the continuous generation of H_2O_2. In both systems, product formation was inhibited by competitive $^{\cdot}OH$ scavengers (Table 1). The degree of inhibition was consistent with literature values for the second order rate constants for reactions of $^{\cdot}OH$ with the scavengers.

The yield of product can be calculated in the direct Fenton system (Fe^{2+}-DTPA/H_2O_2). In Fig 7B, the combined yield of 2-OHDA, 5-OHDA, and 6-OHDA was 5.55 ug/10 ml (3.26 uM) at 20 minutes. Assuming complete conversion of 44 uM H_2O_2 to $^{\cdot}OH$, the yield of ring-monohydroxylated products is 7.4%. Senoh et al. (1959) had reported side-chain beta-hydroxylation to form norepinephrine in the iron-EDTA/ascorbate system. We confirmed the formation of small amounts of norepinephrine in both experimental systems. The ring-hydroxylated products are of greater interest because these compounds should not be present in tissue preparations in the absence of $^{\cdot}OH$, whereas norepinephrine is a naturally-occurring catecholamine. We did not seek to confirm the formation of other possible or presumed products such as 1,2,4-trihydroxybenzene, polyhydroxylated dopamine, dopamine quinone or polymerized products. Small shoulders preceding the 5-OHDA and dopamine peaks (e.g., Fig. 7, panel

B) may represent phenolic metabolites.

6-OHDA is a known neurotoxin that is selectively taken up into catecholamine nerve terminals and destroys them (Kostrzewa and Jacobowitz, 1974). The mechanism of cytotoxicity has been shown to be dependent, in part, upon the generation of oxygen-derived free radicals (superoxide and $^{\bullet}OH$) during the spontaneous, rapid autoxidation of 6-OHDA (Cohen et al., 1976). 2-OHDA and 5-OHDA are not cytotoxic.

Senoh et al. (1959) reported the formation of 6-OHDA-like material during incubation of Fe^{2+}-EDTA/ascorbate with dopamine. They detected similar ^{14}C-labelled material in the urine of rats that had been injected with ^{14}C-dopamine. Numerous investigators have quoted these observations to suggest that 6-OHDA can be generated from dopamine in the central nervous system in vivo, and that such an event may underlie cellular damage to dopamine neurons; relationships to schizophrenia and Parkinson's disease, which entail defects in dopaminergic neurons, have been suggested (Stein and Wise, 1971; Graham et al., 1978). However, the studies of Senoh et al. (1959) were performed in 1959 with paper chromatography as a major analytic tool. The unique analytic capabilities of modern HPLC methodology indicates that 6-OHDA is indeed a product of the reaction, but that 2-OHDA and 5-OHDA are formed in greater amounts. The urinary excretion data with rats appear more problematical.

Material excreted in urine would not have the benefit of high ascorbate concentrations that are needed to maintain 6-OHDA in the reduced form. It appears likely that the ^{14}C-labelled material excreted in the urine of rats could not have been 6-OHDA. Moreover, recent studies have shown that tyrosinase, the melanin-forming enzyme found in skin, will hydroxylate 3,4-dihydroxyphenylalanine in the 5-position (Agrup et al., 1982); therefore, 5-OHDA may appear in urine. These considerations raise questions about the significance of the 6-OHDA-like material reportedly excreted in rat urine, as well as the extrapolation to ideas about the etiology of diseases involving dopamine neurons.

Our observations indicate that $^{\cdot}OH$, generated by two model non-enzymatic hydroxylating systems, will react with dopamine to generate a mixture of the three possible ring-monohydroxylated products. The ability to study the products of $^{\cdot}OH$ attack on dopamine should prove relevant as a detection system in other biochemical or biologic systems in which H_2O_2 is generated and ring-hydroxylation of dopamine can occur. The axon terminals of dopaminergic neurons in the central nervous system are highly enriched in that neurotransmitter, with concentrations estimated at 8 mg/g (or 47 mM) (Anden et al., 1966). H_2O_2 is generated within these neurons during the oxidative deamination of dopamine by mitochondrial monoamine oxidase; the rate of H_2O_2 production should follow neuronal activity and turnover of neurotransmitter. The potential toxicity of generated

H_2O_2 (via $^{\cdot}OH$ formation) has been discussed (Cohen et al., 1976; Graham et al., 1978; Sinet et al., 1980; Cohen, 1983). The techniques presented in this paper may prove valuable for evaluating the generation of $^{\cdot}OH$ in dopamine neurons and the potential pathologic consequences.

CHAPTER 4: REDUCED AND OXIDIZED GLUTATHIONE IN HUMAN AND MONKEY BRAIN.

Materials and Methods:

We measured GSH and GSSG in grey and white matter from autopsy specimens of human cortex. Specimens of right parietal cortex were obtained from 5 patients (4 male and 1 female) who had died without central nervous system disease. The average age was 73.4 + 8.5 years, and the death to assay time interval was 19.4 + 4.7 hours. Tissue samples were homogenized in 10 volumes of ice-cold 0.4 M perchloric acid containing 40 mg diethylenetriaminepentaacetic acid/L. The precipitated protein was pelleted by centrifugation at 11,000 x g for 15 minutes. The supernatant fluid was analyzed for GSH and GSSG.

Determinations of GSH and GSSG were also performed on cortical grey and white matter, as well as on caudate nucleus, from three male monkeys (Macaca fascicularis, Charles River Breeders). These animals were made available to us at the termination of other experiments. The monkeys were anesthetized with sodium pentobarbital (40 mg/kg), the skull was removed, and the brain was excised immediately following a lethal intravenous dose of pentobarbital. A piece of frontal cortex and the head of the caudate nucleus were obtained. The frontal cortex was dissected into grey and white matter. All procedures were performed in a cold room ($4^{o}C$), and the dissected specimens were frozen over dry ice until weighed and processed as described for human

tissue.

Some assays were also performed on rats (male Sprague-Dawley, 225-250 g, Perfection Breeders). The animals were decapitated with a guillotine and the brain was removed and rinsed by immersion in ice-cold isotonic saline. A piece of frontal cortex was obtained, weighed, and processed as described above. The assays with rats served to compare our results to literature values of GSH and GSSG.

GSH analyses were performed directly on the acidic supernatant by high performance liquid chromatography (HPLC) with electrochemical detection (BAS Inc., 1982). The HPLC equipment consisted of a pump and injector (Waters Associates, Milford, Mass.), a 25 cm octadecylsilane column with 5 um beads (Altex, Berkley, Ca.), and an electrochemical detector equipped with a sulfhydryl-sensitive mercury/gold amalgam electrode (BAS Inc., West Lafayette, Ind.), which was operated at an oxidizing potential of +0.15 volts vs a Ag/AgCl reference electrode. The mobile phase was 96 parts 0.15 M monochloroacetic acid, pH 3.0, containing 1.25 mM sodium octyl sulfate (paired ion reagent), and 4 parts methanol. A flow rate of 1.0 mL/min was used.

GSSG was measured by a modification of the method of Teitze (1969). A 100 uL aliquot of the acidified supernatant was added to 900 uL of 11 mM N-ethylmaleimide (NEM) in 100 mM potassium phosphate buffer, containing 5 mM EDTA, at pH 7.5, in order to remove GSH. After 20 min.

incubation at room temperature, this solution was passed over Sep-Pak C-18 cartridges (Waters) to remove unreacted NEM. The cartridges were rinsed once with an equal volume of buffer; the final pH was 7.0. Assays were performed with 1.5 ml of this eluate, to which 5,5'-dithiobis-(2-nitrobenzoic acid) (DTNB), NADPH, and GSSG-reductase were added in amounts described by Cooper et al. (1980). The final assay volume was 2.0 mL. The rate of color formation was monitored at 412 nm and ambient temperature with a Stasar III flow-through spectrophotometer (Gilford Inst., Oberlin, OH.) and compared to rates obtained with standards which were subjected to the same procedure; the blank rate, consisting of the rate of reduction of DTNB by GSSG reductase, was subtracted from observed values.

Results:

Table 2 is a summary of literature values for brain GSH and GSSG in rodents, along with calculated values of the % GSSG. The formula used was % GSSG = 100 x 2GSSG/(GSH + 2GSSG). Our own values for rat cortex are also shown at the bottom of the Table. The method of tissue extraction and the analytical techniques employed are also listed in the Tables, as these parameters may affect the apparent concentrations of GSH and GSSG. Most authors used variants of the same analytical procedure to measure reduced and oxidized forms of glutathione.

Table 2. Mean levels of reduced glutathione (GSH) and oxidized glutathione (GSSG) in rat brain.

The % GSSG (defined as 100% x 2GSSG/[GSH + 2GSSG]) is presented in descending order. Values in parentheses are the number of animals (N). Abbreviations used: PCA, perchloric acid; TCA, trichloroacetic acid; SA, sulphosalicylic acid; MeOH, methanol; NEM, N-ethylmaleimide; 2-VP, 2-vinylpyridine. NEM or 2-VP were used to remove GSH prior to assay for GSSG. Analytic methods: A, GSSG reductase with NADPH fluorescence; B, glyoxylase; C, GSSG reductase with DTNB colorimetry; and D, GSSG reductase with DTNB colorimetry for GSSG, and HPLC for GSH. Methods A-C employed variants of the same procedure to determine GSH and GSSG. *SEM ± 0.02 mM GSH and ± 0.0019 mM GSSG.

BRAIN REGION (N)	EXTRACTION	ANALYTIC METHOD	GSH (mM)	GSSG (mM)	% GSSG	REFERENCE
Cortex (16)	HCl+MeOH/PCA/NEM	A	2.05	0.062	5.7	Folbergrova et al., 1979
Cerebellum (4)	HCl+MeOH/NEM	A	2.01	0.049	4.6	"
Brain stem (4)	HCl+MeOH/NEM	A	1.37	0.028	3.9	"
Whole Brain (6)	SA	B	3.34	0.05	2.9	Martin and McIlwain, 1959
Cortex (6)	TCA/NEM	A	2.03	0.014	1.4	Folbergrova et al., 1979
Cortex (6)	TCA/NEM	A	2.07	0.0123	1.2	Rehncrona et al.,1980
Cortex (7)	TCA/NEM	A	1.86	0.0096	1.0	"
Frontal cortex(4)	PCA/NEM	D	1.45*	0.0038*	0.5	This study
Forebrain (13)	"Freeze blow"/ PCA/2-VP	C	1.80	0.0017	0.2	Cooper et al., 1980

Table 2 shows that rodent brain exhibits GSH levels ranging from 1.37 mM to 3.34 mM. GSSG values range from 0.0017 mM to 0.15 mM. It is now generally recognized that proper assessment of GSSG values requires that oxidation of GSH to GSSG be curtailed during the processing of tissues for analyses. Cooper et al. (1980) went to great lengths to minimize artifactual formation of GSSG. They used a freeze-blow technique to obtain brain samples, and reported the lowest GSSG levels and the lowest % GSSG for rodent brain, consistent with the lowest artifactual formation of GSSG. They suggested that their values represent only an upper limit for brain GSSG in vivo. Our GSSG values, obtained from tissue that was rapidly removed and homogenized in cold perchloric acid, are low compared to other values in Table 2, but they are not as low as Cooper et al. (1980).

Studies with human brain are few. Surprisingly, they indicate that most of the glutathione is in the oxidized form (Table 3A). Values as high as 1.09 mM GSSG were recorded. To our knowledge, the results listed in Table 3A constitute the only available data on both GSH and GSSG in human brain. Other publications (Marstein et al., 1981; Perry et al., 1981 and Perry, 1982) contain data on human brain, but results are expressed as total glutathione, and a breakdown into GSH and GSSG is not provided. Although post-mortem changes can result in autolytic loss of total glutathione (Perry et al., 1981, and may disturb the ratio of GSSG to GSH, Table 3A shows that even biopsy specimens of

human tissue that were frozen within 10-30 seconds after removal from brain showed remarkably high levels of GSSG. These data of Perry and coworkers (1971 and 1982) appear to indicate that the redox state of the human brain is significantly different from rodent brain and other tissues.

Table 3B shows the results of our measurements of GSH and GSSG in autopsy specimens of human brain. Mean levels of GSSG were 0.0081 mM or less. The % GSSG was 0.5% and 1.2% for cortical grey and white matter, respectively. In the monkey, the % GSSG was 0.5%, 0.3%, and 0.5%, respectively, for cortical grey matter, cortical white matter, and caudate nucleus. The data indicate that in human and monkey cortex, the total glutathione pool is predominantly (> 98.8%) in the reduced (GSH) form. These results are similar to those reported for rodent brain (Table 2), but do not agree with the prior reports concerning human brain (Table 3A).

The levels of GSH in human brain in our study were significantly lower than monkey brain (Table 3B). This difference may be species related, but more likely reflects, at least in part, post-mortem autolytic loss of glutathione: the death to assay interval was 19.4 $\pm$ 4.7 hours for human brain and less than than 30 minutes for monkey brain.

Table 3. Levels of reduced glutathione (GSH) and oxidized glutathione (GSSG) in human and monkey brain. The number of brain samples is shown in parentheses. Abbreviations used: PCA, perchloric acid; tr, trace.

3A. LITERATURE VALUES: Data are from Perry et al. (1971, 1982). Biopsy material was from patients with a variety of neurologic conditions; autopsy material was from a pooled heterogeneous group of patients. Mean values are given where available. Other data show the range. Tissues were processed with liquid nitrogen and PCA. Analyses were conducted by automated amino acid analysis with ninhydrin.

BRAIN REGION	GSH (mM)	GSSG (μM)	% GSSG
BIOPSY:			
Frontal Cortex (33)	0.91	0.89	66.0
Frontal Cortex (16)	0.64	0.85	72.5
Cerebellar Cortex (9)	0.71	1.09	75.4
AUTOPSY:			
Frontal Cortex (42)	0.61	0.45	59.6
Occipital Cortex (47)	0.45	0.46	67.2
Cerebellar Cortex (47)	0.66	0.54	62.1
Caudate (47)	0.66	0.61	64.9
Substantia Nigra (50)	0.13	0.54	89.3

Table 3 Continued

3B. VALUES FROM THE CURRENT STUDY: Autopsy specimens of human brain were from patients who died without central nervous system involvement. Tissues were processed in the cold with PCA. GSH was measured by high performance liquid chromatography and electrochemical detection with a sulfhydryl-sensitive electrode. GSSG was measured with GSSG reductase and DTNB by the assay of Teitze (1969). Values shown are the mean ± SEM.

BRAIN REGION	GSH (mM)	GSSG (mM)	% GSSG
HUMAN BRAIN, AUTOPSY (5)			
Parietal Cortex, grey matter	0.83 ± 0.03	0.0020 ± 0.0005	0.5
Parietal Cortex, white matter	1.18 ± 0.09	0.0068 ± 0.0020	1.2
MONKEY BRAIN, AUTOPSY (3)			
Frontal Cortex, grey matter	2.64 ± 0.43	0.0067 ± 0.0011	0.5
Frontal Cortex, white matter	2.51 ± 0.43	0.0039 ± 0.0002	0.3
Head of Caudate Nucleus	3.10 ± 0.58	0.0081 ± 0.0032	0.5

Discussion:

The results of our analyses for GSSG in human brain conflict with previous published results. The factors responsible need to be elucidated. The factors may include differences in tissue storage, tissue extraction, or method of analysis. In our assays, an average delay of 19 hours before autopsy was unavoidable. However, very low levels of GSSG were confirmed for monkey brain, which was obtained rapidly after death and assayed immediately. On the other hand, Perry et al. (1971) performed assays on biopsy specimens that were rapidly frozen, and then stored frozen for 1-2 h prior to analyses; these brains gave high GSSG values similar to those observed for autopsied and stored specimens. Both Perry et al. (1971 and 1982) and we used 0.4 M perchloric acid to deproteinize brain. Whereas they remove the perchloric acid by precipitation with KOH at pH 2.8, we proceed with analyses without removal of perchloric acid. With regard to analytic methodology, Perry et al. (1971 and 1982) used an automated amino acid analyzer, with post-column derivatization with ninhydrin. An obvious advantage of this method as a research tool is that it permits survey of many amino acids and small peptides in a tissue sample; a possible drawback is that the detection system views too many compounds. We used analytic techniques that were selective for the compounds under study. Assays were performed immediately, without storage. The analysis of GSH by HPLC is based on a sulfhydryl-

sensitive detector. Acid-soluble sulfhydryls are separated in an acidic mobile phase within 10 minutes after injection. GSH, which is the major soluble sulfhydryl constituent of tissues, is the major peak on the chromatogram; cysteine is also visible. For the analysis of GSSG, acidified tissue extracts are brought to neutral pH in the presence of NEM to remove GSH from the samples (Teitze, 1969). This step effectively prevents artifactual formation of GSSG during the assay, and also permits the selective determination of GSSG when GSH is present in the tissue extract.

GSSG levels constituting 41-100% of the total glutathione, as previously reported by Perry et al. (1971 and 1982) for human brain (Table 2A), are difficult to rationalize. These data indicate a very unusual state for the redox couple GSH/GSSG in human brain. The high levels of GSSG would be expected to lead to extensive mixed disulfide formation and inactivation of key SH-dependent enzymes. It is difficult to imagine that this represents the basal condition for human brain.

Perry et al. (1982) also measured GSH and GSSG levels in various brain regions obtained at autopsy on patients with Parkinson's disease. They reported that all of the glutathione in the substantia nigra was GSSG, compared to a level of 89.3% GSSG in control substantia nigra. They considered that key findings were that the levels of GSH and total glutathione (GSH + {2 x GSSG}) were significantly

lower in the substantia nigra compared to other regions of control human brain, and that nigral GSH was significantly further reduced in Parkinson's disease compared to controls. However, these results cannot be accepted at face value unless the reason for the apparent high GSSG in normal brain is resolved.

A number of investigators (Cohen, 1983; Bannon et al., 1984; Yong et al., 1986) have considered the possibility that levels of GSH and oxidant stress within dopamine neurons may be pathologic vectors in both idiopathic and toxin-induced parkinsonism (e.g., MPTP toxicity). Study of brain GSH and GSSG in neurodegenerative disorders is warranted, as is the study of brain response to selected neurotoxins. In view of the cellular heterogeneity of brain, methods that can specify the localization of GSH or GSSG to cell type or region are needed.

CHAPTER 5: HISTOCHEMICAL ANALYSIS OF GLUTATHIONE IN BRAIN.

Materials and Methods:

Male Swiss-Webster mice (30-50 gm., Perfection Breeders) were decapitated and their brains were quickly removed, rinsed with cold isotonic saline, and cut into blocks. Male Sprague-Dawley rats (200-220 gm., Perfection Breeders) and male Mongolian gerbils (50-70 gm., Tumblebrook Farms) were similarly handled. The tissue blocks were placed on a drop of Tissue-Tek compound (Miles Pharm., Naperville, Ill.) on a cork disk and immersed in liquid propane that was pre-cooled in liquid nitrogen. After 30 seconds, the tissue blocks were placed into a cryostat and allowed to equilibrate with the chamber temperature ($-20^{o}C$) for 1-2 hr. prior to sectioning. Liver was excised and prepared as above. Some of the animals received diethyl maleate (DEM [Sigma Chem. Co., St. Louis, Mo.], 1 ml/kg i.p. in lubinol [Purepac Pharm., Elizabeth, N.J.]) or vehicle alone. After 30 min., blocks from brain and liver were prepared for staining as described above. Some tissues were homogenized in 0.4M perchloric acid with diethylenetriaminepentaacetate (40 ug/ml) and N-acetylcysteine (5 ug/ml, as an internal standard), centrifuged at 10,000 x g for 10 min., and the supernatants were analyzed for GSH by high performance liquid chromatography (HPLC).

Two male monkeys (Macaca fascicularis, 2.5 kg, Charles River Breeders) were anesthetized with sodium pentobarbital

(40 mg/kg), the skulls were removed, and the brains were excised immediately following a lethal i.v. dose of pentobarbital. The tissues from the monkey brains were available from control animals used in other experiments. The left caudate, cerebellum, hippocampus, and a piece of frontal cortex were dissected. Blocks of tissue were mounted as above, and frozen for 60 sec. in n-hexane pre-cooled in a dry ice-ethanol slurry. The use of a different medium for freezing monkey brain, compared to rodents, is not an essential part of the procedure. All of the procedures for obtaining the monkey tissue were performed in a cold room (4^{o}C). The frozen tissue blocks were transported to the cryostat on dry ice and sectioned as described above.

Staining was performed according to the protocol of Asghar et al. (1975), and modified by Chieco and Boor (1983). Briefly, 8 um sections were thawed on glass slides and immediately immersed in 50 uM Mercury orange (Sigma Chem. Co., St. Louis, Mo.) in ice-cold toluene. After 4 min, the slides were rinsed in cold toluene to remove unreacted Mercury orange, and then either air dried and mounted directly in non-flourescent medium (Entellan, Merck, Damstadt, W. Germany) or fixed (10% neutral buffered formalin, 15 min) for counterstaining with toluidine blue (0.1% aqueous solution, 5 min). Slides were viewed by dark-field, bright field, phase-contrast, transmission

fluorescence (transmitted light from a mercury bulb passed through a BG-38 and BG-12 excitation filter, and emitted light passed through a K-550 barrier filter [Leitz Wetzlar, Germany]), and epi-fluorescence (excitation filter BP 450-490, chromatic beam splitter FT 510, and barrier filter LP 520 [Zeiss, Germany]) microscopy.

HPLC analysis of GSH with electrochemical detection was performed as described by Bioanalytic Systems Inc. (1982). The HPLC equipment consisted of a pump and injector (Waters Assoc., Milford, Mass.), a 15 cm octadecylsilane column with 5 um beads (Altex, Berkley, Ca.), and an electrochemical detector equipped with a mercury/gold amalgam electrode (BAS Inc., West Lafayette, Ind.) set at an oxidizing potential of + 0.15 volts. The mobile phase was 96% 0.15 M monochloroacetic acid pH 3.0, 1.25 mM sodium octyl sulfate (paired-ion reagent), and 4% methanol. A flow of 0.5 ml/min was used.

Results:

Tissue sections from a variety of brain regions from mice, rats, gerbils, and two monkeys, were stained with Mercury orange and examined. When viewed by fluorescence microscopy, the sections exhibit granular deposits of brightly-fluorescent orange material. The Mercury orange stain is, however, conspicuously sparse in neuronal somata. For example, Figure 10 illustrates a section of monkey cerebellum that was treated with Mercury orange. Figure 10A

is the section viewed by dark field illumination, in which a purkinje cell with its apical dendrite is clearly visible. When the same field is viewed by transmission fluorescence (Figure 10B), the Mercury orange-stained regions (which appear white in the photographs) are seen mostly outside of the neuronal soma. Some fluorescent material, particularly that with a peri-nuclear distribution, is present in the perikarya; the nucleus is unstained.

Figure 10. Localization of GSH in a section of monkey cerebellum stained with Mercury orange.

In Figure 10A, dark field illumination reveals the morphology of a purkinje neuron. Figure 10B shows the same field viewed by transmission fluorescence microscopy. Mercury orange-positive staining consists of granular orange fluorescent deposits, which appear white in the photograph (Figure 10B); the neuronal soma is relatively unstained. Some fluorescent material is located within the perikaryon, particularly with a peri-nuclear distribution. The nucleus is unstained. The apical dendrite is visualized as a relatively unstained (dark) process extending into the well-stained molecular layer. Magnification x 500.

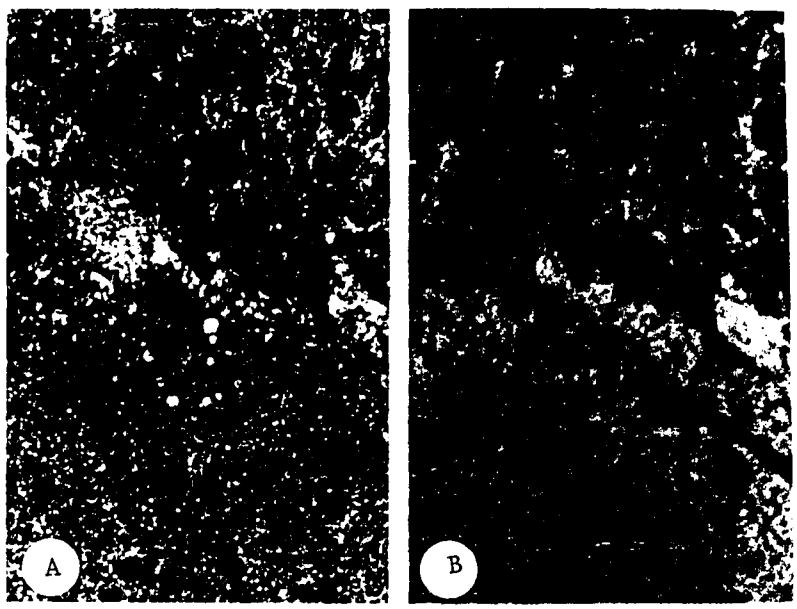

Another example of this staining pattern is seen in the thalamus (Figure 11). Figure 11A illustrates the distribution and morphology of cells in a section of mouse thalamus that was counterstained with toluidine blue and viewed by bright field illumination. Once again, the same field viewed by transmission fluorescence microscopy (Figure 11B) exhibits a relative absence of stained material in the neuronal cell bodies (arrow). Examination of sections by dark field illumination (e.g. Figure 10A) or counterstained sections by bright field microscopy (e.g. Figure 11A) indicates that the relative absence of staining in neuronal somata (Figures 10B and 11B) is not due to morphological artifacts caused by tissue processing. The same pattern was observed consistently in all regions of brain examined, which included sections taken from most rostral to most caudal regions of several mouse brains. Similar observations were made when selected regions of the brains of rats and gerbils were examined.

Figure 11. Localization of GSH in a section of mouse thalamus stained with Mercury Orange and counterstained with toluidine blue.

In Figure 11A, toluidine blue reveals the morphology and distribution of thalamic neurons (arrow) under bright field microscopy. In Figure 11B, the same cells, examined by transmission fluorescence microscopy, appear dark; most of the Mercury Orange-positive fluorescence (white areas) lies outside of the neuronal somata. Magnification x 400.

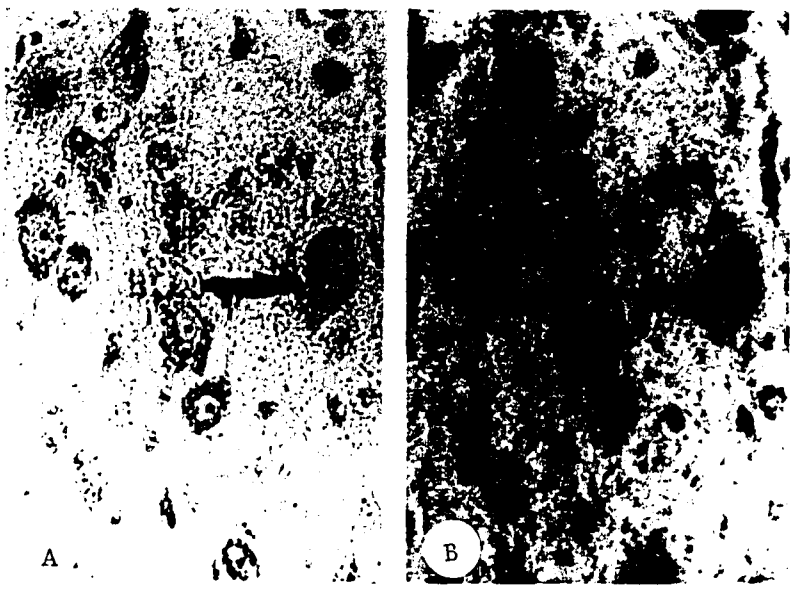

Figures 12 and 13 illustrate similar staining characteristics in other regions of monkey brain. These sections were stained with Mercury orange and viewed directly by transmission fluorescence microscopy. In the hippocampus, the neuronal somata of the pyramidal cells (Figure 12A) lack significant fluorescence. Similarly, the cells of the dentate gyrus of the hippocampus (Figure 12B) lack fluorescence.

In the cortex (Figure 13A), the neuronal somata contain slight fluorescent material, as do apical dendrites which are visible (arrows) as relatively unstained regions. Figure 13B is a higher power view of the boxed area delineated in Figure 13A. Cell bodies and apical dendrites are clearly visible against a more-brightly stained background; slight fluorescent staining is more apparent in the cell cytoplasm at the higher magnification. Examination of sections that were not counterstained with toluidine blue and viewed by dark field, phase contrast, and epi-fluorescence microscopy confirmed that the relative absence of Mercury Orange stain in neuronal somata was not due to morphological artifacts caused by tissue processing.

Figure 12. Localization of GSH in sections of monkey hippocampus stained with Mercury orange and viewed directly (no counterstaining) by transmission fluorescence microscopy.

Figure 12A illustrates the relative absence of staining (dark regions) in neuronal somata of pyramidal cells; the surrounding areas contain abundant fluorescent material (white regions). A higher power view of the neurons of the dentate gyrus of hippocampus (Figure 12B) illustrates similar staining characteristics. Magnification for Figure 12A x 160 and for Figure 12B x 400.

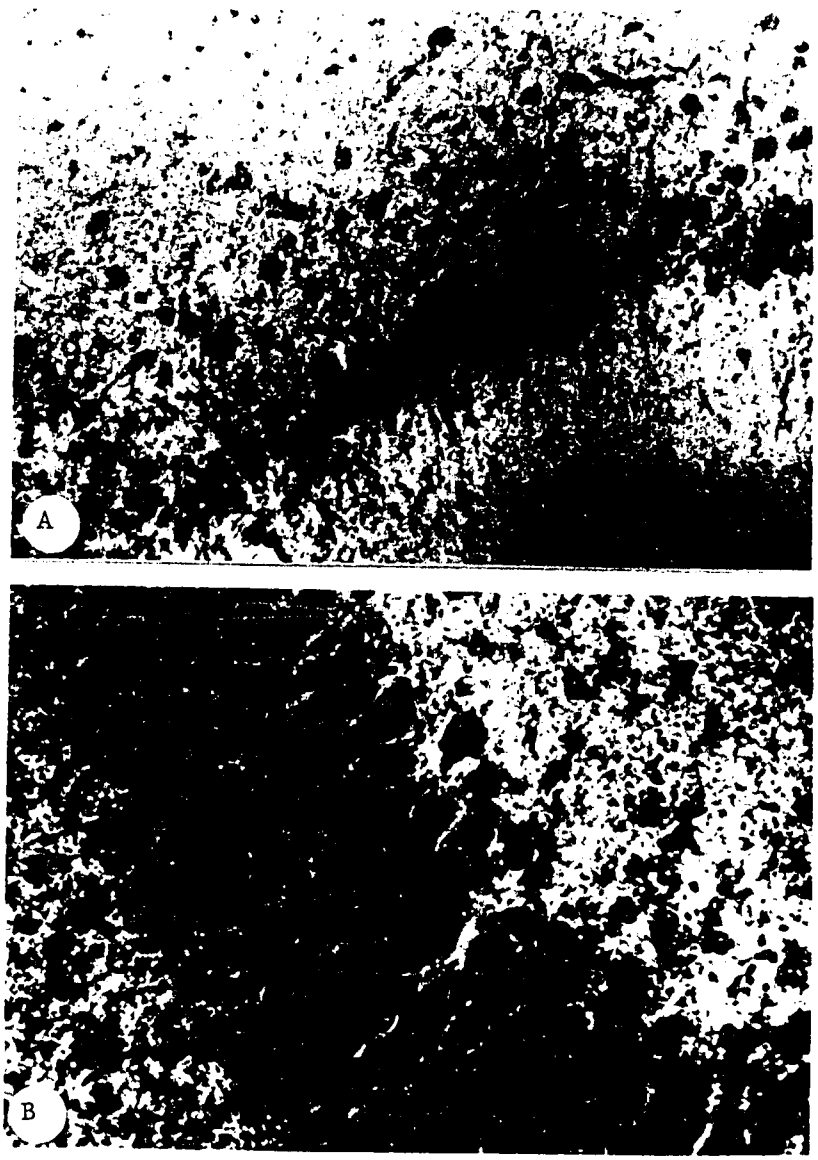

Figure 13. Localization of GSH in a section of monkey cortex, stained with Mercury orange and viewed directly by transmission fluorescence microscopy.

In Figure 13A, the neuronal somata and some large apical dendrites (arrows) are poorly stained by Mercury orange. Figure 13B is a higher magnification of the boxed area in Figure 13A. The neuronal somata and apical dendrite (arrows) contain slight fluorescent stain compared to the well-stained surrounding regions. Some of the larger fluorescent deposits within neuronal somata are lipofuscin, which appears bright yellow in contrast to the Mercury-orange stained material. Magnification for Figure 13A x 400 and for Figure 13B x 864.

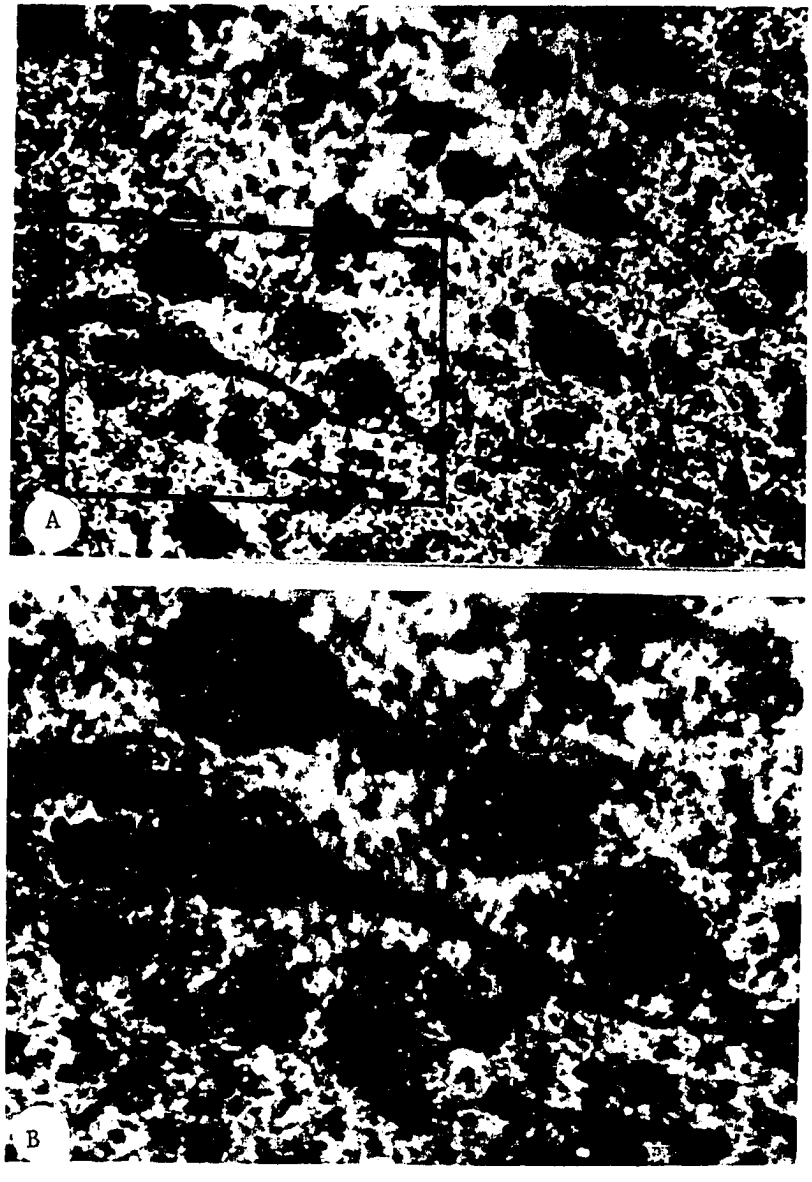

Since liver had been used in previous histochemical studies of GSH distribution (Asghar et al., 1975; Deml and Oesterle, 1980; Harisch and Meyer, 1985), we also examined liver and compared it to the staining pattern seen in brain. Figure 14A shows the staining characteristics of mouse liver. In agreement with the prior reports, the stained material appears in the cytoplasm of hepatocytes with a relatively uniform distribution throughout the section. The nuclei of the hepatocytes are not stained. Some mice were injected with DEM, an agent that depletes cellular GSH via a reaction catalyzed by the enzyme glutathione-S-transferase. Mice receiving DEM showed marked reduction in staining (Figure 14B). Analyses of GSH by HPLC in other mice indicated that DEM depleted liver GSH by an average of 85% (control = 7.02 $\pm$ 0.80 mM and DEM-treated = 1.05 $\pm$ 0.50 mM, N=6 per group).

The staining characteristics of liver, namely, well-stained cytoplasm with relatively uniform stain distribution, contrast with those of brain, where the stain distribution is heterogeneous.

Figure 14. Localization of GSH in liver of a control mouse (Figure 14A) and a mouse that was injected with DEM in order to reduce tissue levels of GSH (Figure 14B).

Sections were stained with Mercury orange and viewed directly by transmission fluorescence microscopy. Figure 14A shows the staining characteristics of normal liver. A relatively homogeneous distribution of stain appears throughout the cytoplasm of hepatocytes; the nuclei do not stain. A pronounced reduction in Mercury orange staining is seen (Figure 14B) after GSH has been lowered (see text) by treatment with DEM. Magnification x 160.

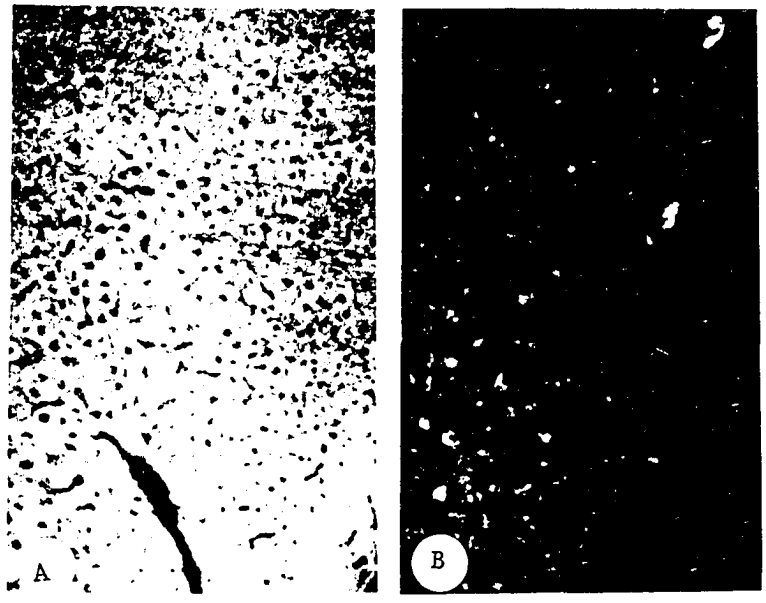

Figure 15 shows the effect of DEM treatment on the GSH staining of brain. Figure 15A illustrates the staining characteristics of the striatum, adjacent lateral ventricle with the choroid plexus, and the corpus callosum, of a control mouse. While stained material is present in the striatum, many of the unstained regions give the appearance and distribution of neuronal cell bodies. In the choroid plexus, the borders of the epithelial cells are particularly well stained. The corpus callosum shows brightly stained fibers. Figure 15B shows a similar region from a DEM-treated animal: The stain intensity is significantly reduced.

When other areas of brain were examined, DEM induced similar reductions in Mercury orange staining. Examination of GSH levels by HPLC in other groups of mice indicated that whole brain GSH levels were reduced by 66% (control = 1.98 ± 0.08 mM and DEM-treated = 0.68 ± 0.39 mM, N=6 per group). HPLC also verified that acid-soluble (perchloric acid) tissue sulfhydryls were comprised mainly of GSH (>95%; see Figure 34, Appendix I).

Figure 15. Reduction of Mercury orange staining in brain following depletion of GSH by pretreatment with DEM.

Sections were stained with Mercury orange and viewed directly by transmission fluorescence microscopy. Figure 15A shows the staining characteristics of striatum (s), adjacent lateral ventricle with choroid plexus, and corpus callosum (cc). Stained material is present in the fibers of the corpus callosum, in the epithelial cells of the choroid plexus, and in the striatum. In the striatum, many of the unstained regions, which appear dark, have the distribution and morphology of neuronal somata. When a similar section of brain from a mouse treated with DEM is examined (Figure 15B), marked reduction in Mercury orange staining is apparent in all structures. Magnification x 160.

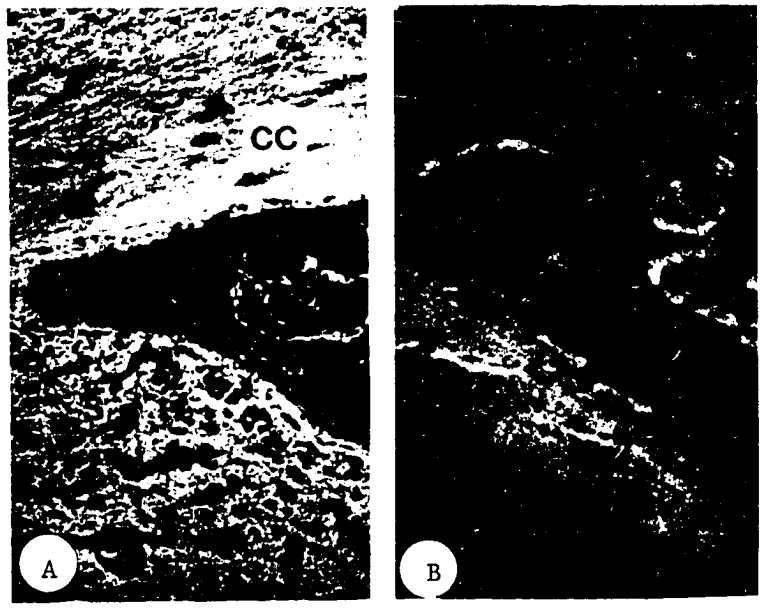

Discussion:

The relative absence of stained material in neuronal somata is an interesting and unexpected finding. In addition to neuronal cell bodies, an absence of stain is also seen in apical dendrites in monkey cortex and cerebellum. Since the cells are sliced open by the sectioning procedure, there is no reason to believe that the Mercury orange does not have access to GSH in the neuronal somata. Moreover, liver cells are easily stained (Figure 14A) and heterogeneity of stain has been reported in other tissues, such as kidney and lung (Asghar et al., 1975). These observations indicate that GSH in brain may be localized to non-neuronal elements, as well as fibrous and terminal regions of neurons.

Asghar et al. (1975) reported that non-specific uptake of Mercury orange by tissue lipids does not take place under the staining conditions employed, which include a post-stain rinse in organic solvent. Therefore, artifactual staining of lipids is not likely to contribute to the staining pattern in brain. This observation is supported by the reduction of staining that occurs after treatment of animals with DEM. It should be noted, however, that quantitative relationships between fluorescence intensity and GSH level have not been established, other than the qualitative observation that decreases in tissue GSH evoked by DEM result in clear decreases in Mercury orange stain.

Griffith and Meister (1979) have reported that freezing of certain tissues prior to biochemical analysis leads to a

marked decrease in chemically-measured GSH, compared to the analysis of unfrozen tissue. However, the brain and liver are listed among the organs resistant to the loss in GSH due to freezing.

The resolution obtained in this study was not high enough to identify non-neuronal cells, such as glia and capillary endothelial cells. The staining observed in the brain may include these cells. Previous studies with radiolabeled precursors suggest that GSH turnover is more rapid in the glial compartment: incorporation of glutamic acid derived from glial glutamine into GSH is more rapid than incorporation of total brain glutamate into GSH (Berl et al., 1961). These data indicate that there is an increased turnover of GSH in the glia as compared to the whole brain, and may suggest a relative enrichment of GSH in glia.

It is of interest that the borders of the epithelial cells in the choroid plexus contain positively-stained material. The brush borders of these cells contain enzymes of the gamma-glutamyl cycle, a transport system that utilizes GSH for membrane transport of amino acids (Orlowski and Meister, 1970). Therefore, increased concentrations of GSH in this region appears reasonable.

GSH appears to be present at relatively low concentrations in neuronal cell bodies in rodent and monkey brain, as well as in apical dendrites of monkey cortex and

cerebellum. The concentration of GSH in cerebrospinal fluid of rats is 0.037 ± 0.007 mM (Rehncrona and Seijo, 1979), which is too low for extracellular fluid to contribute significantly to the observed Mercury orange stain in brain. Morphologic limitations do not allow for a determination of whether terminal regions of neurons are positively stained, and whether neuronal axons contribute to the staining seen in the fiber bundles. However, it would appear that the GSH stain must be present in glia or nerve terminals, or in both. A compartmentalization of GSH within neurons, with accumulation in axon terminals, could reflect an adaptive response of these cells, in which the concentration of GSH is increased in regions where the turnover of GSH is higher. The low levels of GSH in neuronal somata may render these regions susceptible to potentially damaging events, such as the formation of peroxides or exposure to xenobiotic agents, which require GSH for detoxification.

CHAPTER 6: DEPLETION OF BRAIN GSH IN PREWEANLING MICE WITH BUTHIONINE SULFOXIMINE.

Materials and Methods:

Six Swiss-Webster mice at 14 days of age and three 25-30 gm adults (male, Camm Breeders) were injected subcutaneously four times daily at 2.5 hr. intervals, between the hours of 9:00 AM and 4:30 PM, with 20 uL/gm body weight of either 0.20 M L-buthionine-S,R-sulfoximine (L-BSO; 4 mmoles/kg body weight) in 0.10 M sodium chloride (n=3) or with 0.30 M sodium chloride (control, n=3) for three successive days as previously described by Calvin et al. (1986), except for the omission of ether anesthesia. On the fourth experimental day, a single injection was administered at 9:00 AM, and four hours later, the mice were decapitated. The brain, spinal cord, and a section of liver were removed rapidly and rinsed in cold isotonic saline. The brain was divided into left and right hemispheres by a mid-sagittal incision. The right hemisphere was cut into two blocks by mid-coronal incision and processed by histochemistry and fluorescence microscopy for assessment of tissue GSH. The cerebellum and the remainder of the left hemisphere, as well as the spinal cord and liver, were weighed and homogenized in 10 volumes of ice-cold 0.4 M perchloric acid, which contained 40 mg diethylenetriaminepentaacetic acid/L. The homogenates were centrifuged at $4^{o}C$ for 12 min. at 11,000 x g.

Analyses for GSH and cysteine were performed directly

on the acidic supernatants by high performance liquid chromatography (HPLC) with electrochemical detection (BAS Inc., 1982). The HPLC equipment consisted of a pump and injector (Waters Associates, Milford, Mass.), a 25 cm octadecylsilane column with 5 um beads (Altex, Berkley, Ca.), and an electrochemical detector equipped with a sulfhydryl-sensitive mercury/gold amalgam electrode (BAS Inc., West Lafayette, Ind.), which was operated at an oxidizing potential of +0.15 volts vs a Ag/AgCl reference electrode. The mobile phase was 96 parts 0.15 M monochloroacetic acid, pH 3.0, containing 1.25 mM sodium octyl sulfate (paired ion reagent), and 4 parts methanol. A flow rate of 1.0 mL/min was used.

For histochemical analysis of GSH, blocks of tissue from the right hemisphere were placed on a drop of Tissue Tek mounting medium (Miles Lab Inc., Naperville, Ill.) on a cork disk, and immersed in iso-pentane that was pre-cooled in a dry-ice/ethanol slurry. The blocks were then placed in a cryostat and allowed to equilibrate with the chamber temperature ($-20^{o}C$) for 90 min. Staining was performed according to the protocol of Asghar et al. (1975), as modified by Chieco and Boor (1983). Briefly, 8 um thick sections were thawed on glass slides and immediately immersed in 50 uM Mercury orange (Sigma Chem. Co., St. Louis, Mo.) in ice-cold toluene. After 4 min, the slides were rinsed in cold toluene to remove unreacted Mercury orange, and then they were air dried and mounted directly in

non-flourescent medium (Entellan, Merck, Damstadt, W. Germany). Short staining time permits GSH to be distinguished from protein sulfhydryls (Asghar et al., 1975) and cold temperature reduces artifactual staining (Chieco and Boor, 1983). This procedure had been used previously in experiments described in Chapter 5. Slides were viewed by transmission fluorescence microscopy with incident light from a mercury bulb passed through BG-38 and BG-12 excitation filters, and emitted light passed through a K-550 barrier filter (Leitz Wetzlar, Germany).

Results:

HPLC analyses for GSH and cysteine are shown in Table 4. BSO reduced GSH in preweanling mice by 79.6-86.5% in nervous tissues, and an even greater reduction (91.5%) was observed for liver. The concentration of cysteine was slightly reduced in nervous tissue; the reduction was significant only in the cerebellum.

Figure 16 compares sections of brain from control and BSO-treated preweanling mice that were stained for GSH with Mercury orange. The staining pattern of normal brain was described previously (Chapter 5); it is characterized by slight fluorescence within neuronal somata, contrasting with a brightly fluorescent surround. A marked reduction in fluorescence was observed in L-BSO-treated animals in all brain regions. Representative observations are shown for

the frontal cortex of a control (Fig. 16A) and an L-BSO-treated animal (Fig. 16B).

Table 5 shows the effect of repeated subcutaneous injections of L-BSO on GSH and cysteine levels in nervous tissues and liver of adult mice. L-BSO reduced GSH by 17.8-55.9% in nervous tissues and by 61% in liver. L-BSO had no statistically significant effect on the concentration of cysteine in any of the adult tissues.

Table 4. Effect of L-BSO on GSH and cysteine levels in central nervous system and liver of preweanling mice. Brain refers to all tissue remaining after removal of cerebellum. Results are expressed as the mean ± SEM mM (N=6).

	Control		L-BSO			
	mM GSH	mM Cysteine	mM GSH	(% Control)	mM Cysteine	(% Control)
Brain	1.86 ± 0.25	0.040 ± 0.004	0.38 ± 0.06	(20.4)**	0.033 ± 0.0	(82.5)
Cerebellum	1.88 ± 0.28	0.056 ± 0.006	0.31 ± 0.05	(16.5)**	0.039 ± 0.0	(69.6)*
Spinal Cord	1.33 ± 0.19	0.067 ± 0.067	0.18 ± 0.03	(13.5)**	0.039 ± 0.0	(58.2)
Liver	2.93 ± 0.34	0.105 ± 0.037	0.25 ± 0.02	(8.5)**	0.188 ± 0.019	(179.0)

* $p < 0.05$

** $p < 0.001$

Figure 16. Reduction of Mercury orange staining in brain following depletion of GSH by pretreatment with L-BSO.

In panel A, a section of frontal cortex from a control preweanling mouse was stained with Mercury orange and viewed by transmission fluorescence microscopy. Mercury orange-reactive material appears as bright orange fluorescent granular deposits. Neuronal somata can be visualized due to their relative lack of fluorescent material. Panel B shows a section of frontal cortex from an animal that was pretreated with L-BSO. A marked reduction in fluorescent material is noted; the distribution of fluorescence appears to be similar to controls. Magnification x 350.

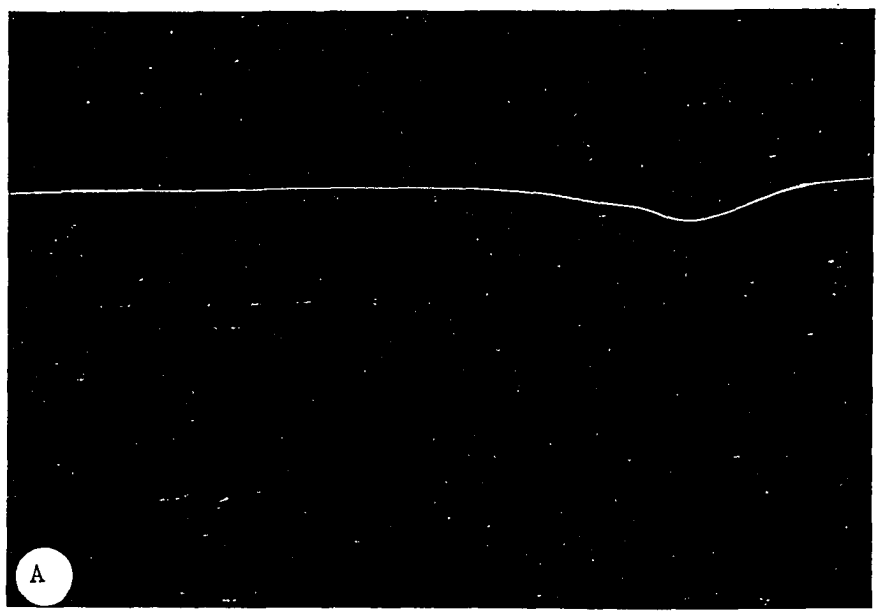

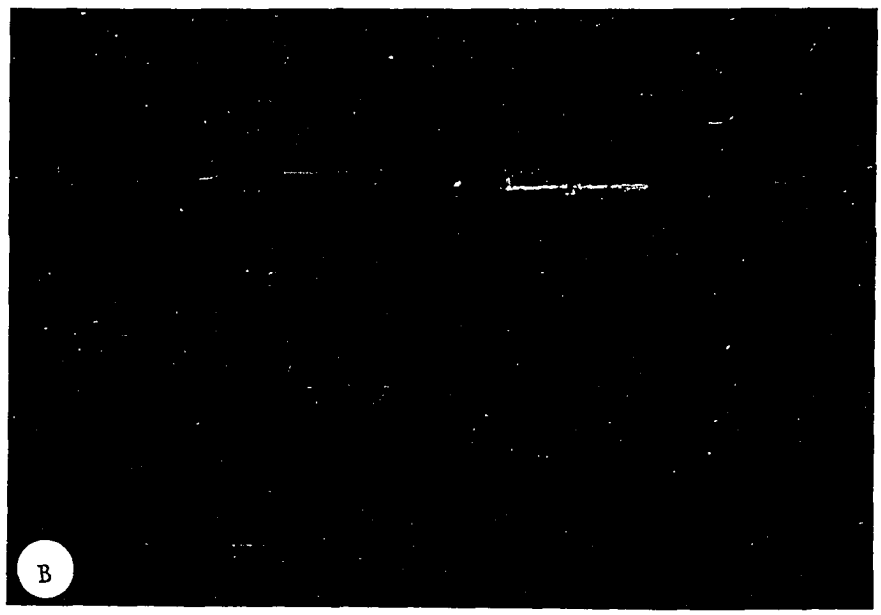

Table 5. Effect of L-BSO on GSH and cysteine levels in central nervous system and liver of adult mice. Brain refers to all tissue remaining after removal of cerebellum. Results are expressed as the mean ± SEM mM (N=3).

	Control		L-BSO	
	mM GSH	mM Cysteine	mM GSH (% Control)	mM Cysteine (% Control)
Brain	1.06 ± 0.08	0.046 ± 0.004	0.75 ± 0.06 (70.8)*	0.040 ± 0.003 (86.9)
Cerebellum	1.01 ± 0.03	0.065 ± 0.008	0.83 ± 0.05 (82.2)*	0.058 ± 0.007 (89.2)
Spinal Cord	0.68 ± 0.07	0.039 ± 0.010	0.30 ± 0.00 (44.1)**	0.036 ± 0.004 (92.3)
Liver	5.23 ± 0.65	0.081 ± 0.008	2.04 ± 0.33 (39.0)*	0.063 ± 0.005 (77.8)

* $p < .05$

** $p < .001$

Discussion:

This study shows that levels of GSH in mouse brain are lowered when L-BSO is administered by repeated subcutaneous injections to adults, and that this effect is greatly enhanced when the drug is given during the neonatal period. The increased susceptibility of neonates compared to adults may reflect increased permeability of the blood-brain barrier in neonates. Alternatively, perhaps the developing nervous system exhibits a higher turnover of GSH compared to adults.

L-BSO also caused a modest reduction in cysteine in the central nervous system of preweanling mice. The availability of intracellular cysteine may be rate limiting for GSH synthesis, as this amino acid is present intracellularly at concentrations below the Km for gamma-glutamylcysteine synthetase (0.35 mM, Orlowski and Karkowski, 1976). In studies with cultured cells, Brodie and Reed (1985) found that the presence of cysteine in the feeding medium is a poor source for cellular synthesis of GSH, but that cellular uptake of cystine with subsequent reduction to cysteine is more effective. BSO (D,L- and L-) causes less cystine to be taken up cultured cells. This effect appears to be due to both diminished intracellular utilization of cysteine by gamma-glutamylcysteine synthetase and also to direct effects on cystine uptake (Brodie and Reed, 1985). These factors may be responsible for the mild decreases in cysteine seen in brain. The slight decrease in

cysteine compared to the marked decrease in GSH seen in the nervous tissue of preweanling mice exposed to L-BSO suggests that the drug is lowering GSH levels mainly by inhibiting gamma-glutamylcysteine synthetase rather than interfering with the accumulation of intracellular cysteine.

Histochemical assessment of GSH by fluorescence microscopy with Mercury orange verifies the loss of GSH throughout the brain. In control neonates, the staining pattern is the same as that previously reported for adult mice and other species (Chapter 5). It was suggested previously that the Mercury orange stain in brain is distributed in glia, nerve terminals, and axons (see Chapt. 5). It is known that GSH turnover in glia is rapid, compared to neurons (Berl et al., 1961); therefore, glia should be more sensitive than neurons to L-BSO-mediated depletion of GSH. With regard to neuronal somata, the sparse fluorescence normally seen there makes it difficult to evaluate the effects, if any, of L-BSO.

Treatment of preweanling mice with multiple injections of L-BSO represents an experimental approach for lowering GSH in brain in vivo. Diethylmaleate, a substrate for GSH-S-transferase, also lowers brain GSH (Richardson and Murphy, 1975; Chapter 5), but the reduction is relatively small and it is associated with toxicities due to non-specific interactions (Meister, 1985). The use of L-BSO in neonatal rodents may permit the evaluation of the biologic roles for

GSH in the nervous system. In this regard, the hind limb paralysis that has been reported in some neonatal mice after L-BSO treatment (Calvin et al., 1986) may derive from GSH depletion in the nervous system. It is noteworthy that patients with gamma-glutamylcysteine synthetase deficiency have reduced levels of GSH in red cells, white cells, and skeletal muscle, and exhibit a clinical syndrome of hemolytic anemia, spinocerebellar degeneration, peripheral neuropathy, myopathy, and aminoaciduria (Konrad et al., 1972; Richards et al., 1974). L-BSO administration to preweanling mice represents an experimental model to study aspects of this disease. Similarly, L-BSO may prove useful in evaluating the roles of GSH and GSH peroxidase in protecting the nervous system from oxidative stress.

Chapter 7: GSH AND GSSG IN ISCHEMIC BRAIN.

Materials and Methods:

Production of unilateral cerebral ischemia.

Left hemispheric cerebral ischemia was produced by the method of Lust et al. (1975). Male gerbils (50-70 gm; Tumblebrook Farms, Port Washington, N.Y.) were lightly anesthetized with approximately 35 mg methohexital i.p. Animals were unconscious, but could breathe unassisted. The level of anesthesia was tested by a foot pinch test. Occasionally, the dose of anesthetic had to be supplemented when an animal showed a pain response.

Surgery was initiated by a midline incision through the skin of the paratracheal region; the left common carotid artery was exposed and isolated from the left vagus nerve and the left jugular vein by blunt dissection. Blood loss during the procedure was minimal. Two sutures were placed around the carotid, but were not ligated until the animal had partially recovered from the anesthetic. The surgical wound was closed with autoclip staples (Clay Adams). In sham operated controls, the animals were anesthetized and the left carotid artery was isolated. Sutures were placed around the artery, but they were not ligated prior to surgical closure.

After surgery, animals were observed for behavioral signs of stroke which included: ipsilateral hemiparesis, ptosis, and rotational behavior (Kahn, 1972). Only those animals exhibiting all three signs were included in this

study. Some animals with strokes also exhibited seizure activity. Tissue processing:

At 2 hr., 4 hr., and 8 hr. after carotid ligation, those gerbils exhibiting signs of stroke were decapitated by guillotine, and the cerebra were removed and rinsed in ice-cold isotonic saline. For histochemical studies, the cerebra were divided into rostral and caudal halves by a mid-coronal incision. These blocks were mounted and frozen as described in Chapter 5. For biochemical studies, the cerebra were divided into right and left hemispheres by a mid sagittal incision; the striata and hippocampi from each side were removed by blunt dissection and placed in ice-cold isotonic saline. The isolated regions were then weighed and homogenized in 0.5 mL of ice-cold 0.4 M perchloric acid containing: 40 mg/L DTPA, 0.1 mM ascorbic acid, 5 mg/L N-acetyl cysteine (an internal standard for sulfhydryl compounds), 0.1 mg/L alpha-methyl dopamine (an internal standard for dopamine), and 0.1 mg/L 4-hydroxy,3-methoxyphenylproprionic acid (HMPPA, internal standard for DOPAC and HVA). The time interval between decapitation and homogenization was less than 10 min. The precipitated protein was removed by centrifugation at 11,000 x g for 15 min. at $4^{o}C$.

Biochemical analyses of GSH and GSSG:

GSH in the acidic supernatant was assayed by HPLC with electrochemical detection as described in Chapter 4.

Cysteine was also quantitated with this system. Peak heights and retention times of standard solutions were compared to experimental samples and used to calculate tissue concentrations of GSH and cysteine. Observed concentrations were corrected for the recoveries of the internal standard, N-acetylcysteine. A sample chromatogram appears in Figure 34 of Appendix I.

GSSG was analyzed in the acidic supernatant by an enzymatic assay with GSSG reductase. The method is based on the rate of enzymatic reduction of the mixed disulfide formed from GSH and DTNB (slow rate limiting step) following the rapid reduction of GSSG (Teitze, 1969). Prior to analyses, endogenous GSH is removed by Sep-Pak (Waters Associates, Milford, Mass.) chromatography (Adams et al., 1983). Details of this protocol are described in Chapter 4.

Histochemical analyses of GSH:

GSH histofluorescence was produced using a variation of the modified protocol (Chieco and Boor, 1983) of Asghar et al. (1975), as described in Chapter 5.

Analyses of amino acids and peptides:

Tissue levels of free amino acids and peptides were determined on aliquots of the deproteinized supernatants from which the PCA was removed by the addition of 5 N KOH until the pH was approximately 5.0. The precipitated $KClO_4$ was pelleted by centrifugation at 11,000 x g for 2 min. at

4°C. The resulting supernatant was subjected to HPLC with a lithium acetate gradient mobile phase and an ion-exchange column (Pickering Laboratories application note). Amino acids and peptides were quantitated by post-column derivitization with orthophthalaldehyde, followed by fluorescence detection (Roth, 1971).

Effect of dopamine levels and metabolism on GSH changes during ischemia:

Some animals were injected with alpha-methyl-para-tyrosine methyl ester (AMPT), 400 mg/kg i.p. 6 hrs. prior to carotid ligation, or with pargyline, 100 mg/kg i.p. 12 hrs. and again 1 hr. prior to carotid ligation. AMPT lowers brain levels of dopamine by inhibiting tyrosine hydroxylase. Pargyline inhibits monoamine oxidase (MAO); a dose of 100 mg/kg will inhibit both MAO-A and MAO-B. Levels of GSH were determined as described above. In addition, levels of DA, DOPAC, and HVA were determined by HPLC with electrochemical detection as described in Chapter 8.

Results:

Mercury orange staining and histofluorescence examination were performed on sections of brain from sham-operated gerbils, and sections that were obtained from animals showing behavioral signs of stroke. Gerbils with stroke were examined at 2 hr., 4 hr., and 8 hr. after carotid ligation. The staining characteristics of normal gerbil brain are similar to other species and are described

in Chapter 5. Stained sections of brain from sham-operated controls could not be distinguished from normal gerbils. In gerbils exhibiting behavioral signs of stroke, there were consistent alterations in the staining characteristics of brain in the left (ischemic) hemisphere, compared to the right (control) hemisphere, at 4 hrs. and 8 hrs. after carotid ligation. It should be emphasized that the brain slice contained both the left (ischemic) and right (control) hemispheres. Thus, the experimental and control hemispheres were processed simultaneously for histofluorescence.

The ischemia-induced alterations included: a) a reduction in the fluorescent intensity in those regions which normally contain fluorescent material, b) an increase in fluorescent material in neuronal somata, and c) a reduction in the granular nature of the fluorescent material. In the ischemic hemisphere, these changes were noted consistently in the striatum and hippocampus. The cortex was variably affected; when changes were noted in the cortex, they appeared in those portions which were contiguous with striatum and hippocampus. Similar changes were observed in corpus callosum contiguous to the striatum and hippocampus. Other areas of brain in the ischemic hemisphere were spared from these alterations.

Figure 17 shows the control (Panels A and B) and ischemic (Panels C and D) striata from a stroked animal at 4

hours after carotid ligation. In Panel A, the control striatum is viewed by dark field microscopy to highlight the fiber bundles that course through the striatum. When the same field is viewed by fluorescence microscopy (Panel B), the fiber bundles which contain fluorescent material, can be discerned. Within the striatum proper, fluorescent material can be seen around relatively unstained regions which have the shape and distribution of neuronal somata. In the ischemic striatum, fiber bundles are easily visible by dark field microscopy (Panel C), but they have lost much of their Mercury orange fluorescent intensity (Panel D), and can barely be discerned from the background. In addition, some neuronal somata appear to contain small amounts of fluorescent material.

Figure 17. Mercury orange staining of a section of gerbil brain containing control and ischemic striata, 4 hr. after left carotid ligation.

Dark field illumination highlights the fiber bundles (bright spherical structures) that course through the control (Panel A) and ischemic (Panel C) striata. When these same fields are viewed by transmission fluorescence microscopy, the fiber bundles in the control striatum (Panel B) can be clearly identified as regions of intense Mercury orange positive staining (appearing white in the photograph). Neuronal cell bodies are identified by their lack of flourescent staining. In the ischemic striatum (Panel D), the fiber bundles have lost much of their fluorescence, and can no longer be differentiated from the surround. In addition, some neuronal cell bodies appear to contain small amounts fluorescent material. Magnification x 440.

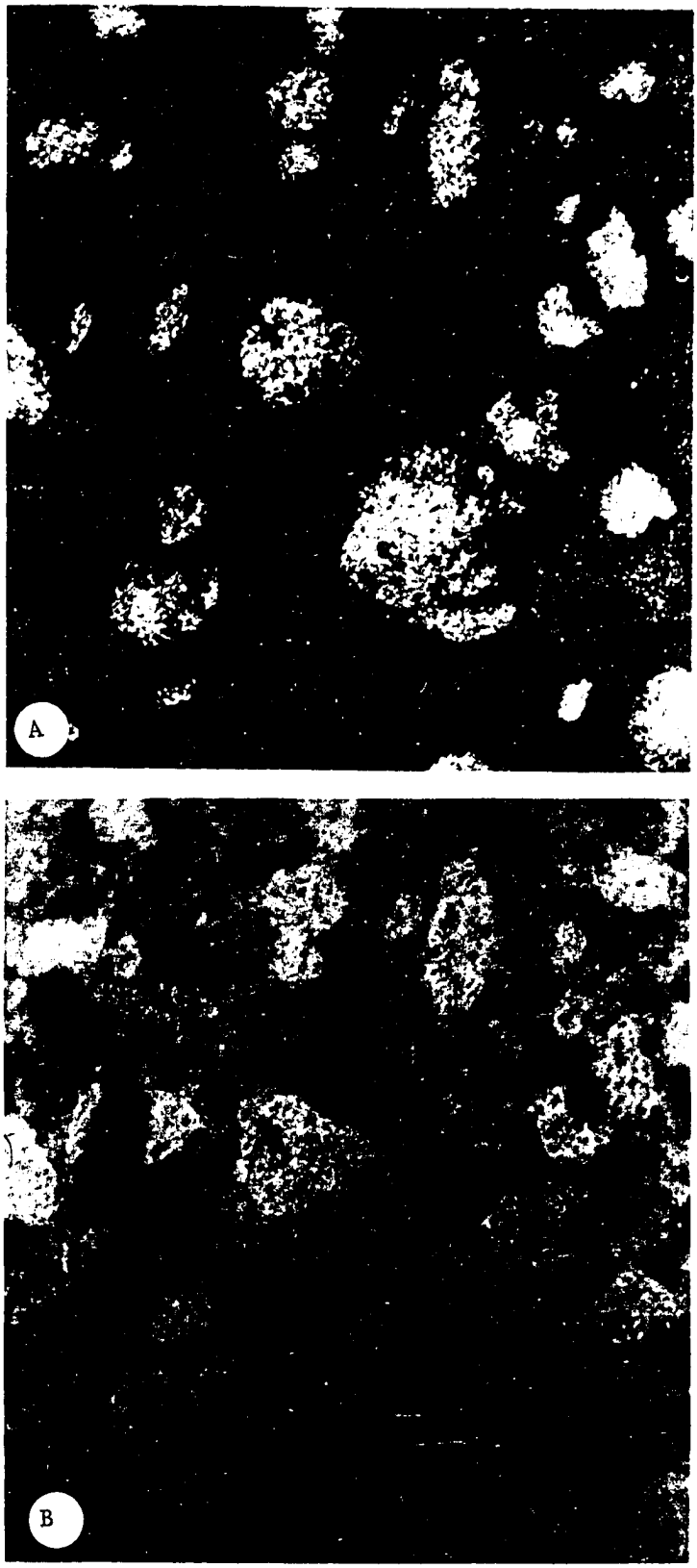

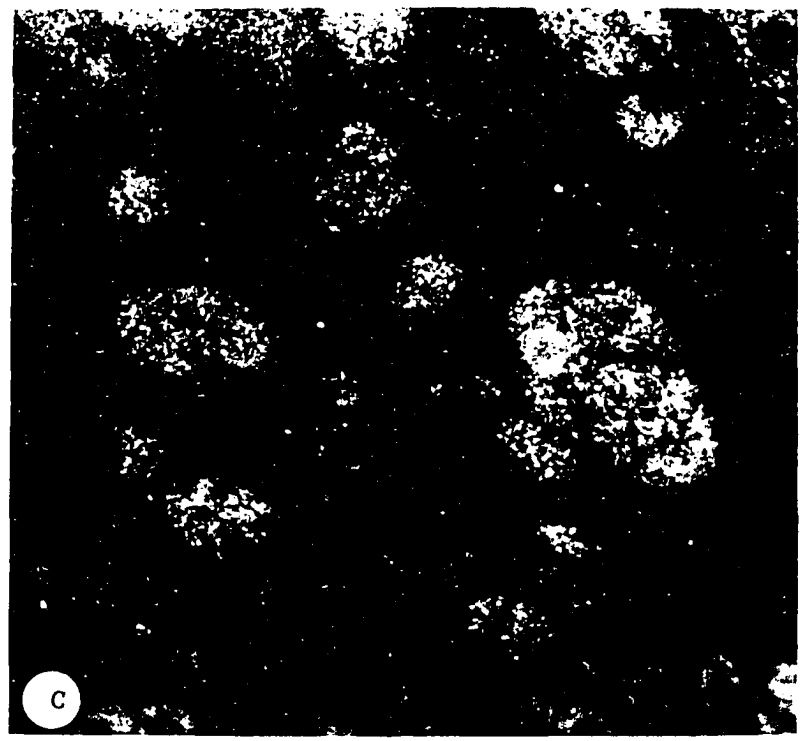

The appearance of fluorescence in neuronal somata is more clearly demonstrated in Figure 18. Panel A shows the dentate gyrus from the control side of the brain from the same animal depicted in Figure 17; neuronal somata are seen as relatively unstained regions surrounded by brightly fluorescent material. On the ischemic side, the neuronal somata of the dentate gyrus contain significant amounts of fluorescent material and are more difficult to distinguish from the surround.

In Figure 19, similar changes are noted in the ischemic pyramidal cell layer from the same gerbil. The arrows indicate the demarcation between the hippocampus and overlying cortex. In this animal, the staining characteristics of the cortex were less affected by ischemia than were the hippocampus or striatum, as evidenced by the maintenance of stain intensity and granularity, when compared to control. However, there appears to be somewhat more fluorescent material in cortical neuronal somata of the ischemic side of the brain compared to the control side. The ischemia-induced changes in Mercury orange staining at 8 hr. were similar to, if not more pronounced, than those seen at 4 hr. However, changes were not particularly apparent at 2 hr. (not shown). At all time points, the right (control) hemisphere was indistinguishable in staining characteristics from sham-operated brains (right or left hemispheres).

Figure 18. Mercury orange staining of a section of gerbil brain containing both the control (Panel A) and ischemic (Panel B) dentate gyrus.

The section was viewed by transmission fluorescence microscopy. Neuronal somata within the dentate gyrus of the control hemisphere are dark and contain little fluorescent material when compared to the surround. In the ischemic hemisphere, the neuronal somata of the dentate gyrus contain significant amounts of flourescent material; the intensity of the stain in the remaining structures is reduced when compared to control. Magnification x 175.

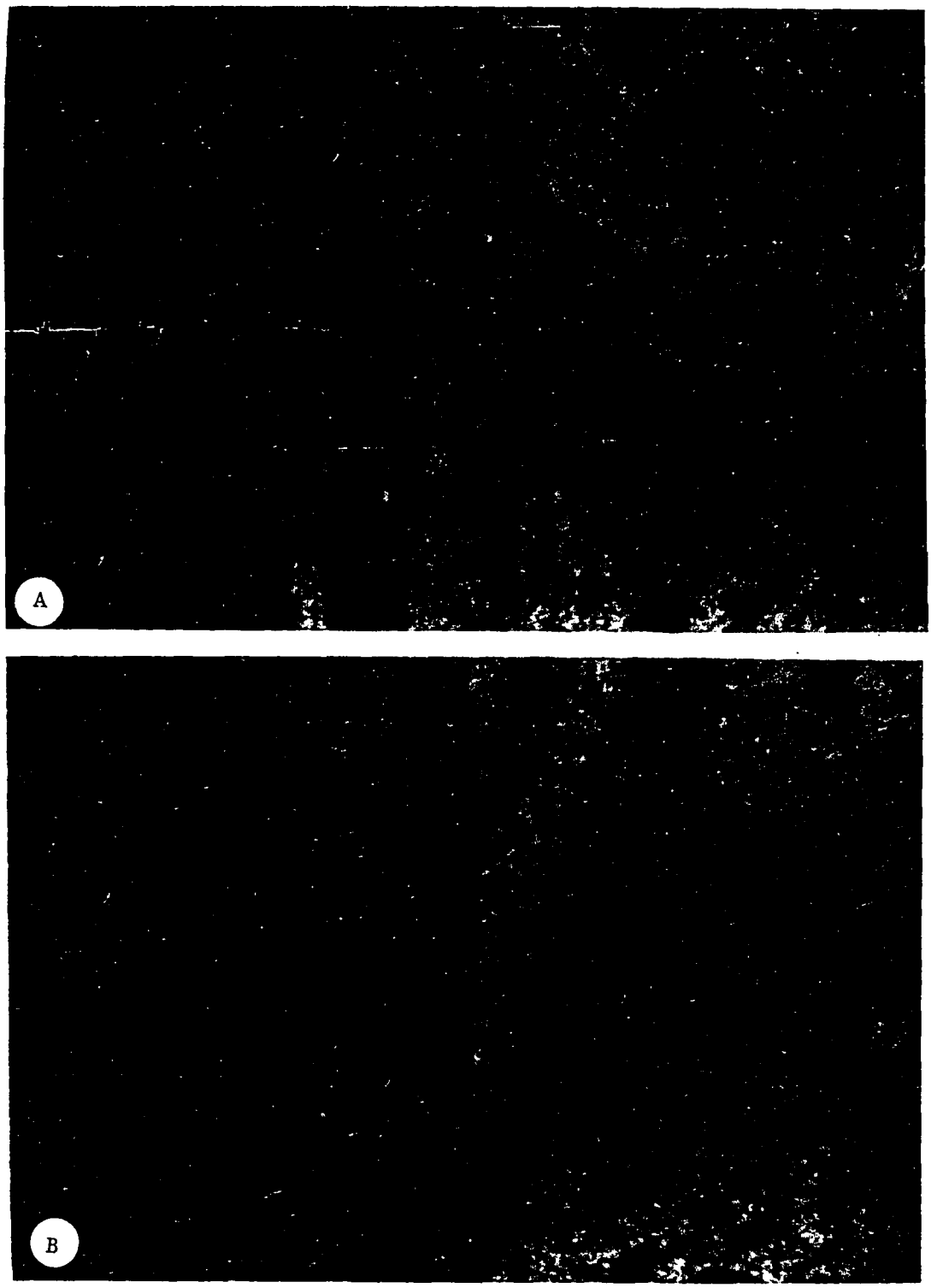

Figure 19. Mercury orange staining of a section of gerbil brain containing both the control (Panel A) and ischemic (Panel B) hippocampus and overlying cortex.

The section was viewed by transmission fluorescence microscopy. In the control hippocampus, the neuronal somata in the pyramidal layer appear as a dark band, containing very little fluorescent material. The demarcation between hippocampus and overlying cortex is marked by arrows. Cortical neuronal somata are relatively unstained, and are outlined by the brightly fluorescent surround. In the ischemic hemisphere, the hippocampus has lost some fluorescent intensity and granularity; however, the neuronal somata within the pyramidal layer contain significant amounts of fluorescent material. The ischemic cortex appears relatively unaffected; however, some increase in fluorescent material within cortical neuronal somata is evident. Magnification x 175.

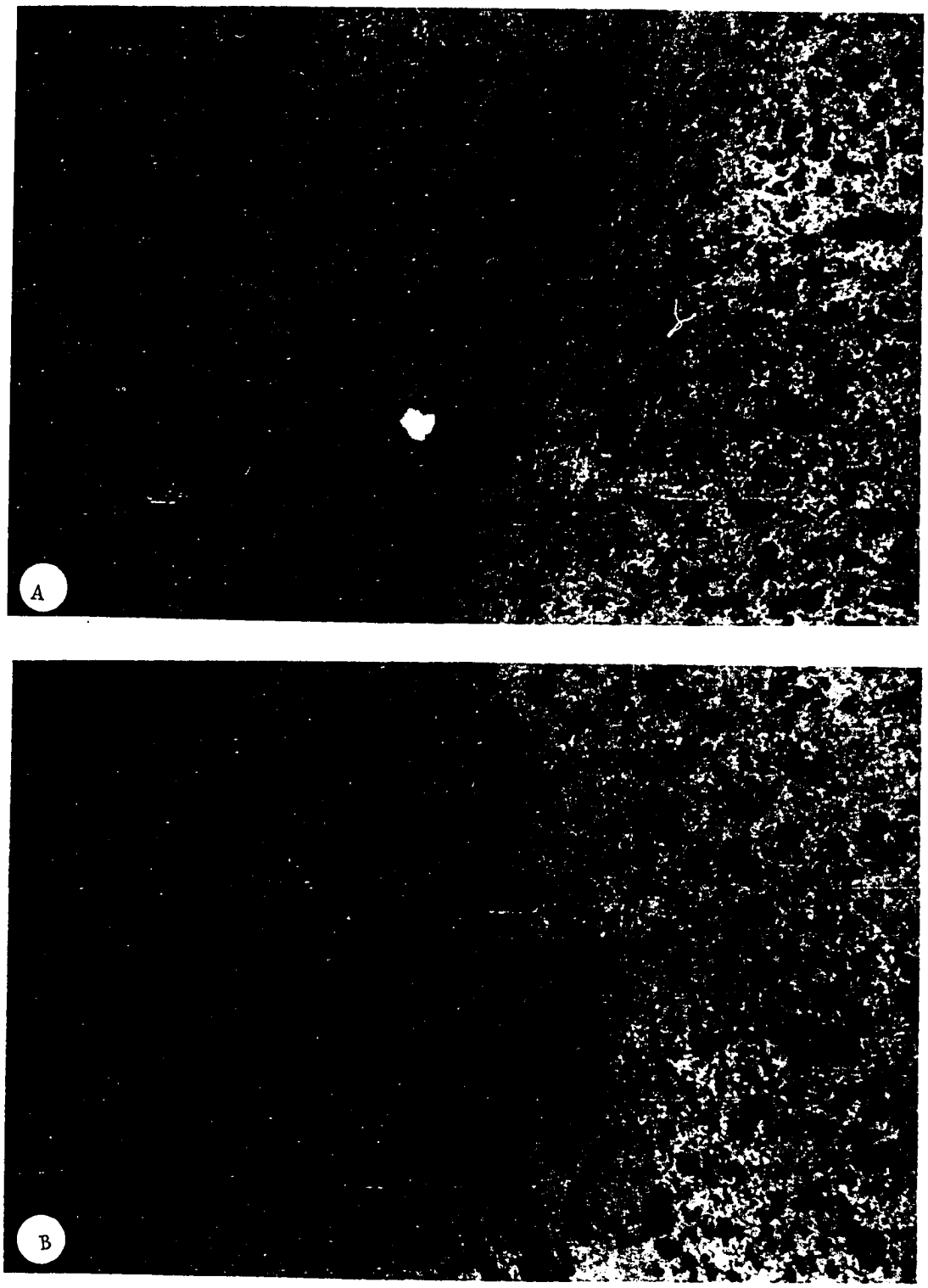

Table 6 lists the mean (+ SD) GSH levels in the left and right striata and hippocampi of control animals and animals exhibiting signs of stroke. Assays were conducted at 2 hr., 4 hr., and 8 hr. after left carotid artery ligation. The control group is comprised of sham-operated animals that were sacrificed at 2 hr. (n=3), 4 hr. (n=3), and 8 hr. (n=2) after surgery. There was no significant difference in GSH level within these groups and , therefore, they were pooled. The data in Table 6 were analyzed by paired T-test to compare the ischemic (left) to control (right) GSH levels for each animal. In striata, there was no significant difference in GSH between the left and right sides in sham-operated controls. The left hippocampi of sham-operated controls contained slightly elevated levels of GSH when compared to the right side. At 2 hr. after carotid ligation, the GSH on the ischemic left side was significantly less than the control right side for both striata and hippocampi. This left to right difference persisted and increased in magnitude at 4 hr. and 8 hr. in both striata and hippocampi.

Figure 20 shows the changes in GSH concentration with time in left and right striata and hippocampi. In these analyses, comparisons are made to sham-operated controls, rather than to the control hemisphere in an animal with with stroke, as in Table 6. When compared to sham-operated controls (i.e. zero time values), there were no significant decreases in GSH concentrations at 2 hr. in left striata or

left hippocampi. At both 4 hr. and 8 hr., significant decreases in GSH levels were seen in left striata and hippocampi, compared to sham-operated controls. On the right side, there was a slight but significant increase in GSH concentration compared to controlat 2 hr. after ligation in hippocampi, but not striata, and a slight but significant decrease in GSH concentration at 4 hr. after ligation in both striata and hippocampi. By 8 hr., the levels of GSH in right striata and hippocampi had returned to levels found in the sham-operated controls.

Table 6: GSH (mM) in striata and hippocampi at 2 hr., 4 hr., and 8hr. after occlusion of the left common carotid artery.

		STRIATA		HIPPOCAMPI	
		Right	Left	Right	Left
SHAM (8)	mean	1.59	1.58	1.27	1.46*
	SD	0.09	0.22	0.22	0.24
2 hr. (8)	mean	1.71	1.51*	1.59	1.29**
	SD	0.12	0.26	0.10	0.20
4 hr. (7)	mean	1.11	0.71**	1.00	0.55**
	SD	0.16	0.24	0.12	0.14
8 hr. (6)	mean	1.36	0.74**	1.42	0.52**
	SD	0.40	0.26	0.29	0.20

* $p<0.05$
** $p<0.005$

The number of gerbils is in parenthesis. Sham-operated animals were decapitated at 2 hr., 4 hr., or 8 hr. after surgery; there was no effect of length of time after surgery on GSH concentration in this group. All other values are for animals that exhibited behavioral signs of stroke and were decapitated 2 hr., 4 hr., or 8 hr. after surgery. The concentrations of GSH in the left striata and hippocampi are compared to the concentrations in the right striata and hippocampi by paired T-test analyses.

Figure 20. Changes in GSH in control and ischemic striata and hippocampi with time after left common carotid ligation.

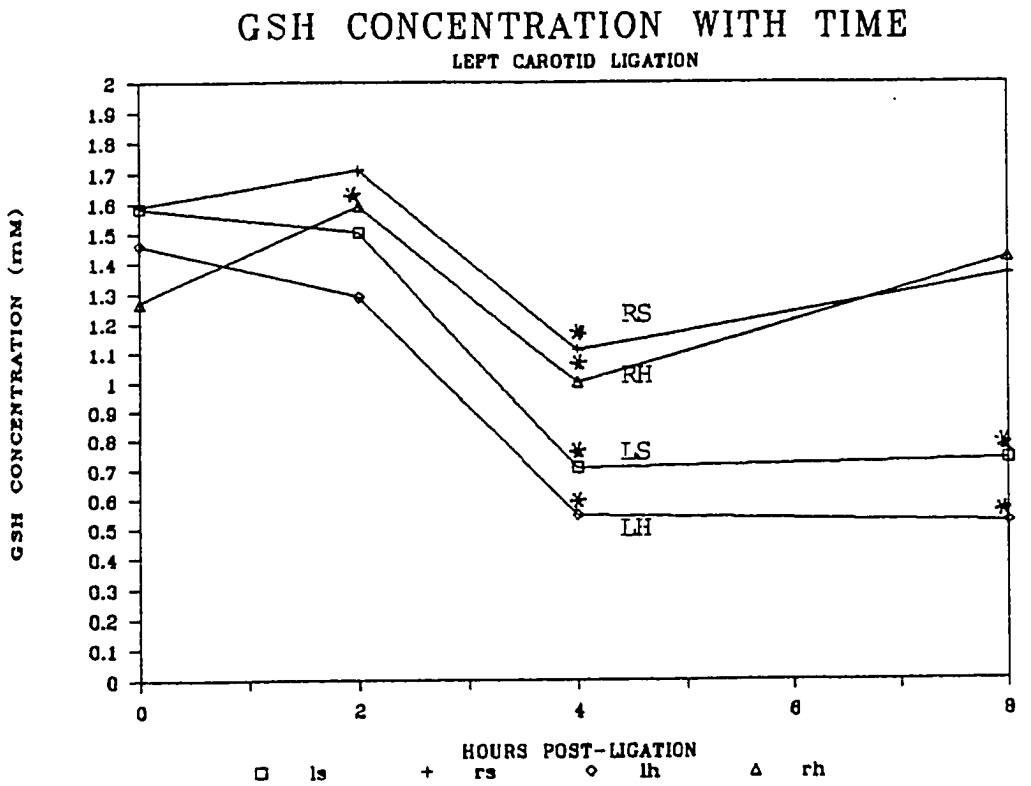

left striatum (LS)

right striatum (RS)

left hippocampus (LH)

right hippocampus (RH)

*Significantly different from 0 time, alpha=0.05

This figure depicts the same data listed in Table 6. The concentration of GSH in left or right striata and hippocampi are compared to sham-operated controls (i.e., zero time values). Assays were performed in gerbils exhibiting behavioral signs of stroke at 2 hr., 4 hr., and 8 hr. after left common carotid artery ligation. Comparisons were conducted by one-way analyses of variance.

Analyses of tissue samples for GSSG (Table 7) showed no significant changes in the ischemic striata or hippocampi at 2 hr., but at both 4 hr. and 8 hr. after ligation, the concentration of GSSG was significantly lower in both regions when compared to controls.

Table 8 lists the mean (± SD) cysteine concentration in left and right striata and hippocampi of sham-operated animals and animals exhibiting signs of stroke after arterial ligation. Similar to the levels of GSH, there was no left to right difference in cysteine concentration in striata of sham-operated controls, but the left hippocampi contained slightly more cysteine than the right. However, at 2 hr., 4 hr., and 8 hr. after arterial ligation, there was a marked elevation in cysteine concentration in the left ischemic side compared to the right control side in both striata and hippocampi.

Table 7: GSSG (uM) in striata and hippocampi at 2 hr., 4 hr., and 8 hr. after occlusion of the left carotid artery.

		STRIATA		HIPPOCAMPI	
		Right	Left	Right	Left
SHAM (4)	mean	5.1	4.7	4.8	5.6
	SD	0.9	1.1	1.2	1.7
2 hr. (4)	mean	3.0	2.3	3.8	2.4
	SD	0.8	0.6	1.2	0.4
4 hr. (4)	mean	4.2	2.3*	5.1	2.4*
	SD	0.6	0.3	1.4	0.2
8 hr. (3)	mean	4.8	3.0*	4.5	2.1*
	SD	0.8	0.4	1.0	0.3

* $p<0.05$

The number of animals is in parenthesis. Sham-operated animals were decapitated at 2 hr. after surgery. All other points represent animals that exhibited behavioral signs of stroke after ligation of the left common carotid artery and were decapitated 2 hr., 4 hr., or 8 hr. after surgery. The concentrations of GSSG in the left striata and hippocampi are compared to the concentrations in the right striata and hippocampi by paired T-test analyses.

Table 8: Cysteine (uM) in striata and hippocampi at 2 hr., 4 hr., and 8 hr. after occlusion of the left carotid artery.

		STRIATA		HIPPOCAMPI	
		Right	Left	Right	Left
SHAM (8)	mean	62.8	61.1	42.6	50.9*
	SD	19.5	21.3	16.6	20.9
2 hr. (8)	mean	56.4	247.0*	40.0	273.9*
	SD	23.2	173.3	17.1	244.6
4 hr. (7)	mean	60.9	521.1**	43.0	545.8**
	SD	10.7	265.2	5.9	260.3
8 hr. (6)	mean	122.8	616.2**	84.5	663.5*
	SD	100.8	327.0	41.4	370.4

* $p<0.05$
** $p<0.005$

The number of animals is in parenthesis. Sham-operated animals were decapitated at 2 hr., 4 hr., or 8 hr. after surgery; there was no effect of length of time after surgery on cysteine concentration in this group. All other points represent animals that exhibited behavioral signs of stroke after ligation of the left common carotid artery and were decapitated 2 hr., 4 hr., or 8 hr. after surgery. The concentrations of cysteine in the left striata and hippocampi are compared to the concentrations in the right striata and hippocampi by paired T-test analyses.

Figure 21 shows changes in cysteine concentration with time in left and right striata and hippocampi of stroked animals when compared to sham-operated controls. At 2 hr. after ligation, ischemia induced elevations in cysteine concentrations were apparent in both striata and hippocampi, but they did not achieve statistical significance. The levels of cysteine were increased further and significantly at 4 hr. and 8 hr. on the ischemic side in both striata and hippocampi. Levels of cysteine on the control side were not different from sham-operated controls at 2 hr. and 4 hr. after carotid ligation in both striata and hippocampi. The levels of cysteine were slightly but significantly elevated in the control (non-ischemic) right striata and hippocampi at 8 hr. after ligation when compared to sham-operated controls.

Figure 21. Changes in cysteine in control and ischemic striata and hippocampi with time after left common carotid ligation.

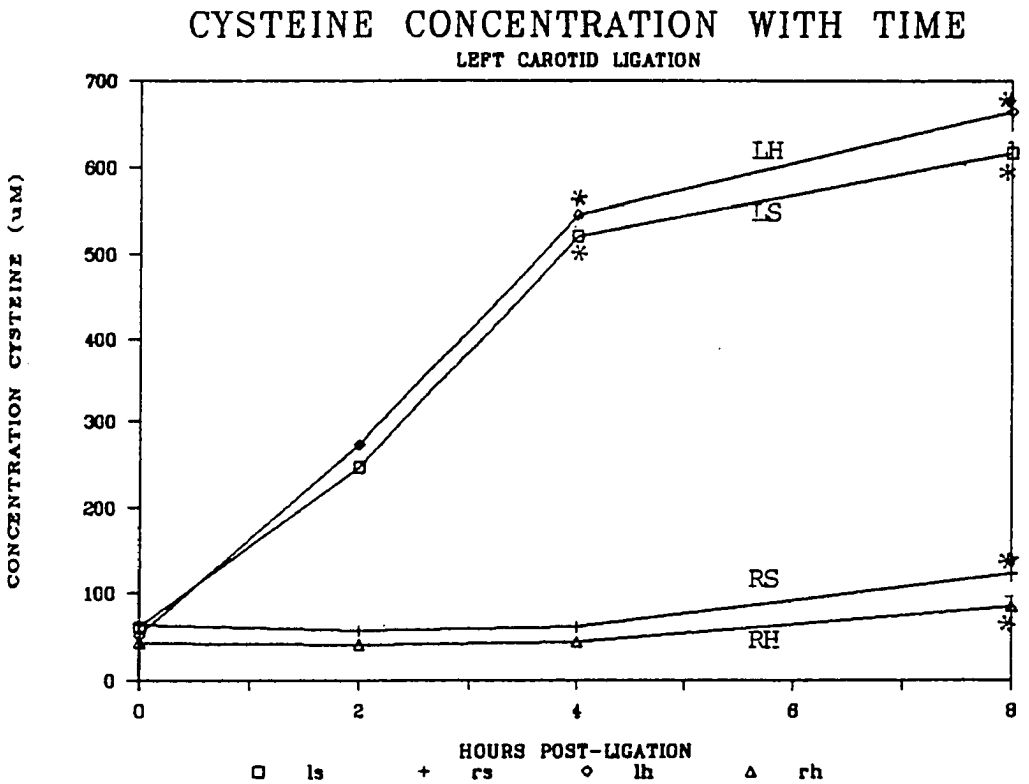

left striatum (LS) left hippocampus (LH)

right striatum (RS) right hippocampus (RH)

*Significantly different from 0 time, alpha=0.05

This figure depicts the same data listed in Table 8. The concentration of cysteine in left or right striata and hippocampi are compared to sham-operated controls (i.e., zero time values). Assays were performed in gerbils exhibiting behavioral signs of stroke at 2 hr., 4 hr., and 8 hr. after left common carotid artery ligation. Comparisons were conducted by one-way analyses of variance.

HPLC analyses of some free amino acids was performed on samples of ischemic and control striata in 3 animals exhibiting signs of stroke 4 hr. after carotid ligation (Figure 22). Although there were left to right differences in the mean levels of several amino acids, only the elevation of histidine in the ischemic striata was statistically significant when analyzed by paired T-test analysis. A significant increase in cysteine had been noted earlier (Figure 21).

Pre-treatment of animals with AMPT diminished levels of dopamine and metabolites to an undetectable range in striata and hippocampi (dopamine < 0.2 ug/gm, DOPAC < 0.1 ugm/gm, and HVA < 0.25 ug/gm wet weight), but had no protective effect on the ischemia-induced depletion of GSH at 4 hr. in both striata and hippocampi (Table 9). Inhibition of monoamine oxidase by pretreatment with pargyline also failed to inhibit the ischemia- induced depletion of GSH in striata and hippocampi (Table 9).

Figure 22. Concentrations of some amino acids in control and ischemic striata, 4 hr. after left carotid artery ligation.

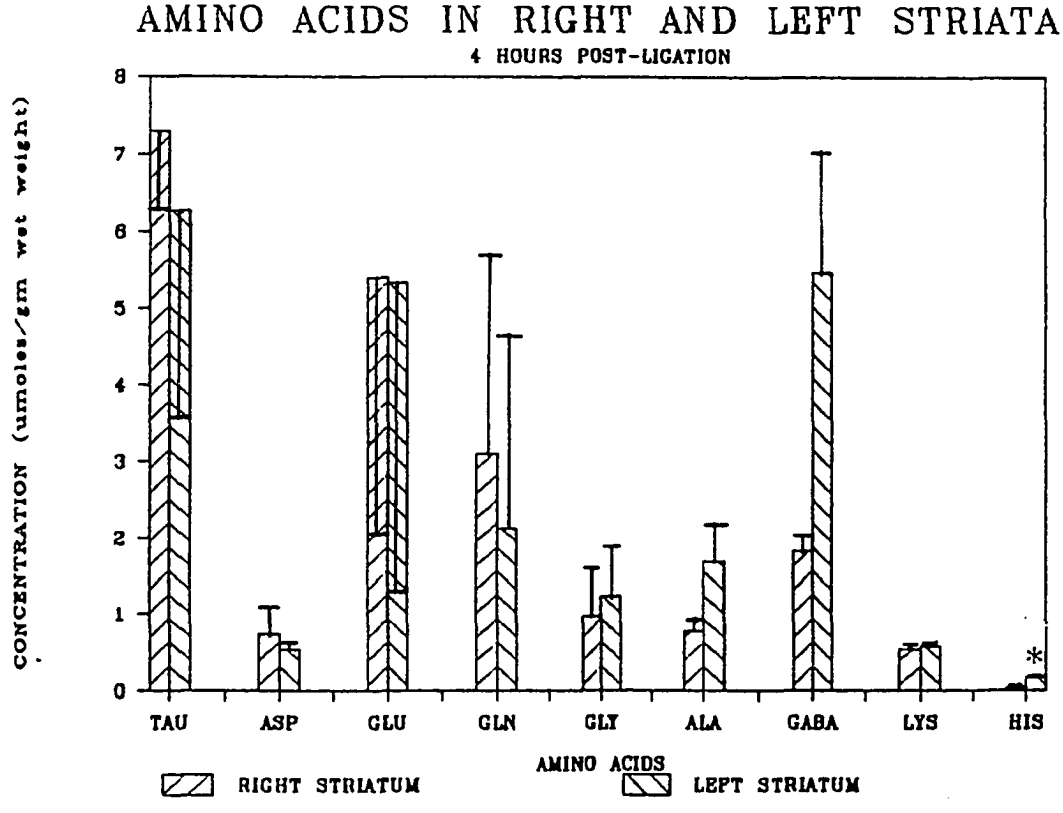

*$p<0.01$

Levels (mean ± SD) of selected amino acids were measured in the striata of gerbils (n=3) exhibiting behavioral signs of stroke at 4 hr. after ligation of the left common carotid artery. Comparisons between the left and right striata were made by paired T-test analyses.

Table 9. Effects of alpha-methyl-para-tyrosine methyl ester (AMPT) or pargyline (Parg) on ischemia-induced decreases in GSH at 4 hr. after ligation of the left carotid artery. The number of animals is in parenthesis. Values are the mean ± SD.

	% Control GSH (Left/Right x 100)	
Pretreatment	Striatum	Hippocampus
none (7)	63.7 ± 20.6	55.3 ± 17.6
AMPT (3)	52.7 ± 5.5	52.6 ± 4.9
Parg (3)	50.7 ± 18.2	43.3 ± 9.2

Discussion.

The results of this study demonstrate that unilateral hemispheric ischemia produced by irreversible left common carotid artery ligation in the Mongolian gerbil leads to histochemical alterations in mercury orange staining, measured reductions in GSH, and elevations in free cysteine in the ipsilateral striatum and hippocampus. The decrease in GSH was apparent at 2 hr., when compared to the contralateral (control) side, and persisted at 4 hr. and 8 hr. after arterial ligation. There was no concomitant increase in GSSG at any time point studied. Oxidative stress, due to the formation of peroxides and oxygen radicals, has been suggested as an initiating factor in ischemia-induced tissue damage (Demopolus et al. 1977). Normally, elevation in tissue peroxides is associated with elevation of tissue levels of GSSG (Sies and Cadenas, 1985). Rehncrona et al. (1980) demonstrated that in vitro lipid peroxidation, induced by incubating cortical tissue homogenates with ferrous sulfate and ascorbate, was associated with elevations in GSSG. A decrease in GSH without a corresponding elevation in GSSG, as reported in this study, has been demonstrated in other models of cerebral ischemia (Folbergrova et al., 1979; Cooper et al., 1980; Rehncrona et al., 1980). These results provide no evidence for peroxide-mediated oxidation as the cause of ischemia-induced depletion of GSH. The decreased level of GSSG that was seen after 4 hr. and 8 hr. of ischemia may be

the result of similar processes operative in the ischemia-induced decrease in GSH. Brain ATP has been shown to be depleted during ischemia (Lowry et al. 1964), and it has been postulated that ischemia-mediated decreases in GSH concentration reflect an imbalance between synthesis and degradation (Rehncrona et al. 1980); synthesis of GSH requires 2 molecules of ATP (reviewed by Orlowski and Karkowski, 1976).

In this study, levels of free cysteine were elevated in the ischemic regions at 2 hr., 4 hr., and 8 hr. following carotid artery ligation, when compared to control regions. The magnitude of this elevation was similar to, but somewhat less than the decrease in GSH when compared on a molar basis; the cysteine may arise from the autolytic breakdown of GSH. Perry et al. (1981) studied post-mortem changes of amino compounds in human and rat brain and found that the total glutathione in rat brain fell with time while the concentration of cystine (oxidized cysteine) and glycine gradually increased. However, the elevation of the latter two amino acids was much less than expected when compared to the loss of GSH. Free cysteine was not measured in the latter study.

Determination of several amino acids in control and ischemic striata of 3 animals at 4 hours post-ligation in the present study showed changes in mean levels that paralleled the post-mortem findings of Perry et al. (1981)

at 4 hours post-mortem; however, in the present study, the N was small and only the elevation in histidine on the ischemic striata achieved statistical significance by paired T-test analysis. Glycine levels (mean ± SD) were 0.97 ± 0.35 um/gm in the right (control) striata and 1.23 ± 0.76 um/gm in the left (ischemic) striata; similar to the elevation in cysteine, this is slightly less than, but similar to what might be expected if glycine were arising from GSH breakdown. The glutamate concentration might also be expected to rise if autolytic breakdown of GSH was occurring in ischemic tissue. However, glutamate analyses in this study failed to show any difference in concentration in ischemic striata, compared to control. It is noted that in the post-mortem study of Perry et al. (1981), glutamate content did not change significantly with time. Possible explanations include the occurrence of concurrent processes which tend to both elevate and reduce glutamate concentration. The rise in GABA levels seen in ischemic brain (Lust et al. 1975) and post-mortem brain (Perry et al., 1981) is thought to arise from continued activity of glutamic acid decarboxylase, a process which would consume glutamate. In addition, the glutamyl portion of GSH might be transferred to other amino acids via gamma-glutamyl transpeptidase, or converted to pyroglutamate via gamma-glutamyl cyclotransferase, thus resulting in no net increase in free glutamate during breakdown of GSH. Alternatively, glutamate levels may rise following ischemic-mediated

release from glutamatergic neurons (Benveniste et al., 1984; Drejer et al., 1985) and autolytic breakdown of proteins and peptides.

The biochemical findings of decreased GSH and increased cysteine may explain the ischemia-induced alterations in mercury orange staining. Mercury orange reacts with soluble SH groups in the protocol which was utilized (Asghar et al., 1975); it should react equally with both free GSH and free cysteine. Normally, the level of cysteine is very low (uM; Table 8) compared to GSH (mM; Table 6). However, the cysteine rises dramatically in ischemic tissue (up to 0.67 mM; Table 8). The modest decrease in stain intensity with partial loss of granularity in regions which normally contain abundant fluorescence, may reflect the observed depletion of GSH in striata and hippocampus (Cf. Table 6). However, the depletion of fluorescence in these regions would be hindered by the appearance of free cysteine, which also reacts with Mercury orange. The appearance of free cysteine should be particularly evident in neuronal somata, which normally contain only slight fluorescence; the Mercury orange stain revealed increased fluorescent material in neuronal somata in ischemic regions.

An alteration in catecholamine histofluorescence (Falk-Hillarp technique) was reported in ischemic striata of gerbils at one hour after left carotid ligation (Ahagon et al., 1980). These investigators described a slight decrease

in intensity of fluorescence in dopamine terminals on the ligated side, when compared to the control (non-ligated) side, as well as an appearance of fluorescence in myelinated fiber bundles in the ischemic striata. These authors interpreted their observations to indicate an extraneuronal leakage and diffusion of dopamine. An interesting parallel can be drawn between their results and the results of the present study. Ahagon et al. (1980) reported the appearance of DA-fluorescence in fiber bundles, detectable at one hour, and disappearance of DA-fluorescence from nerve-terminals. The present study describes a reduction of mercury orange staining in both fiber bundles and regions surrounding neuronal somata, as well as an increase of staining in neuronal somata in ischemic striata, first visible at four hours.

A previous study by Weinberger et al. (1985) found that depletion of catecholamines by pre-treatment of gerbils with AMPT protected nerve terminals from ischemia-induced injury in the unilateral carotid artery ligation model. It was proposed that products of the oxidative metabolism or autoxidation of catecholamines (H_2O_2 and quinones respectively; see section 1.1.6 a) may be involved in ischemic damage. In this study, inhibition of enzymatic oxidative deamination of catecholamines via monoamine oxidase by pretreatment with pargyline, or reduction in the level of catecholamines by pre-treatment with AMPT failed to inhibit the ischemia-induced depletion of GSH. One may

conclude that the processes that are responsible for the ischemia-induced damage to nerve terminals are different from the processes which are responsible for the ischemia-induced depletion of GSH. The stoichiometric relationship between the depletion of GSH and the elevation of cysteine and glycine as well as the lack of elevation of GSSG, support the idea that the GSH depletion seen in ischemic tissue in this study is due to autolytic hydrolysis of the tripeptide. This hypothesis is further supported by the similarity between the post-mortem changes in amino acids described by Perry et al. (1981) and the changes seen in ischemic tissue in this study. The possibility that decreased levels of brain GSH may have deleterious effects on brain function or may contribute to further ischemic damage by other mechanisms can not be ruled out.

CHAPTER 8: STRIATAL DOPAMINE AND METABOLITES DURING ISCHEMIA.

Materials and methods.

Left hemispheric ischemia was produced in male gerbils by the method of Lust et al.(1975) as described in Chapter 7. At 2 hr., 4 hr., and 8 hr. after carotid ligation, those gerbils exhibiting signs of stroke were decapitated by guillotine, and the cerebra were removed and rinsed in ice-cold isotonic saline. The cerebra were divided into right and left hemispheres by a mid- sagittal incision; the striata from each side were removed by blunt dissection and placed in ice-cold isotonic saline. The isolated striata were then weighed and homogenized as described in Chapter 7. Analyses for hydroxylated products of dopamine were performed as described in Chapter 3. Analyses of DA, DOPAC, and HVA by HPLC with electrochemical detection (Bioanalytic Systems, West Lafayette, Ind) were carried out as follows: The mobile phase consisted of 93 parts 150 mM monochloroacetic acid pH 3.0 with 7 mM EDTA and 1.25 mM sodium octylsulfate, and 7 parts acetonitrile. The column used was 25 cm. long containing octadecylsilane reverse-phase packing. Peak heights and retention times of standard solutions were compared with samples and used to calculate tissue concentrations. Recoveries of the internal standards, alpha-methyldopamine and HMPPA, were used in the calculations for DA and DOPAC, and HVA, respectively. Some samples were further purified by alumina chromatography for

isolation of catechol-containing compounds (i.e. DA and DOPAC) prior to HPLC analyses, as follows: 250 uL of the deproteinized supernatant was added to 500 uL of a mixture of 1 part 10% EDTA and 10 parts 0.5 M TRIS base pH 9.2 in 1 mL centrifuge tubes containing 13 mg acid-washed alumina, and the tubes were shaken immediately by hand. The final pH of this solution was between 8.1 and 8.2. The tubes were placed in a mechanical rotator for 3 min. Subsequently, they were centrifuged at 10,000 x g for 30 sec. at 4^{o}C, and the pellets of alumina were washed twice by 1 min. rotation in 800 uL distilled deionized water, followed by centrifugation to pellet the alumina. Catechol compounds were eluted from the alumina pellets by addition of 250 uL of 0.4 M PCA with 40 mg/L DTPA and 0.1 mM ascorbic acid. This procedure was run simultaneously on standard solutions of DA and DOPAC in the presence of internal standards, and recoveries were included in the final calculations. Recoveries of DA and DOPAC were in the range of 80-90% and 70-80% respectively; HVA is lost during this procedure (viz., it is not bound to alumina).

Construction of intracerebral dialysis (ICD) probes:

The system used for ICD is similar to that described by Phebus et al. (1986). The probe consisted of two parallel 23 gauge stainless steel cannulae which were constructed from Butterfly infusion sets (Abbott Hospitals Inc., Chicago), trimmed and soldered together. A length of

cellulose dialysis tubing with a molecular cut-off of 15,000 Daltons and a wet outer diameter of 250 umeter was inserted into each end of the probe and glued in place with epoxy resin. The length of the loop was adjusted to contain approximately 5 mm of exposed tubing.

In vivo ICD:

Male gerbils (50-70 gms) were anesthetized with 400 mg/kg chloral hydrate i.p. The animals remained anesthetized throughout the remainder of the experiment; some animals received additional i.p. injections of anesthetic if they responded to foot pinch stimulus. Chloral hydrate has been demonstrated not to effect the metabolism of dopamine in rats in vivo (Berger and Weiner, 1977). The left common carotid artery was isolated and sutures were placed around it, not tied, as described in Chapter 7. The animals were then placed in a stereotaxic device, and the dialysis probes were inserted into the left striatum, utilizing the following coordinates: 0.8 mm anterior and 2.8 mm lateral to bregma, and 3.8 mm below dura. The probe was perfused with normal saline at 8.8 uL/min. and collected in microcentrifuge tubes containing 20 uL 0.4 M PCA with 40 mg/L DTPA, at 20 min. intervals. Three or four samples were collected prior to ligation of the carotid artery. Subsequently, samples were collected at 20 min. intervals for up to 280 min. The acidified dialysates were vortexed and assayed directly for DA, DOPAC, and HVA by

HPLC as described above. Some of these samples were also assayed for ascorbic acid by HPLC with electrochemical detection (Cf., Thrivikraman et al. 1974; Pachla and Kissinger, 1976).

In vivo electrochemistry (IVED) with ICD:

In some experiments, in vivo electrochemistry was performed simultaneously with ICD. Working electrodes were constructed from teflon coated silver wire (0.2 mm diameter) packed with carbon paste (1.0 mL silicon oil, 1.5 gm Ultra F carbon powder; source) and were glued onto the ICD probes so that the working electrode tip was in close proximity to the tip of the dialysis loop (approximately 1 mm lateral and 1 mm anterior to the loop tip). The reference electrode was a chloridized silver wire and the control electrode was a silver wire attached to a cortical screw. The working electrode-ICED probe complex was lowered into the striatum; the probe was perfused and the dialysate collected as described above. Simultaneous with ICED collections, in vivo chronoamperometric measurements were performed every 60 sec. by applying a 250 mV pulse of 1 sec. duration and recording the average current generated during the last 100 msec. of each pulse.

After completion of all ICD experiments, animals were decapitated and the position of the probe in the striatum was verified by inspection under a dissecting microscope. Each probe was calibrated after it was removed from the

animal; the probe was immersed in a solution containing 0.1 mg/L DA, DOPAC, and HVA in artificial CSF (Myers, 1971) and perfused under identical conditions as the in vivo experiments. Dialysis and dilution of the stock compounds resulted in final concentrations that varied between 3 and 6% of the initial concentration, depending on the probe. The dilution during dialysis was included in the calculations.

Results:

Table 10 shows the concentration of dopamine and acid metabolites in the left and right striata of sham-operated animals, and animals exhibiting behavioral signs of stroke. Animals with stroke were analyzed at 2 hr., 4 hr., and 8 hr. after left carotid ligation. The sham-operated animals were analyzed at 2 hr. (n=3), 4 hr. (n=2), and 8 hr. (n=2) after surgery. There was no significant difference in the values for dopamine, DOPAC, or HVA concentration in the right and left striata of the animals within the sham-operated group and, therefore, these values were pooled. Concentrations of DA and metabolites in the left and right striata were compared by paired T-test. There was a significant decrease in dopamine in the left ischemic striata of animals at 2 hr., 4 hr., and 8 hr. after arterial ligation; in addition, there was a significant elevation of DOPAC in the left striata 2 hr. after ligation. There was no significant difference in the concentration of HVA in the left striata when compared to the right, at any time point.

Table 10. Dopamine and acid metabolites in control and ischemic striata at 2 hr., 4 hr., and 8 hr. after left carotid ligation.

	DOPAMINE		DOPAC		HVA	
	Right	Left	Right	Left	Right	Left
SHAM (7)	9.65± 1.74	9.25± 1.78	0.94± 0.26	0.81± 0.15	2.07± 0.42	2.08± 0.25
2 hr. (8)	12.18± 2.17	6.52±* 3.48	1.32± 1.16	2.91±* 1.45	2.98± 2.23	3.46± 1.82
4 hr. (5)	10.98± 1.52	3.61±* 2.13	0.91± 0.38	1.68± 0.87	2.51± 0.89	2.31± 0.66
8 hr. (8)	10.91± 3.11	1.51±* 0.36	0.91± 0.30	1.09± 0.45	2.76± 1.01	2.43± 0.70

* $p<0.05$
** $p<0.005$

The number of animals is in parenthesis. Values are the mean ± SD in ugm/gm wet weight. Sham-operated animals were decapitated at 2 hr., 4 hr., or 8 hr. after surgery; there was no effect of length of time after surgery on DA, DOPAC, or HVA concentration in this group and therefore, the values are pooled. All other data are from animals that exhibited behavioral signs of stroke after ligation of the left common carotid artery and were decapitated 2 hr., 4 hr., or 8 hr. after surgery. The concentration of DA, DOPAC, or HVA in the left striata are compared to the concentration in the right striata by paired T-test.

Figure 23 shows the changes in DA, DOPAC, and HVA concentration with time in left and right striata and hippocampi. In these analyses, comparisons are made to sham-operated controls, rather than to the control hemisphere in an animal with with stroke, as in Table 10. There was a significant decrease in dopamine on the left (ischemic) side at 2 hr., 4 hr., and 8 hr., and a slight but significant increase in dopamine on the right (control) side at 2 hr. The concentration of both DOPAC and HVA was significantly elevated at 2 hr. post-ligation on the left striata, but not at 4 hr. and 8 hr.; there was no significant change in either metabolite in the right striata at any time point.

Hydroxylated isomers of dopamine were not detected at any time point in either control or ischemic striata.

Figure 23. Changes in DA, DOPAC, and HVA with time in control and ischemic striata after left carotid ligation.

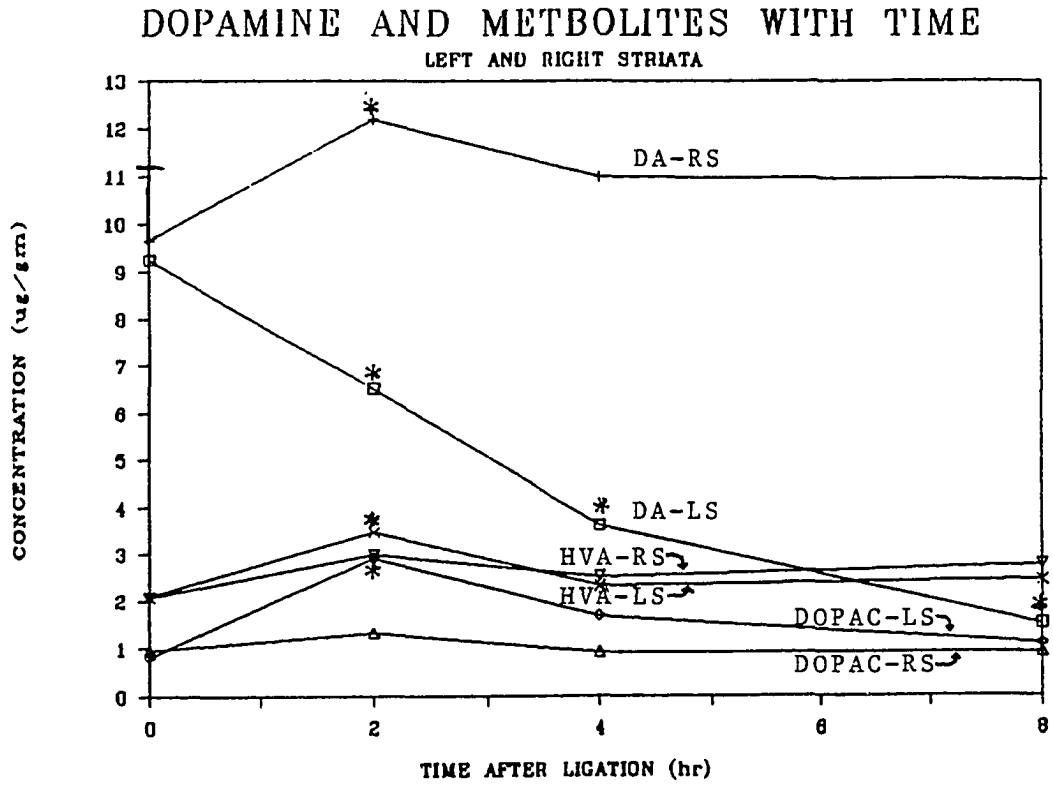

DA-left striatum (DA-LS) **DA-right striatum (DA-RS)**

DOPAC-left striatum (DOPAC-LS) **DOPAC-right striatum (DOPAC-RS)**

HVA-left striatum (HVA-LS) **HVA-right striatum (HVA-RS)**

*Significantly different from 0 time, alpha=0.05

This figure depicts the same data listed in Table 10. The concentration of DA, DOPAC, and HVA in left or right striata are compared to sham-operated controls (i.e., zero time values). Assays were performed in gerbils exhibiting behavioral signs of stroke at 2 hr., 4 hr., and 8 hr. after left common carotid artery ligation. Comparisons were conducted by one-way analyses of variance.

The concentrations of dopamine and its acid metabolites in the extracellular space of the left striata (ipsilateral to carotid ligation) were obtained by intracerebral dialysis, in anesthetized gerbils both prior to and after left carotid ligation. Samples were analyzed by HPLC with electrochemical detection (Figure 24). The first sample, taken during the 20 min. after placement of the dialysis probe, but before left carotid ligation, usually contained substantial amounts of dopamine, as well as DOPAC and HVA. With time, prior to ligation, the level of dopamine tended to fall while the level HVA rose slightly; these changes did not achieve statistical significance by one-way analysis of variance. Immediately prior to left carotid ligation, the mean ($\pm$ SEM) extracellular fluid concentrations of dopamine, DOPAC, and HVA were 6.05 $\pm$ 2.13, 39.32 $\pm$ 6.27, and 127.35 $\pm$ 21.27 uM. Behavioral assesment of stroke with these gerbils was not possible because the animals were anesthetized. In 9 of 19 animals studied (Figure 24), there was a marked increase in dopamine in the extracellular fluid detected in the first sample (20 min. after arterial ligation), which continued to rise during the next 20 min. (second sample). The extracellular dopamine concentration then fell, but remained elevated over baseline. There were no significant changes in extracellular fluid levels of DOPAC with time after arterial ligation. The extracellular fluid level of HVA fell, reaching statistical significance by 40 min. after ligation, and persisting up to 260 min. post-ligation.

Figure 24. Dopamine, DOPAC, and HVA in extracellular fluid of ischemic striata after left carotid ligation.

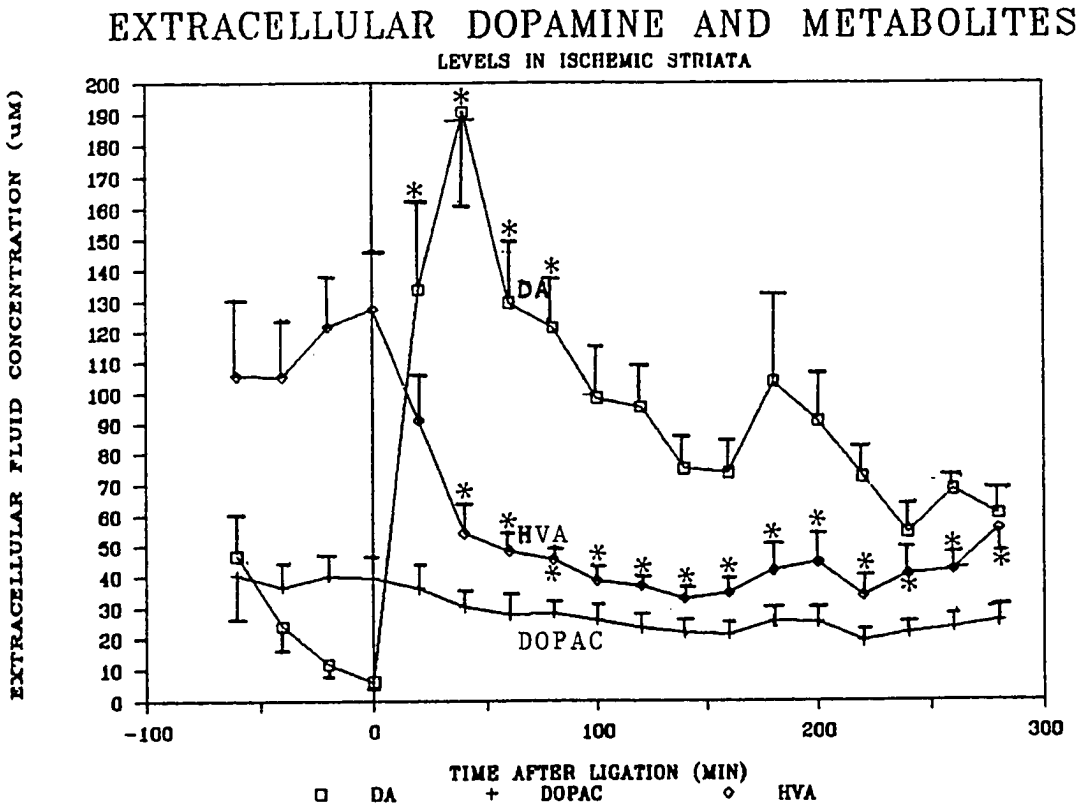

* Significantly different from 0 time, alpha=0.05

Samples were collected from the left striata of gerbils by intracerebral dialysis, before and after ligation of the left common carotid artery. Samples were analyzed by HPLC with electrochemical detection. Only those animals exhibiting a rise in dialysate DA are plotted (9 of 19). Values are presented as the mean ± SEM of the calculated concentration of the compound in the extracellular fluid. Asterisks mark significant changes from time 0, as determined by one-way analyses of variance.

In order to study the relationship between in vivo chronoamperometric signal and the concentration of some electrochemically active compounds in the extracellular fluid during stroke, 6 anesthetized gerbils were analyzed simultaneously by in vivo chronoamperometry and intracerebral dialysis. Prior to arterial ligation, the level of dopamine (Figure 24) and ascorbate (Figure 25) in the left striata, as well as the electrochemical signal (Figure 26), fell with time after placement of the electrochemistry-dialysis probe complex. In 3 of 6 animals, there was a marked increase in the electrochemical signal above baseline (61 ± 30%) evident within minutes, as well as an increase in the level of dopamine (Figure 24) which obtained statistical significance at 40 min. after carotid ligation. The level of ascorbate (Figure 25) was unaffected after ligation, when compared to baseline. The three animals that did not exhibit a rise in electrochemical signal were killed by intracardiac injection of 5 cc of air. Within minutes after death, there was a rise in the chronoamperometric signal; in the first 20 min. sample after death, and in subsequent samples, there was a rise in the extracellular concentration of dopamine (See Figure 26).

Figure 25. Ascorbate in the extracellular fluid of ischemic striata after left carotid ligation.

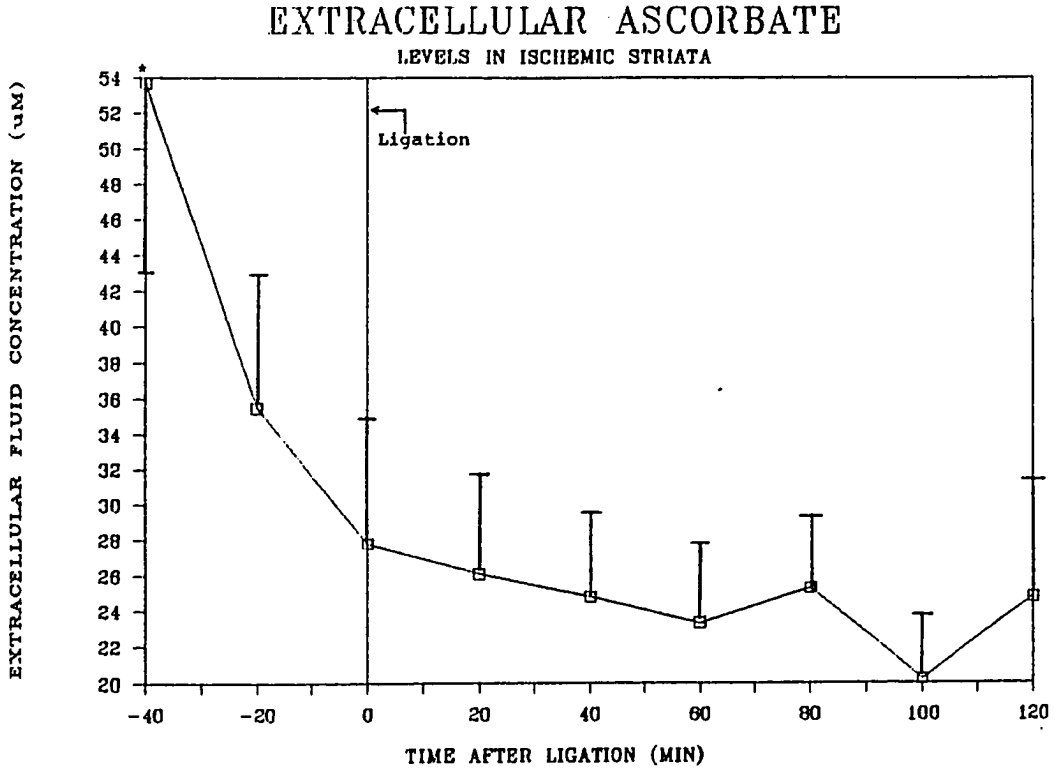

* Significantly different from 0 time, alpha=0.05

Samples were collected from the left striata of gerbils by intracerebral dialysis, before and after ligation of the left common carotid artery. Samples were analyzed by HPLC with electrochemical detection. Concurrently, chronoamperometric signals were obtained from left striata by IVED. Only those animals exhibiting a rise in chronoamperometric signal are plotted (3 of 6). These 3 animals had an elevation in extracellular fluid DA, and are included in Figure 24. Values are presented as the mean ± SEM of the calculated concentration of ascorbate in the extracellular fluid.

Figure 26. Post-mortem changes in extracellular DA, DOPAC and HVA and chronoamperometric signal in the striata of an animal that did not exhibit a rise in extracellular DA after left carotid ligation.

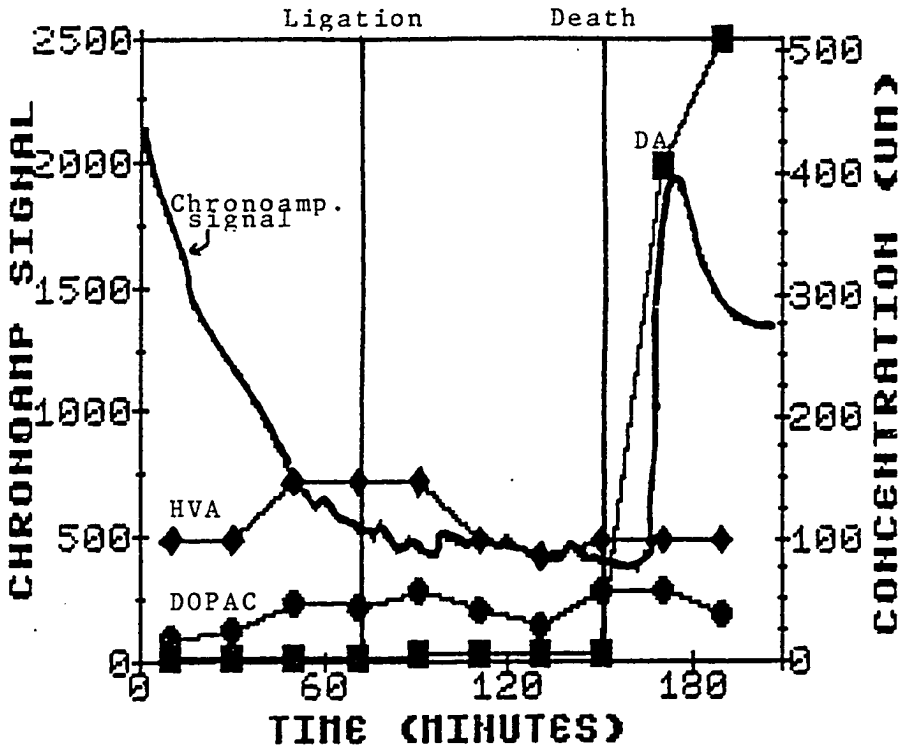

Samples were collected from the left striata of a gerbil by intracerebral dialysis, before and after ligation of the left common carotid artery. Concurrently, chronoamperometric signals were obtained from left striata by IVED. Samples were analyzed by HPLC with electrochemical detection. These data are from one representative animal that did not show an elevation in extracellular DA or chronoamperometric signal after arterial ligation (3 of 6). The animals were killed by intracardiac injection of 5 cc air at the time point indicated. Values are presented as the mean ± SEM of the calculated concentration of DA, DOPAC, and HVA in the extracellular fluid.

Discussion

Analyses of striatal levels of DA and its metabolites DOPAC and HVA in gerbils exhibiting behavioral signs of stroke (Table 10) show that ligation of the common carotid artery induces a decrease in the concentration of DA and an increase in the concentration of DOPAC on the side ipsilateral to ligation. The concentration of HVA was not affected by arterial ligation. In these analyses, the contralateral side served as a control for the ischemic side (ipsilateral to arterial occlusion) and allows the use of the paired T-test for comparisons. The use of the contralateral hemisphere as an internal control diminishes the impact of animal to animal variations in neurotransmitter concentrations and responses to ischemia. However, several investigators have suggested that changes in blood flow, neurotransmitter metabolism, and tissue energy charge also occur on the side contralateral to arterial ligation, and that this tissue may not represent a true control (Levy and Duffy, 1977; Harrison et al., 1979; Mayevsky et al., 1983 and 1986). In addition, there are documented differences in the concentration of neurotransmitters, including DA, in the right versus the left hemisphere within animals (Glick et al., 1976). For these reasons, the data were also analyzed for changes in DA, DOPAC, and HVA, by comparison with sham-operated controls. The concentrations of compounds present in the striata of sham-operated gerbils was used as a zero time

control for comparison with the striata of animals exhibiting behavioral signs of stroke at 2 hr., 4 hr., and 8 hr. after arterial ligation. Comparisons were made by one-way analysis of variance (Fig. 23). These analyses demonstrated a loss of DA in the striata ipsilateral to ligation at all time points studied. Although DOPAC was elevated in the ipsilateral striata at all time points following ligation, only the 2 hr. values achieved statistical significance. In addition, the 2 hr. values for HVA were also significantly elevated in the ipsilateral striata.

The ischemia-induced decrease in striatal DA seen in this study agrees with previous reports using the same animal model (Lust et al., 1975; Lavyne et al., 1975; Mrsulja et al., 1976; Zervas et al., 1977). Lust et al. (1975) attributed the fall in DA during ischemia to a decreased availability of O_2 for the rate-limiting biosynthetic enzyme, tyrosine hydroxylase. The elevated levels of DOPAC seen in this study confirm the observations of Weinberger et al. (in press) and indicate that sufficient O_2 is available for the intracellular oxidative deamination of DA by MAO.

Hydroxylated isomers of DA (i.e., products of $^{\cdot}OH$ attack on DA, Chapt. 3) were not detected at any time point in ischemic or control striata. These data indicate that $^{\cdot}OH$ is either not generated during ischemia, or that

insufficient quantities are generated to result in detectable levels of hydroxylated DA. In experiments utilizing ICD to analyze changes in the extracellular fluid levels of DA, DOPAC, and HVA in the ipsilateral striatum, the data support the hypothesis that ischemia induces a release of DA (Wurtman and Zervas, 1974; Lavyne et al., 1975; Brannan et al., in press). In 9 of 19 (47%) animals studied, there was a significant increase in extracellular fluid concentrations of DA in the striata following ipsilateral carotid ligation. This percentage compares favorably with the percentage of gerbils exhibiting behavioral signs of stroke after unilateral carotid ligation (30-60%, Ito et al., 1975; Harrison et al., 1973). In addition, when IVED was coupled to ICD analyses, every animal that showed an increase in electrochemical signal showed an elevation in extracellular DA. The current data support and extend the findings of Brannan et al. (1987) who demonstrated that animals exhibiting behavioral signs of stroke following unilateral carotid ligation showed a marked increase in electrochemical signal on the ipsilateral striata.

Several electrochemically active substances have been postulated to contribute to the signal that was detected in this study, the most notable of which is ascorbic acid (O'Neill et al., 1983; Clemens and Phebus, 1983; Echizen and Freed, 1986). However, no rise in extracellular ascorbic acid was detected in animals exhibiting a rise in

electrochemical signal after carotid ligation (Figure 25). Pre-treatment of animals with AMPT markedly attenuated the initial increase in the in vivo electrochemical signal (Brannan et al., 1987), providing evidence that the rise in the signal was due to DA. In this current study, positive identification by HPLC of elevated DA in the extracellular fluid of animals exhibiting a rise in the in vivo electrochemical signal provides further evidence for an acute release of DA during ischemia and simultaneously indicates that the in vivo signal is due to extracellular DA.

Animals that did not exhibit a rise in electrochemical signal following arterial occlusion were killed by intracardiac injection of 5 cc of air. Immediately following death, there was a rapid rise in both the electrochemical signal, and in the concentration of DA in the extracellular fluid (Fig. 26). A post-mortem rise in electrochemical signal, identified as DA by ICED and HPLC, has been previously reported (Phebus et al., 1986), and served as an indication of proper functioning of equipment in the present study.

The ICD studies also showed no change in extracellular DOPAC and a decrease in extracellular HVA following carotid ligation. DOPAC is formed intracellularly and might not be expected to be elevated in the extracellular fluid, even in the face of increased metabolism of DA. Although the

extracellular levels of HVA prior to ligation may be somewhat higher than the "true resting state" levels, due to metabolism of DA liberated from cells following the trauma of probe placement, the sharp decline in HVA that occurred immediately after arterial ligation must be assumed to result from the ensuing ischemia. Extracellular DA can be metabolized to form 3-O-methyldopamine (3-O-MeDA). Extracellular 3-O-MeDA has been shown to be elevated following the release of striatal DA induced by the neurotoxin MPP^+ (Rollema et al., 1986). 3-O-MeDA could not be detected by the chromatographic conditions employed in this study; elevations of this metabolite in the extracellular fluid might be expected following ischemia-induced release of DA, but have yet to be proven experimentally.

Comparison of the extracellular fluid data (Fig. 24) with the tissue data (Fig. 23 and Table 9) must be guarded, as the ICD studies were conducted with anesthetized animals. Although chloral hydrate has been shown not to effect DA metabolism in rat brain tissue in vitro (Berger and Weiner, 1976), other effects of general anesthesia on aspects of DA release and clearance, as well as other tissue responses to ischemia, cannot be ruled out.

The data presented in this study offers evidence that during striatal ischemia produced by unilateral carotid ligation in gerbils, an acute release of DA occurs and that sufficient O_2 is available for the intracellular oxidative

metabolism of DA to DOPAC. Extracellular DA or products of its oxidative metabolism may play a role in the ensuing tissue damage.

APPENDIX I: CALIBRATION CURVES FOR ANALYTIC TECHNIQUES.

Figure 27: Amino acid calibration curve 1.

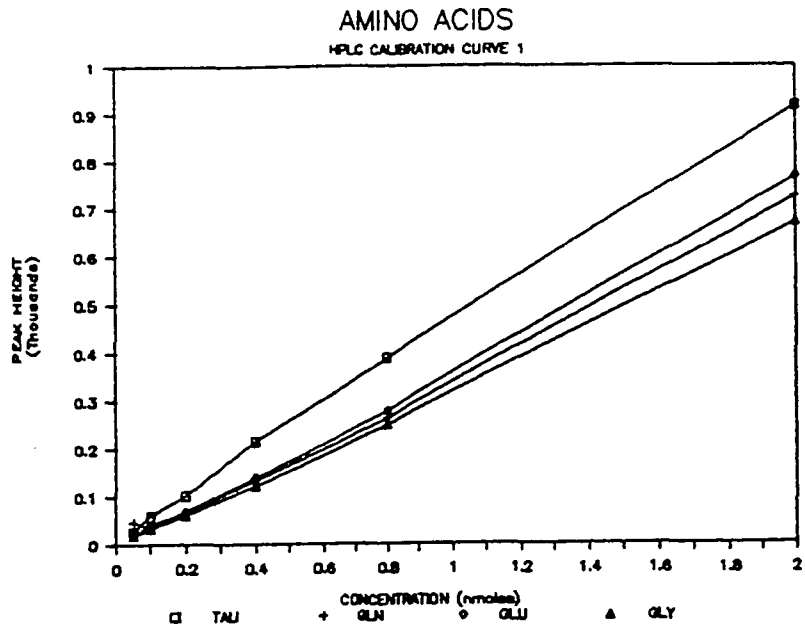

Amino acids were separated by ion exchange HPLC in a lithium acetate gradient mobile phase, and identified following post-column derivitization with orthophthalaldehyde by fluorescence detection. Each point represents the mean peak height of three injections.

Figure 28: Amino acid calibration curve 2.

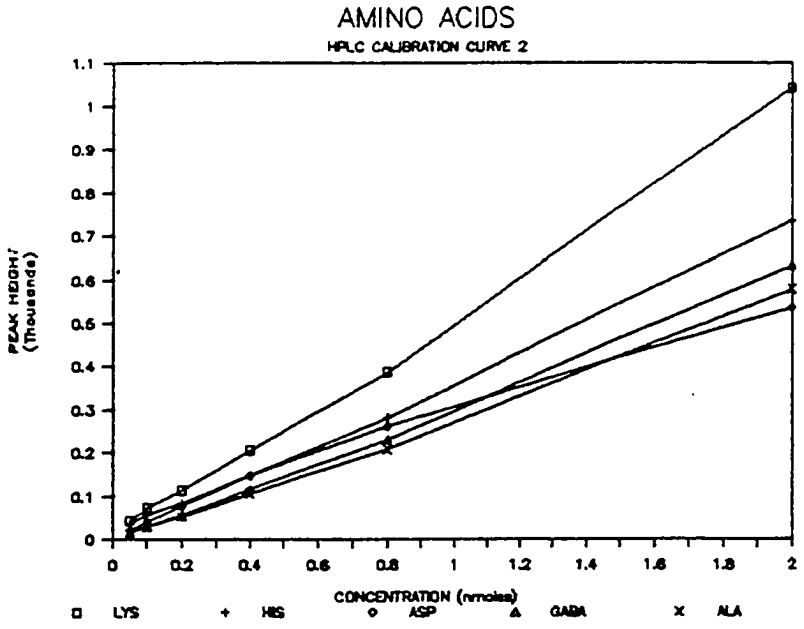

Amino acids were separated by ion exchange HPLC in a lithium acetate gradient mobile phase, and identified following post-column derivitization with orthophthalaldehyde by fluorescence detection. Each point represents the mean peak height of three 10 ul injections.

Figure 29: Ascorbic acid calibration curve.

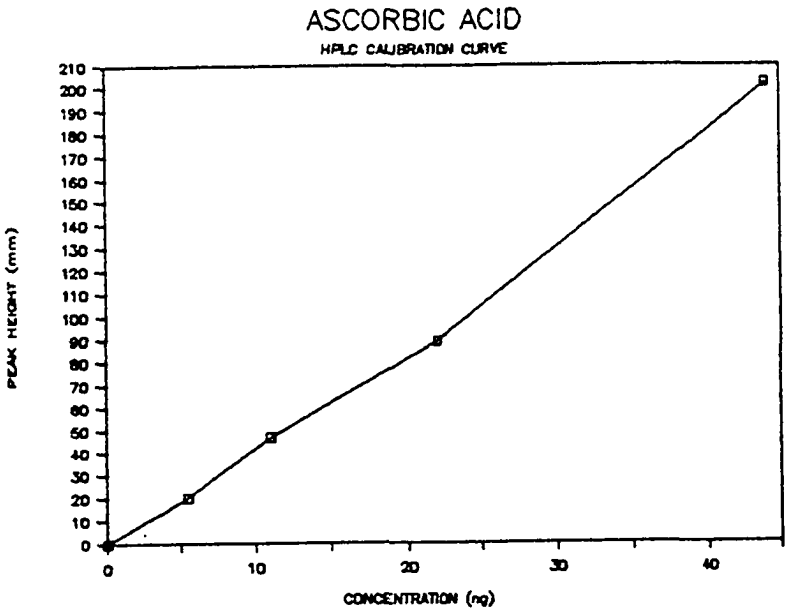

Ascorbic acid was analyzed by HPLC with electrochemical detection. A mobile phase consisting of 0.08 M acetate buffer pH 4.75, containing 1.0 mM sodium octylamine and 20 % methanol was used at a flow rate of 1.0 ml/min. A glassy carbon detector electrode potential was set at + 0.7 volts. Each point represents the mean of three 25 ul injections.

Figure 30: Calibration curves for dopamine (DA), dihydroxyphenylacetic acid (DOPAC), and homovanillic acid (HVA).

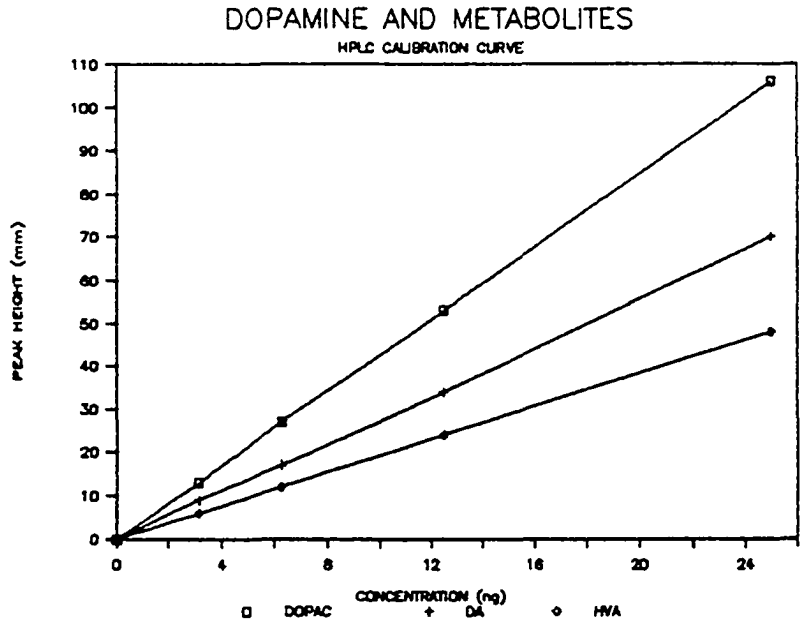

Dopamine, DOPAC and HVA were analyzed by HPLC with electrochemical detection. A mobile phase consisting of 0.15 M monochloroacetic acid, pH 3.0, containing 0.7 mM ethylenediaminetetraacetic acid, 1.25 mM sodium octylsulfate, and 7 % acetonitrile was run at 1.0 ml/min. A glassy carbon detector electrode potential was set at + 0.8 volts. Each point represents the mean of three 25 ul injections.

Figure 31: Calibration curve for glutathione (GSH) and cysteine.

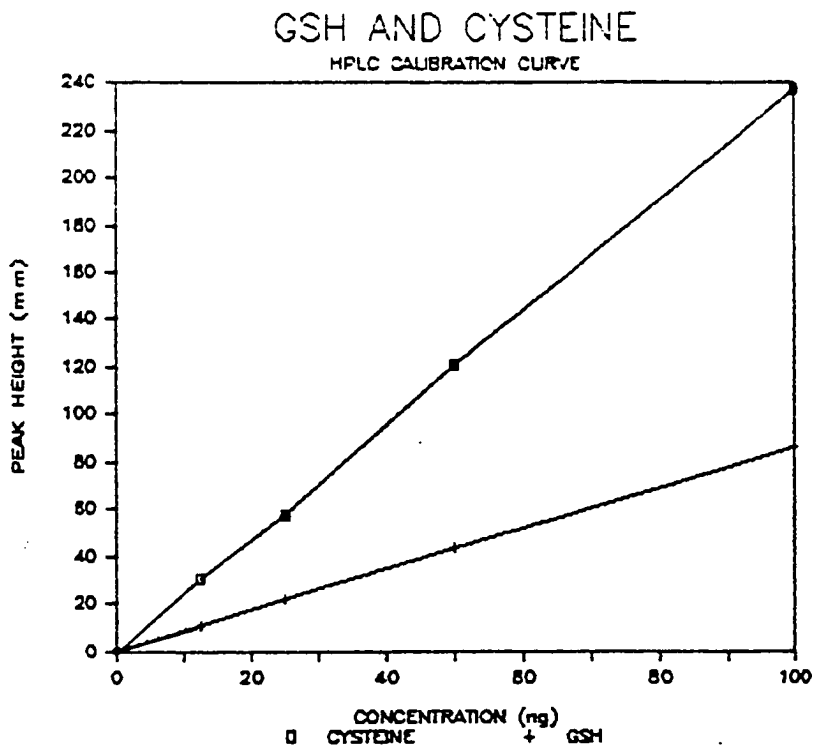

GSH and cysteine were analyzed by HPLC with electrochemical detection. A mobile phase consisting of 0.15 M monochloroacetic acid, pH 3.0, containing 1.25 mM sodium octylsulfate, and 4 % methanol was used at a flow rate of 1.0 ml/min. A mercury/gold amalgam detector electrode was operated at an oxidizing potential of + 0.15 volts. Each point represents the mean of three 25 ul injections.

Figure 32: Calibration curve for oxidized glutathione (GSSG).

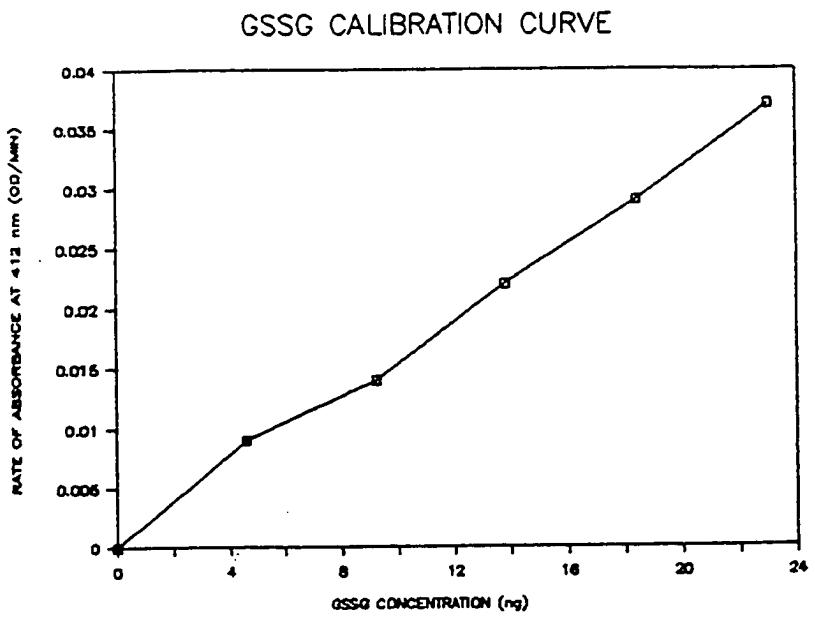

GSSG was analyzed by following the enzymatic reduction of the mixed disulfide formed from GSH and dithionitrobenzoic acid by GSSG reductase and NADPH (slow), after the reduction of GSSG by the same enzyme system (fast). The rate of color formation is monitored at 412 nm; the rate obtained in the absence of added GSSG standard (blank) is subtracted from the rates obtained in the presence of known amounts of authentic GSSG. Each point represents the mean of 3 assays.

Figure 33: Calibration curve for hydroxydopamine isomers.

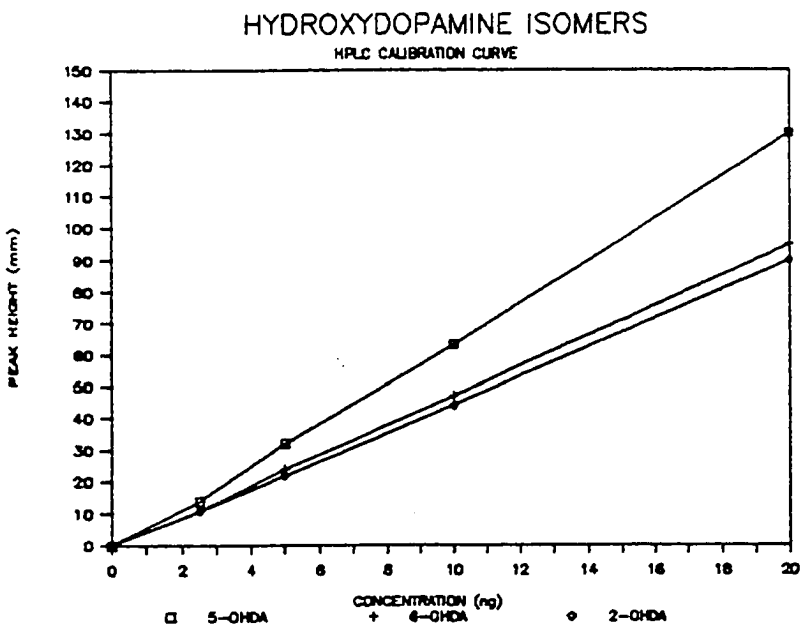

Isomers of hydroxydopamine were analyzed by HPLC with electrochemical detection. A mobile phase consisting of an aqueous solution of citric acid (0.125 M) and sodium phosphate (0.125 M), pH 2.5, containing ethylenediaminetetraacetic acid (100 mg/liter) and sodium octylsulfate (30 mg/liter) was used at a flow rate of 1.0 ml/min. A glassy carbon detector electrode was operated at an oxidizing potential of + 0.8 volts for 2-OHDA and 5-OHDA and at + 0.2 volts for 6-OHDA. Each point represents the mean of 3 20 ul injections.

Figure 34: Sample chromatogram showing changes in GSH and cysteine in striata and hippocampi during ischemia.

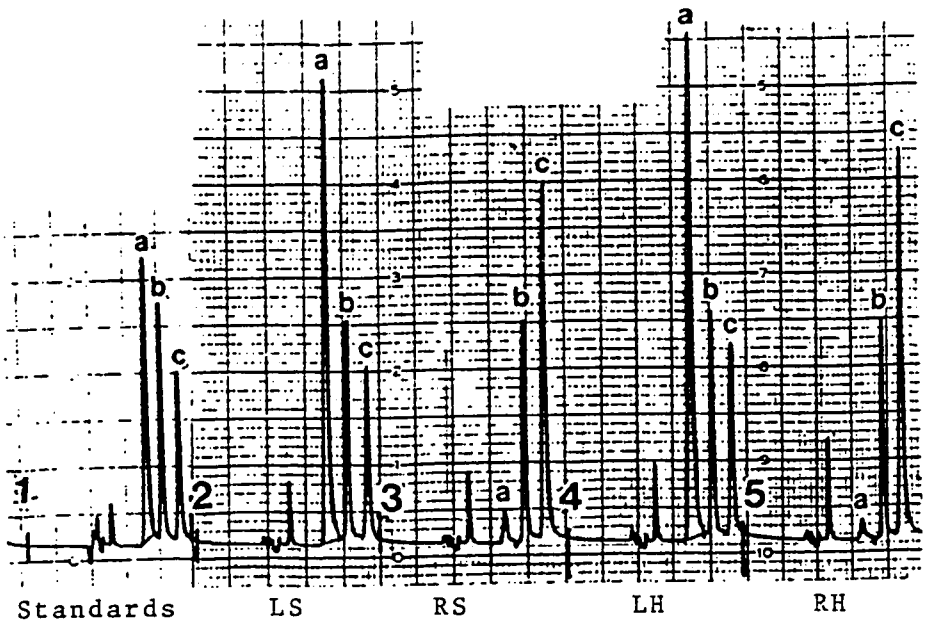

LS = left striatum
RS = right striatum
LH = left hippocampus
RH = right hippocampus

The first chromatographic run (1) shows the separation of a standard solution containing cysteine (peak a), N-acetylcysteine (internal standard; peak b), and GSH (peak c). The standard solution was prepared in 0.4 M perchloric acid with 0.4 mg/L diethylenetriaminepentaacetic acid, and contained 5 ug/ml cysteine and N-acetylcysteine and 10 ug/ml GSH. Control striatum (run 3) and hippocampus (run 5) contain very low levels of cysteine (peak a) when compared to GSH (peak c). Ischemia induced a significant decrease in GSH and an increase in cysteine in both striatum (run 2) and hippocampus (run 4). The tissue preparation and chromatographic conditions are described in Chapter 4. All injection volumes were 25 uL.

APPENDIX II: HYDROXYL RADICALS AND THE TOXICITY OF ORAL IRON.

Ferrous ions in solution are readily oxidized by molecular oxygen. Products of the overall reaction include the superoxide radical (O_2^-, Equation 9), hydrogen peroxide (Equation 10), and the hydroxyl radical ($^{\cdot}OH$, Equation 6).

$$Fe^{2+} + O_2 \text{ ------> } Fe^{3+} + O_2^- \quad \text{(Eq. 9)}$$

$$O_2^- + O_2^- + 2H^+ \text{ ------> } O_2 + H_2O_2 \quad \text{(Eq. 10)}$$

$$Fe^{2+} + H_2O_2 \text{ ------> } Fe^{3+} + {}^{\cdot}OH + OH^- \quad \text{(Eq. 6)}$$

The hydroxyl radical, in particular, is a highly reactive species, whose formation is generally associated with pathologic consequences (Freeman and Crapo, 1982; Cohen, 1978).

We wished to determine if ingestion of iron salts could lead to the formation of $^{\cdot}OH$ in the gastrointestinal tract. These experiments were prompted by the knowledge that poisoning by oral iron preparations is a major cause of accidental death in young children (Lacoutre and Lovejoy, 1983). In addition, intolerance to oral iron can be a serious problem when iron is prescribed for a variety of medical reasons (Finch, 1980). The mechanisms for the toxicity of oral iron have not been elucidated. If evidence were available for the generation of $^{\cdot}OH$ in vivo, then methods to treat acute iron poisoning or to suppress oral intolerance to iron might become apparent.

Almost all oral iron preparations contain a ferrous salt (rather than a ferric salt) as the source of elemental

iron (Lacoutre and Lovejoy, 1983; Physicians Desk Reference, 1985). The reason is that iron is absorbed from the gastrointestinal tract most efficiently when it is in the ferrous form. Many preparations additionally contain ascorbic acid, which is intended to maintain the iron in the ferrous state. In our experiments, we used a ferrous salt combined with ascorbic acid. It should be noted that ascorbic acid reduces the ferric ion to the ferrous state, but it does not inhibit equation 1. Hence, reactive products of reduced oxygen, including $^{\cdot}OH$, will still be formed.

Female Sprague-Dawley rats (220-250 g) received 100 mg of ascorbic acid (Fisher) and 100 mg of ferrous sulfate ($7H_20$, Fisher; equivalent to 20 mg elemental iron) in aqueous solution by gastric intubation (Table 11). The animals had first received an aqueous solution of 100 mg of 2-keto-4-methiolbutyric acid (KMB, a potent $^{\cdot}OH$ scavenger; Sigma), by gastric intubation. KMB reacts vigorously with $^{\cdot}OH$ and generates ethylene, a hydrocarbon gas, as a product (Equation 20; Diguiseppi and Fridovich, 1980; Cohen et al., 1976).

$$CH_3\text{-}S\text{-}CH_2\text{-}CH_2\text{-}CO\text{-}COOH + {}^{\cdot}OH \text{ ------>}$$

$$CH_2{=}CH_2 + \text{other products} \quad \text{(Eq.20)}$$

KMB has been used in numerous in vitro studies to detect $^{\cdot}OH$ (Cohen et al., 1976; Hoidal et al., 1979). In studies conducted with biochemical or chemical systems in vitro, ethylene production is blocked by catalase (Cf. Equation 6)

or by competitive scavengers for $^{\cdot}OH$ (Diguiseppi and Fridovich, 1980; Cohen et al., 1976; Hoidal et al., 1979; Beauchamp and Fridovich, 1970).

Previous studies from this laboratory described methodology for concentrating volatile hydrocarbons evolved from living animals in order to facilitate analyses by gas chromatography (Lawrence and Cohen, 1982). In the experiments reported here, the animals were placed into sealed rebreathing chambers in which the ethylene accumulated in the chamber atmosphere (Lawrence and Cohen, 1982). Samples of chamber air were removed for assay of ethylene.

In Table 11, the rats receiving KMB alone showed a relatively low background rate of ethylene production. This rate was not significantly different from that for untreated rats (viz. 3.59 ± 1.76 nmoles/kg/2 hr, mean $\pm$ S.D., N = 4). Those rats receiving oral iron and ascorbic acid along with KMB showed a marked production of ethylene, which persisted for up to 8 hr. These data indicate the generation of a $^{\cdot}OH$-like species following the oral administration of iron and ascorbic acid. The low level ethylene production seen in untreated animals is consistent with other reports of endogenous production of ethylene and other hydrocarbon gases by normal animals (Sagai and Ichinose, 1980).

Table 11. Hydroxyl radical production from orally administered ferrous sulfate and ascorbic acid: In vivo detection with KMB.

	Rate of ethylene production (nmoles/kg/2 hr)	
Time (hr)	KMB alone	KMB + Iron + Ascorbic acid
0-2	2.39 ± 0.26	45.59 ± 21.69
2-4	3.52 ± 0.90	58.43 ± 26.09
4-6	2.83 ± 1.20	61.38 ± 35.75
6-8	1.12 ± 2.19	9.38 ± 4.64

Gastric instillations of KMB (100 mg), ascorbic acid (100 mg), and ferrous sulfate ($7H_2O$, 100 mg) were made in volumes of 0.5 ml water each, and an additional 0.5 ml water was used as a rinse. Control rats received 0.5 ml of KMB solution and 1.5 ml of water as a rinse (iron and ascorbic acid were omitted). Data are the mean ± S.D. for N=4 except for KMB alone at 6-8 hr, for which N = 3. The differences between the values for KMB alone versus KMB + iron + ascorbate are statistically significant at all time intervals ($P < 0.01$ for 0-2 hr, 2-4 hr, and 4-6 hr, and $P < 0.025$ for 6-8 hr; two-tailed T-test).

Ferrous salts dissolved in phosphate-buffered solution at neutral pH are oxidized by molecular oxygen at extraordinarily rapid rates (e.g. half-life of less than 15 seconds for 0.1 mM solution in 50 mM phosphate at pH 7.0; Cohen and Sinet, 1980). However, higher concentrations (e.g., 10 mM) in pure water are relatively stable to autoxidation. Nonetheless, oxidation of ferrous ions by oxygen does proceed and can be followed by the appearance of yellow color. The stomach exhibits a strongly acidic pH, while the small intestine is mildly alkaline. These experiments show that $^{\bullet}OH$ is observed under naturally-occurring conditions of pH and in the presence of various endogenous biomolecules when the ferrous salt is instilled directly into the stomach.

Although the gastrointestinal tract per se is an obvious site of oxygen radical formation after ingestion of a ferrous salt, it is not clear whether ethylene generation from KMB may additionally reflect the formation of a $^{\bullet}OH$-like species, stimulated by iron, elsewhere in the body. We note that ethylene production continued for up to 8 hrs, whereas KMB in solution may have already cleared from the gastrointestinal tract at the later time points in Table 11. Further studies concerning this aspect are warranted.

Another point of interest is that ascorbate can have both pro- and anti-oxidant actions. The recycling of ferric ions to the ferrous state by ascorbate can promote formation of $^{\bullet}OH$ when the availability of ferrous ions for

Equations 9 and 10 is limiting. Indeed, iron-EDTA plus ascorbate is a well-known system for generating a ·OH-like species at neutral pH (Breslow and Lukens, 1960). On the other hand, ascorbate reacts very effectively with ·OH (Dorfman and Adams, 1973) and, therefore, high concentrations of ascorbate may be capable of scavenging a portion of the ·OH that is formed. These aspects warrant further investigation.

This preliminary report provides experimental evidence for the generation of ·OH in vivo following administration of oral iron and ascorbic acid. The dose of iron used in Table 11 is at the low end of a range (0.08 to 0.32 mg elemental iron/g) known to result in damage to the stomach and proximal small bowel in rats (Nayfield et al., 1976). The damage parallels similar findings made at autopsy following death from acute ferrous sulfate poisoning in human subjects (Lacoutre and Lovejoy, 1983; Whitten and Brough, 1971). We suggest that hydroxyl radicals may be a mediator of damage to the gastrointestinal tract by oral iron.

APPENDIX III: ASCORBIC ACID AND IRON: A NOTE OF CAUTION.

In a recent review, Levine (1986) discusses many aspects of ascorbic acid biochemistry. One clinically relevant aspect that needs to be appreciated more fully is the interaction of ascorbic acid with iron.

Dr. Levine (1986) commented that ascorbic acid enhances the absorption of ingested iron. Iron is absorbed from the gastrointestinal tract most efficiently when it is in the reduced (ferrous) form, and ascorbate is a strong reducing agent. For this reason, many oral iron preparations consist of a ferrous salt plus ascorbic acid (Lacoutre and Lovejoy, 1983). However, it is well documented in the chemical and biochemical literature that solutions of free ferrous salts, and many chelates thereof, are readily oxidized by molecular oxygen and generate potentially toxic forms of reduced oxygen (i.e., superoxide anions, hydrogen peroxide, and hydroxyl radicals; Cohen and Sinet, 1980) These species have been implicated as mediators of tissue pathology in many in vitro and in vivo systems (Freeman and Crapo, 1982). Because ascorbic acid recycles ferric iron back to the ferrous state, it is commonly incorporated into in vitro systems (e.g., iron-EDTA at neutral pH) in order to enhance the generation of hydrogen peroxide and hydroxyl radicals (Breslow and Lukens, 1960). In this way, ascorbate acts as a pro-oxidant, as well as a reducing agent. It is noteworthy that iron salts are corrosive to the gastrointestinal tract mucosa; hemorrhagic necrosis of the

stomach and proximal small bowel are characteristic findings following death from acute iron poisoning (Lacoutre and Lovejoy, 1983). We have recently reported formation of hydroxyl radicals in vivo in rats following gastric instillation of solutions of ferrous sulfate and ascorbic acid (Appendix II; Slivka et al., 1986). In addition, we have preliminary in vitro evidence for a biphasic action of ascorbic acid: at lower concentrations, a pro-oxidant action increases the yield of hydroxyl radicals, but higher concentrations exhibit an antioxidant (radical scavenging) action.

Ascorbic acid may also interact with body stores of iron, as discussed in an editorial in 1981. In his commentary, Nienhuis described how the mobilization of tissue iron stores by administered ascorbic acid in patients with iron overload was associated with deterioration in cardiac function. He cautioned about the administration of ascorbic acid to these patients.

Oxy-radicals may mediate some of the pathology associated with iron toxicity. Ascorbic acid can have a pro-oxidant action by mobilizing body stores of iron and by recycling ferric ions and certain chelates to their autoxidizable ferrous forms. On the other hand, high concentrations of ascorbic acid react directly with hydroxyl radicals in an antioxidant action. It is not clear whether or not ascorbic acid is primarily a pro-oxidant or

antioxidant in vivo when administered with iron salts, but evidence does exist for damaging effects in vivo in iron overload. Further investigation into the complex interactions of ascorbic acid and iron are clearly warranted.

References:

Adams, J.D., Lauterburg, B.H., and Mitchell, J.R., Plasma glutathione and glutathione disulfide in the rat: regulation and response to oxidative stress, J. Pharm. Exp. Therap., 227 (1983) 749-754.

Aebi, H. and Suter, H., Protective function of reduced glutathione (G-SH) against the effect of prooxidative substances and of irradiation in the red cell. In Flohe, L., Benohr, H.Ch., Sies, H., Walker, H.D., and Wendel, A., (Eds.), Glutathione, Georg Thieme, Stuttgart, 1974, pp. 192-199.

Agrup, G., Rorsman, H., and Rosengren, E., 5-OH-DOPA, product of and substrate for tyrosinase, Acta Dermatovener. (Stockholm) 62, (1982) 371-376.

Ahagon, A., Ishikawa, M., and Nanda, H., Histochemical changes of brain dopamine in an acute stage of cerebral ischemia in gerbils, Stroke, 11 (1980) 622-628.

Akerboom, T.P.M. and Seis, H., Assay of glutathione, glutathione disulfide, and glutathione mixed disulfides in biological samples, in W.B. Jakoby (ed.) Methods in Enz., 77 (1981) pp 373-382, Academic Press, New York, N.Y.

Allis, B., and Cohen, G., The neurotoxicity of 5,7-dihydroxytryptamine in the mouse atrium: protection by 1-phenyl-3-(2-thiazolyl)-2-thiourea and by ethanol, Eur. J. Pharmacol., 43, (1977) 269-272.

Allison, L. and Shoup, R., Dual electrode liquid chromatography for thiols and disulfides, Anal. Chem., 55 (1983) 8-12.

Anbar, N. and Neta, P., A compilation of specific bimolecular rate constants for the reactions of hydrated electrons, hydrogen atoms, and hydroxyl radicals with inorganic and organic compounds in aqueous solution, Int. J. Appl. Radiat. Isotopes, 18 (1967) 493-523.

Anden, N.-E., Fuxe, K., Hamberger, B., and Hokfelt, T., A quantitative study on the nigro-neostriatal dopamine neuron system in the rat. Acta Physiol. Scand., 67 (1966) 306-312.

Asghar K, Reddy BG, Krishna G: Histochemical localization of glutathione in tissues, J. Histochem. Cytochem., 23 (1975) 774-779.

Bannon, M.J., Goedert, M., and Williams, B., The possible relation of glutathione, melanin and 1-methyl-4-phenyl-1,2,5,6-tetrahydropyridine (MPTP) to Parkinson's disease, Biochem. Pharm., 33 (1984) 2697-2698.

Barka, T. and Anderson, P.J. (Eds.), Histochemistry. Harper & Row, Publishers, Inc., New York, 1965, p 32-34.

Beauchamp, C. and Fridovich, I., A mechanism for the production of ethylene from methional: The generation of the hydroxyl radical by xanthine oxidase, J. Biol. Chem., 245 (1970) 4641-4646.

Bennett HS: The demonstration of thiol groups in certain tissues by means of a new colored sulfhydryl reagent, Anat. Rec., 110 (1951) 231-247.

Benveniste, H., Drejer, J., Schousboe, A., and Diemer, N.H., Elevation of the extracellular concentrations of glutamate and aspartate in rat hippocampus during transient cerebral ischemia monitored by intracerebral dialysis, J. Neurochem., 43 (1984) 1369-1374.

Berger, D. and Weiner, H. Effects of disulfiram and chloral hydrate on the metabolism of catecholamines in rat liver and brain, Biochem. Pharm., 26 (1977) 741-747.

Berl S, Lajtha A, Waelsch H: Amino acid and protein metabolism-VI. Cerebral compartments of glutamic acid metabolism, J. Neurochem., 7 (1961) 186-197.

Betz, A.L. Identification of hypoxanthine transport and xanthine oxidase activity in brain capillaries, J. Neurochem., 44 (1985) 574-579.

Beutler, E., Duron, O., and Kelly, B.M., Improved method for the determination of blood glutathione, J. Lab. Clin. Med., 61 (1963) 882-888.

Bielski, B.H. and Gebieki, J.M. in W.A. Pryor (ed.) Free Radicals in Biology Vol 3, Academic Press, New York, 1977 pp 2-48.

Bioanalytical Systems Inc., Glutathione in whole blood, LCEC Application Note 46 (1982).

Booth J, Boyland E, Sims P: An enzyme from rat liver catalysing conjugations with glutathione, Biochem. J., 79 (1961) 516-524.

Boveris, A., Mitochondrial production of superoxide radical and hydrogen peroxide, Adv. Exptl. Med. and Biol., 78 (1973) 67-82.

Brannan, T.S., Maker, H.S., Weiss, C., and Cohen, G., Regional distribution of glutathione peroxidase in the adult rat brain, J. Neurochem., 35 (1980a) 1013-1014.

Brannan, T.S., Maker, H.S., Raes, I., and Weiss, C., Regional distribution of glutathione reductase in the adult rat brain, Brain Res., 200 (1980b) 474-477.

Brannan, T.S., Maker, H.S., and Raes, I.P., Regional distribution of catalase in the adult rat brain, J. Neurochem., 36 (1981) 307-309.

Brannan, T.S., Weinberger, J., Knott, P., Taff, I., Kaufman, H., Togasaki, D., Nieves-Rosa, J., and Maker, H., Direct evidence of acute massive striatal dopamine release in gerbils with unilateral strokes, Stroke, 18 (1987) 108-110.

Brawn, K. and Fridovich, I., DNA strand scission by enzymically generated oxygen radicals, Arch. Biochem. Biophys., 206 (1981) 414-419.

Breslow R, Lukens LN. On the mechanism of action of an ascorbic acid-dependent nonenzymatic hydroxylating system, J. Biol. Chem., 235 (1960) 292-296.

Brodie A. and Reed D., Buthionine sulfoximine inhibition of cystine uptake and glutathione biosynthesis in human lung carcinoma cells, Toxic. and Pharm., 77 (1985) 381-387.

Calvin H., Medvedovsky C., and Worgul B.V., Near-total glutathione depletion and age-specific cataracts induced by buthionine sulfoximine in mice, Science, 233 (1986) 553-555.

Chance, B., An intermediate compound in the catalase-hydrogen peroxide reaction, Acta. Chem. Scand., 1 (1947) 236-267.

Chieco, P. and Boor, P.J., Use of low temperature for glutathione histochemical stain, J. Histochem. Cytochem., 31 (1983) 975-976.

Clemens, T.A. and Phebus, L.A., Changes in brain chemistry produced by dopaminergic agents: In vivo electrochemical monitoring reveals opposite changes in anesthetized versus unanesthetized rats, Brain Res., 267 (1983) 183-186.

Cohen, G., The generation of hydroxyl radicals in biologic systems: Toxicological aspects, Photochem. and Photobiol., 28 (1978) 669-675.

Cohen, G., The fenton reaction. In: Greenwald, R.A. (Ed.), Handbook of Methods for Oxy Radical Research, CRC Press, Boca Raton, 1985, pp. 55-64.

Cohen, G., The pathobiology of Parkinson's disease: biochemical aspects of dopamine neuron senescence, J. Neural Transm. (suppl.), 19 (1983) 89-103.

Cohen, G. and Cederbaum, A.I., Microsomal metabolism of hydroxyl radical scavenging agents: relationship to the microsomal metabolism of alcohols, Arch. Biochem. Biophys., 199 (1980) 438-447.

Cohen, G. and Heikkila, R.E., The generation of hydrogen peroxide, superoxide radical and hydroxyl radical by 6-hydroxydopamine, dialuric acid, and related cytotoxic compounds, J. Biol. Chem., 249 (1974) 2447-2452.

Cohen, G. and Hochstein, P., Glutathione peroxidase: the primary agent for the elimination of hydrogen peroxide in erythrocytes, Biochem., 2 (1963) 1420-1428.

Cohen, G. and Sinet, P.M., Fenton's reagent- Once more revisited, Dev. Biochem., 11A (1980) 27-37.

Cohen, G., and Sinet, P.M., The Fenton reaction between ferrous diethylenetriaminepentaacetic acid and hydrogen peroxide, FEBS Lett., 138 (1982) 258-260.

Cohen, G., Heikkila, R.E., Allis, B., Cabbat, F., Dembiec, D., MacNamee, D., Mytilineou, C., and Winston, B., Destruction of sympathetic nerve terminals by 6-hydroxydopamine: protection by 1-phenyl-3-(2-thiazolyl)-2-thiourea, diethyldithiocarbamate, methimazole, cysteamine, ethanol, and n-butanol, J. Pharm. Exp. Therap., 199 (1976) 336-352.

Cohen, G., Lewis, D., and Sinet, P.M., Oxygen consumption during the Fenton-type reaction between hydrogen peroxide and a ferrous chelate (Fe^{2+}-DTPA), J. Inorg. Biochem., 15 (1981) 143-151.

Colman, R.F. and Black, S., On the role of flavin adenine dinucleotide and thiol groups in the catalytic mechanism of yeast glutathione reductase, J. Biol. Chem., 240 (1965) 1796-1803.

Cooper, A.J.L., Pulsinelli, W.A., and Duffy, T.E., Glutathione and ascorbate during ischemia and postischemic reperfusion in rat brain, J. Neurochem., 35 (1980) 1242-1245.

Cummings, J.N., The copper and iron content of brain and liver in the normal and in hepato-lenticular degeneration, Brain, 71 (1948) 410-415.

DeDuve, C. and Baudhuin, P., Peroxisomes (microbodies and related particles, Physiol. Rev., 46 (1966) 323-357.

Del Maestro, R.F., An approach to free radicals in medicine and biology, Acta. Physiol. Scand., 492 (1980) 153-168.

DeMarchena, O., Guarnieri, M., and McKhann, G., Glutathione peroxidase levels in brain, J. Neurochem., 22 (1974) 773-776.

Demaster, E., Shirota, F., Redfern, B., Goon, D., Nagasawa, H., Analysis of hepatic reduced glutathione, cysteine and homocysteine by cation-exchange high-performance liquid chromatography with electrochemical detection, J. Chromatog. 308 (1984) 83-91.

Deml, E. and Oesterle, D., Histochemical demonstration of enhanced glutathione content in enzyme-altered islands induced by carcinogens in rat liver, Cancer Res., 40 (1980) 490-491.

Demopoulos, H., Flamm, E., Seligman, M., Power, R., Pietronigro, D., and Ransohoff, J. Molecular pathology of lipids in CNS membranes, in Oxygen and physiological function (Jobsis, F.F., ed.) 1977 pp 491-501 Professional Information Library, Dallas, TX.

Dethmers J.K. and Meister A., Glutathione export by human lymphoid cells: Depletion of glutathione by inhibition of its synthesis decreases export and increases sensitivity to irradiation, Proc. Natl. Acad. Sci. U.S.A., 78 (1981) 7492-7496.

Diguiseppi, J. and Fridovich, I. Ethylene from 2-keto-4-thiomethyl butyric acid: the Haber-Weiss reaction, Arch. Biochem. Biophys., 205 (1980) 323-329.

Dorfman, L.M. and Adams, G.E., Reactivity of the hydroxyl radical in aqueous solution, NSRDS Nat. Bur. Stand. no. 46, (1973) Washington, D.C.

Dormandy, T.L., An approach to free radicals, Lancet, 2 (1983) 1010-1014.

Echizen, H. and Freed, C.R. Factors affecting in vivo electrochemistry: Electrode-tissue interactions and the ascorbate amplification effect, Life Sci., 39 (1986) 77-89.

Fee, J., Biological and Clinical Aspects of Superoxide and Superoxide Dismutase In: Bannister, W.H., and Bannister, J.V. (Eds.) Developments in Biochem. Vol 11 B, Elsevier/North-Holland, New York, 1980, pp. 41-48.

Fenton, H.J.H., Oxidation of tartaric acid in the presence of iron, J. Chem. Soc., 65 (1894) 899-910.

Finch, C.A., In: The Pharmacological Basis of Therapeutics (Eds. A.G. Gilman, L.S. Goodman and A. Gilman), 6th Edn, p. 1315. Macmillan, New York (1980).

Fligiel, S.E.G., Ward, P.A., Johnson, K.J., and Till G.O. Evidence for a role of hydroxyl radical in immune-complex-induced vasculitis, Am. J. Path., 115 (1984) 375-382.

Floyd, R.A., Watson, J.J., and Wong, P.K., Sensitive assay of hydroxyl free radical formation utilizing high performance liquid chromatography with electrochemical detection of phenol and salicylate hydroxylation products, J. Biochem. Biophys. Meth., 10 (1984) 221-235.

Folbergrova, J., Rehncrona, S., and Siesjo, B.K., Oxidized and reduced glutathione in the rat brain under normoxic and hypoxic conditions, J. Neurochem., 32 (1979) 1621-1627.

Freeman BA, Crapo JD. Biology of disease. Free radicals and tissue injury, Lab. Invest., 47 (1982) 412-426.

Fridovich, I., Hypoxia and oxygen toxicity. In: Fahn, S. (Ed.), Adv. Neurol., Vol 26 , Raven Press, New York, 1977 pp. 255-257.

Fridovich, I., The biology of oxygen radicals, Science, 201 (1978) 875-880.

Fried, R. and Mandel, P., Superoxide dismutase of mammalian nervous system, J. Neurochem., 24 (1975) 433-438.

Gaunt, G.L. and DeDuve, C., Subcellular distribution of D-amino acid oxidase and catalase in rat brain, J. Neurochem., 26 (1976) 749-759.

Glick, S.D., Jerussi, T.P., Waters, D.H., and Green, J.P., Amphetamine-induced changes in striatal dopamine and acetylcholine levels and relationship to rotation (circling behavior) in rats, Biochem. Pharm., 23 (1974) 3223-3225.

Goldstein, S. and Czapski, G., Mannitol as an OH$^{\bullet}$ scavenger in aqueous solution and biological systems, Int. J. Radiat. Biol., 46 (1984) 725-729.

Graham, D.G., Tiffany, S.M., Bell, W.R., and Gutknecht, W.F. (1978) Molec. Pharm. 14, 644-653

Greenstock, C.L., Redox processes in radiation biology and cancer, Rad. Res., 86 (1981) 196-211.

Gregory, J.D., The stability of N-ethylmaleimide and its reaction with sulfhydryl groups, J. Am. Chem. Soc., 77 (1955) 3922-3923.

Griffith, O. and Meister, A., Glutathione: interorgan translocation, turnover, and metabolism, Proc. Natl. Acad. Sci., 76 (1979) 5606-5610.

Griffith O., Anderson, M., and Meister A., Inhibition of glutathione biosynthesis by prothionine sulfoximine (s-n-propyl homocysteine sulfoximine), a selective inhibitor of gamma-glutamyl cysteine synthetase, J. Biol. Chem., 254 (1979) 1205-1210.

Hagberg, H., Lehmann, A., Sandberg, M., Nystrom, B., Jacobson, I., and Hamberger, A., Ischemia-induced shift of inhibitory and excitatory amino acids from intra to extracellular compartments, J. Cereb. Blood Flow and Metab., 5 (1985) 413-419.

Hallgren, B. and Sourander, D.P., The effect of age on non-haemin iron in the human brain, J. Neurochem., 3 (1958) 41-51.

Halliwell, B., Superoxide-dependent formation of hydroxyl radicals in the presence of iron chelates, FEBS Lett., (1978) 92 321-325.

Halliwell, B., and Gutteridge, J.M.C., Oxygen radicals and the nervous system, Trends in Neuro. Sci., 8 (1985) 22-26.

Harisch, G. and Meyer, W., Studies on tissue distribution of glutathione and on activities of glutathione-related enzymes after carbon tetrachloride-induced liver injury, Res. Comm. Chem. Path. Pharm., 47 (1985) 399-414.

Harris, R. and Simon, L., Extracellular pH, potassium, and calcium activities in progressive ischemia of rat cortex, J. Cereb. Blood Flow and Metab., 4 (1984) 178-186.

Harrison, M.J.G., Brownbill, D., Lewis, P.D., and Russell, R.W.R. Cerebral edema following carotid artery ligation in the gerbil, Arch. Neurol. (Chic.), 28 (1973) 389-391.

Harrison, M.J.G., Marsden, C.D., and Jenner, P. Effect of experimental ischemia on neurotransmitter amines in the gerbil brain, Stroke, 10 (1979) 165-168.

Harrison, W.W., Netsky, M.G., and Brown, M.D., Trace elements in human brain: copper, zinc, iron, and magnesium, Clin. Chim. Acta, 21 (1968) 55-61.

Heikkila, R.E. and Cohen, G., Further studies on the generation of hydrogen peroxide by 6-hydroxydopamine, Molec. Pharm., 8 (1972) 241-248.

Heikkila, R.E., Winston, B., Cohen, G., and Barden, H., Alloxan-induced diabetes: evidence for hydroxyl radical as a cytotoxic intermediate, Biochem. Pharm. 25 (1976) 1085-1092.

Hill, J.M. and Switzer, R.C.III, The regional distribution and cellular localization of iron in the rat brain, Neuroscience, 11 (1984) 595-603.

Hoidal, J.R., Beall, G.D., and Repine, J.E. Production of hydroxyl radicals by human alveolar macrophages, Infect. Immunity, 26 (1979) 1088-1092.

Ingleman-Sundberg, M. and Ekstrom, G., Aniline is hydroxylated by the cytochrome P-450-dependent hydroxyl radical-mediated oxygenation mechanism, Biochem. Biophys. Res. Comm., 106 (1982) 625-631.

Ito, U., Spatz, M., Walker, J.T.Jr., and Klatzo, I. Experimental cerebral ischemia in mongolian gerbils - light microscopic observations, Acta Neuroph. (Berl.), 32 (1975) 209-223.

Jocelyn, P.C., The effect of glutathione on protein sulphydryl groups in rat liver-liver homogenates, Biochem. J., 85 (1962) 480-485.

Jones, D.P., Eklow, L., Thor, H., and Orrenius, S., Metabolism of hydrogen peroxide in isolated hepatocytes: relative contributions of catalase and glutathione peroxidase in decomposition of endogenously generated H_2O_2, Arch. Biochem. Biophys., 210 (1981) 505-512.

Kahn, K. The natural course of experimental cerebral infarction in the gerbil, Neurology, 22 (1972) 510-515.

Klein, S.M., Cohen, G., and Cederbaum, A.I., The interaction of hydroxyl radicals with dimethylsulfoxide produces formaldehyde, FEBS Lett., 116 (1980) 220-226.

Klug, D., Rabani, J., and Fridovich, I., A direct demonstration of the catalytic action of superoxide dismutase through the use of pulse radiolysis, J. Biol. Chem., 247 (1972) 4839-4842.

Komara, J.S., Nayini, N.R., Bialick, H.A., Evans, A.T., Garritano, A.M., Hoehner, T.J., Jacobs, W.A., Huang, R.R., Krause, G.S., White, B.C., and Aust, S.D., Brain iron delocalization and lipid peroxidation following cardiac arrest, Ann. Emerg. Med., 15 (1986) 384-389.

Konrad, P.N., Richards, F., Valentine, W.N., and Paglia, D.E., Gamma-Glutamyl-Cysteine Synthetase Deficiency - A cause of hereditary hemolytic anemia, N.Engl. J. Med., 286 (1972) 557-561.

Kostrzewa, R.M. and Jacobowitz, D.M., Pharmacologic action of 6-hydroxydopamine, Pharm. Rev., 26 (1974) 199-288.

Lacouture, P.G. and Lovejoy, F.H., Iron. In: Haddad, L.M. and Winchester, J.F. (Eds.), Clinical management of poisoning and drug overdose, W.B. Saunders Co, Philadelphia, 1983, pp. 644-655.

Land, E.J. and Ebert, M., Pulse radiolysis studies of aqueous phenol, Trans. Faraday Soc., 63 (1967) 1181-1190.

Lauterburg, B.H., Smith, C.V., Hughes, H., and Mitchell, J.R., Biliary excretion of glutathione and glutathione disulfide in the rat, J. Clin. Invest., 73 (1984) 124-133.

Lavyne, M.H., Moskowitz, M.A., Larin, F., Zervas, N.T., and Wurtman, R.J. Brain ^{3}H-catecholamine metabolism in experimental cerebral infarction, Neurology, 25 (1975) 483-485.

Lawrence, G.D. and Cohen, G., Ethane exhalation as an index of in vivo lipid peroxidation: concentrating ethane from a breath collection chamber, Analyt. Biochem., 122 (1982) 283-290.

Lawrence, R.A., Sunde, R.A., Schwartz, G.L. and Hoekstra, W.G., Glutathione peroxidase activity in rat lens and other tissues in relation to dietary selenium intake, Exp. Eye Res., 18 (1974) 563-569.

Levine, S. and Payan, H. Effects of ischemia and other procedures on the brain and retina of the gerbil (Meriones unguiculatus), Exp. Neurol., 16 (1966) 255-262.

Levy, D.E. and Duffy, T.E. Cerebral energy metabolism during transient ischemia and recovery in the gerbil, J. Neurochem., 28 (1977) 63-70.

Little, C. and O'Brien, P.J., An intracellular GSH-peroxidase with a lipid peroxide substrate, Biochem. Biophys. Res. Comm., 31 (1968) 145-150.

Lowry, O.H., Passonneau, J.V., Hasselberger, F.X., and Schultz, D.W. Effect of ischemia on known substrates and cofactors of the glycolytic pathway in brain, J. Biol. Chem.,239 (1964) 18-30.

Lust, W.O., Mrsulja, B.B., Mrsulja, B.J., Passonneau, J.V., and Klatzo, I. Putative neurotransmitters and cyclic nucleotides in prolonged ischemia of the cerebral cortex, Brain Res., 98 (1975) 394-399.

Maker, H.S., Weiss, C., Silides, D.J., and Cohen, G., Coupling of dopamine oxidation (monoamine oxidase activity) to glutathione oxidation via the generation of hydrogen peroxide in rat brain homogenates, J. Neurochem., 36 (1981) 589-593.

Marstein, S., Jellum, E., Nesbakken, R., and Perry, T.L., Biochemical investigations of biopsied brain tissue and autopsied organs from a patient with pyroglutamic acidemia (5-oxoprolinemia), Clinica Chimica Acta, 111 (1981) 219-228.

Martin, H. and McIlwain, H., Glutathione, oxidized and reduced, in the brain and in isolated cerebral tissue, Biochem. J., (1959) 275-280.

Mayevsky, A., Kaplan, H., Haveri, J., Haselgrove, J., and Chance, B. Three dimensional mapping of the freeze-trapped brain: effect of ischemia in the mongolian gerbil, Brain Res., 367 (1986) 63-72.

Mayevsky, A., Zarchin, N., Kaplan, H., Haveri, J., Haselgrove, J., and Chance, B. Brain metabolic responses to ischemia in the mongolian gerbil: In vivo and freeze-trapped redox scanning, Brain Res., 276 (1983) 95-107.

McCay, P.B., Rajagopalan, S., Lai, E.K., and Crossly, C., In vivo spin trapping of oxy radicals in tissues of irradiated mice, Fed. Proc., 44 (1985) 1126.

McCord, J.M. and Day, E.D., Superoxide-dependent production of hydroxyl radicals catalyzed by iron-EDTA complex, FEBS Lett., 86 (1978) 139-142.

McCord, J.M. and Roy, R.S., The pathophysiology of superoxide: roles in inflammation and ischemia, Can. J. Physiol. Pharmacol., 60 (1982) 1346-1352.

McKenna, O., Arnold, G., and Holtzman, E., Microperoxisome distribution in the central nervous system of the rat, Brain Res., 117 (1976) 181-194.

Mefford, I. and Adams, R.N., Determination of reduced glutathione in guinea pig and rat tissue by HPLC with electrochemical detection, Life Sci., 23 (1978) 1167-1174.

Meister A. (1985) The fall and rise of cellular glutathione levels: enzyme-based approaches. Curr. Topics in Cell. Reg. 26, 383-393.

Meister, A. and Anderson, M.E., Glutathione, Ann. Rev. Biochem., 52 (1983) 711-760.

Mills, G.C., Hemoglobin catabolism I. Glutathione peroxidase, an erythrocyte enzyme which protects hemoglobin from oxidative breakdown, J. Biol. Chem., 229 (1957) 189-197.

Mills, G.C., Glutathione peroxidase and the destruction of hydrogen peroxide in animal tissue, Arch. Biochem. Biophys., 86 (1960) 1-5.

Mokrasch, L.C. and Teschke, E.J., Glutathione content of cultured cells and rodent brain regions: a specific fluorometric assay, Anal. Biochem., 140 (1984) 506-509.

Mrsulja, B.B., Mrsulja, B.J., Spatz, M., Ito, U., Walker, J.T., and Klatzo, I. Catecholamines in brain ischemia - effects of a-methyl-p-tyrosine and pargyline, Brain Res., 104 (1976) 373-378.

Myers, R.D., General laboratory techniques, In: Methods in psychobiology, R.D. Myers (Ed.), Vol. 1 (1971) p 65, London Academic.

Nayfield, S.G., Kent, T.H., and Rodman, N.F., Gastrointestinal effects of acute ferrous sulfate poisoning in rats, Archs. Path. Lab. Med., 100 (1976) 325-328.

Nienhuis, A.W., Vitamin C and iron, N. Engl. J. Med., 304 (1981) 170-171.

Olney, J.W., Excitotoxins: an overview, in Excitotoxins (K. Fuxe, P.J. Roberts, and R. Schwarcz eds) Macmillan, London pp 82-97.

O'Neill, R.D., Fillenz, M., Albery, W.J., and Goddard, N.J. The monitoring of ascorbate and monoamine transmitter metabolites in the striatum of unanaesthetised rats using microprocessor-based voltammetry, Neuroscience, 9 (1983) 87-93.

Ong, H.H., Creveling, C.R., and Daly, T.W., The synthesis of 2,4,5-trihydroxyphenylalanine (6-hydroxydopa). A centrally active norepinephrine-depleting agent, J. Med. Chem. 12, (1969) 458-461.

Orlowski, M. and Karkowsky, A., Glutathione metabolism and some possible functions of glutathione in the nervous system, Int. Rev. Neurobio., 19 (1976) 75-121.

Orlowski, M. and Meister, A., The gamma-glutamyl cycle: a possible transport system for amino acids, Proc. Natl. Acad. Sci., 62 (1970) 1248-1255.

Oshino, N. and Chance, B., Properties of glutathione release observed during the reduction of organic hydroperoxide, demethylation of aminopyrine and oxidation of some substances in perfused rat liver, and their implications for the physiologic functions of catalase, Biochem. J., 162 (1977) 509-525.

Pachla, L.A. and Kissinger, P.T., Determination of ascorbic acid in foodstuffs, pharmaceuticals, and body fluids by liquid chromatography with electrochemical detection, Anal. Chem., 48 (1976) 364-367.

Perry, T.L., Cerebral amino acid pools. In Lajtha, A. (Ed.), Handbook of Neurochemistry, Vol 1, Plenum Press, New York, 1982, pp. 151-180.

Perry, T.L., Godin, D.V., and Hansen, S., Parkinson's disease: a disorder due to nigral glutathione deficiency?, Neurosci. Lett., 33 (1982) 305-310.

Perry, T.L., Hansen, S., Berry, K., Mok, C., and Lesk, D., Free amino acids and related compounds in biopsies of human brain, J. Neurochem., 18 (1971) 521-528.

Perry, T.L., Hansen, S., and Gandham, S.S., Postmortem changes of amino compounds in human and rat brain, J. Neurochem., 36 (1981) 406-412.

Phebus, L.A., Perry, K.W., Clemens, J.A., and Fuller, R.W. Brain anoxia releases striatal dopamine in rats, Life Sci., (1986) 2447-2453.

Physician's Desk Reference, 39th Edn, p. 317. Medical Economics, Oradell, NJ (1985).

Pickering Laboratories application note, Gradient LC. Amino acids in physiologic fluid.

Prasad, K.N. and Kollmorgan, G.M., Effect of dopamine on mammalian cells in vivo and in vitro, Proc. Soc. Exp. Biol. Med., 132 (1969) 428-430.

Que, B.G., Downey, K.M., and So, A.G., Degradation of deoxyribonucleic acid by a 1,10-phenanthroline-copper complex: the role of hydroxyl radicals, Biochem., 19 (1980) 5987-5991.

Radzik, D.M., Roston, D.A., and Kissinger, P.T., Determination of hydroxylated aromatic compounds produced via superoxide-dependent formation of hydroxyl radicals by liquid chromatography/electrochemistry, Anal. Biochem., 131 (1983) 458-464.

Rajan, K.S., Colburn, R.W., and Davis, J.M., Distribution of metal ions in the subcellular fractions of several rat brain areas, Life Sci., 18 (1976) 423-432.

Raghavan, N.V. and Steenken, S., Electrophilic reaction of the OH radical with phenol. Determination of the distribution of isomeric dihydroxycyclohexadienyl radicals, J. Am. Chem. Soc., 102 (1980) 3495-3499.

Rehncrona, S., Folbergrova, J., Smith, D.S., and Siesjo, B.K., Influence of complete and pronounced incomplete cerebral ischemia and subsequent recirculation on cortical concentrations of oxidized and reduced glutathione in the rat, J. Neurochem., 34 (1980) 477-486.

Reichelt, K.L. and Fonnum, F., Subcellular localization of N-acetyl-aspartyl-glutamate, N-acetyl-glutamate, and glutathione in brain, J. Neurochem., 16 (1969) 1409-1416.

Richards F., Cooper M.R., Pearce L.A., Cowan R.J., and Spurr C.L., Familial spinocerebellar degeneration, hemolytic anemia, and glutathione deficiency Arch. Intern. Med., 134 (1974) 534-537.

Richardson R.J. and Murphy S.D., Effect of glutathione depletion on tissue deposition of methyl mercury in rats, Toxic. and App. Pharm., 31 (1975) 505-519.

Richmond, R., Halliwell, B., Chauhan, J., and Darbre, A. Superoxide-dependent formation of hydroxyl radicals: detection of hydroxyl radicals by the hydroxylation of aromatic compounds, Anal. Biochem., 118 (1981) 328-335.

Richter, H.W. and Waddell, W.H., Mechanism of the oxidation of dopamine by the hydroxyl radical in aqueous solution, J. Am. Chem. Soc., 105 (1983) 5434-5440.

Rollema, H., Damsma, G., Horn, A.S., DeVries, J.B., and Westernick, B.H.C. Brain dialysis in conscious rats reveals an instantaneous release of striatal dopamine in response to MPP^+, Europ. J. Pharm., 126 (1986) 345-346.

Roots, R., Chatterjee, A., Chang, P., Lommel, L., and Blakely, E.A., Characterization of hydroxyl radical-induced damage after sparsely and densely ionizing radiation, Int. J. Radiat. Biol., 47 (1985) 157-166.

Rosen, G.H. and Freeman, B.A., Detection of superoxide generated by endothelial cells, Proc. Natl. Acad. Sci., 81 (1984) 7269-7273.

Rowley, D.A. and Halliwell, B., Superoxide-dependent formation of hydroxyl radicals from NADH and NADPH in the presence of iron salts, FEBS Lett., 142 (1982) 39-41.

Rowley, D.A. and Halliwell, B., Formation of hydroxyl radicals from hydrogen peroxide and iron salts by superoxide- and ascorbate-dependent mechanisms: relevance to the pathology of rheumatoid disease, Clin. Sci., 64 (1983) 649-653.

Sachs, C., Jonsson, G., Heikkila, R., and Cohen, G., Control of the neurotoxicity of 6-hydroxydopamine by intraneuronal noradrenaline in rat iris, Acta. Physiol. Scand., 93 (1975) 345-351.

Sagai, M. and Ichinose, T., Age-related changes in lipid peroxidation as measured by ethane, ethylene, butane, and pentane, Life Sci., 27 (1980) 731-738.

Seiden, L.S. and Vosmer, G., Formation of 6-hydroxydopamine in caudate nucleus of the rat brain after a single large dose of methylamphetamine, Pharm. Biochem. Behav., 21 (1984) 29-31.

Senoh, S., Creveling, C.R., Udenfriend, S., and Witkop, B., Chemical, enzymatic, and metabolic studies on the mechanism of oxidation of dopamine, J. Am. Chem. Soc., 81 (1959) 6236-6240.

Sinet, P.M., Heikkila, R.E., and Cohen, G., Hydrogen peroxide production by rat brain in vivo, J. Neurochem., 34 (1980) 1421-1428.

Sies, H., Hydroperoxides and thiol oxidants in the study of oxidative stress in intact cells and organs. In: Sies, H. (Ed.), Oxidative Stress, Academic Press Inc., London, 1983, pp. 73-90.

Sies, H. and Cadenas, E. Oxidative stress: damage to intact cells and organs, Phil. Trans. R. Soc. Lond. B, 311 (1985) 617-631.

Sies, H., Bartoli, G.M., Burk, R.F., and Waydhas, C., Glutathione efflux from rat liver after phenobarbital treatment, during drug oxidations, and in selenium deficiency, Eu. J., Biochem., 89 (1978) 113-118.

Singh, D.R., Mahajan, J.M., and Krishnan, D., Effect of chemical protectors on fast-neutron-induced reversions in yeast, Int. J. Radiat. Biol., 30 (1976) 585-588.

Smith, J.E., Di-gamma-glutamylcystine as a substrate for glutathione reductase, Biochim. Biophys. Acta., 242 (1971) 36-38.

Stein, G. and Weiss, J., Chemical actions of ionising radiations on aqueous solutions. Part II. The formation of free radicals. The action of X-rays on benzene and benzoic acid, J. Chem. Soc., 4 (1949) 3245-3254.

Stein, L. and Wise, D.C., Possible etiology of schizophrenia: Progressive damage to the noradrenergic reward system by 6-hydroxydopamine, Science, 171 (1971) 1032-1036.

Stripe, F. and Della Corte, E., The regulation of rat liver xanthine oxidase. Conversion in vitro of the enzyme activity from dehydrogenase (typeD) to oxidase (type O), J. Biol. Chem., 244 (1969) 3855-3863.

Tietze, F., Enzymic method for quantitative determination of nanogram amounts of total and oxidized glutathione: Applications to mammalian blood and other tissues, Anal. Biochem., 27 (1969) 502-522.

Thomas, T.N., Priest, D.G., and Zemp, J.W., Distribution of superoxide dismutase in rat brain, J. Neurochem., 27 (1976) 309-310.

Thrivikraman, K.V., Refshauge, C., and Adams, R.N. Liquid chromatographic analysis of nanogram quantities of ascorbate in brain tissue, Life Sci., 15 (1974) 1335-1342.

Udenfriend, S., Clark, C.T., Axelrod, J., and Brodie, B.B. Ascorbic acid in aromatic hydroxylation I. A model system for aromatic hydroxylation, J. Biol. Chem., 208 (1954) 731-739.

Walling, C., Partch, R.W., and Weil, T., Kinetics of the decomposition of hydrogen peroxide catalyzed by ferric ethylenediaminetetraacetatae complex, Proc. Nat. Acad. Sci., 72 (1975) 140-142.

Weinberger, J., and Cohen, G. The differential effect of ischemia on the active uptake of dopamine, g-aminobutyric acid, and glutamate by brain synaptosomes, J. Neurochem., 38 (1982) 963-968.

Weinberger, J. and Cohen, G., Nerve terminal damage in ischemia: greater susceptibility of catecholamine nerve terminals relative to serotonin nerve terminals, Stroke, 14 (1983) 986-989.

Weinberger, J. and Nieves-Rosa, J., The role of catecholamines in the evolution of infarction in ischemic striatum, Soc. for Neurosci. 14th Ann. Meeting, Abstr. # 261.4, (1985) p. 889.

Weinberger, J. and Nieves-Rosa, J., Monoamine metabolism in the evolution of infarction in ischemic striatum, J. Neural Trans., in press.

Weinberger, J., Nieves-Rosa, J., and Cohen, G. Nerve terminal damage in cerebral ischemia: protective effect of alpha-methyl-para-tyrosine, Stroke, 16 (1985) 864-870.

Wellner, V.P., Anderson, M.E., Puri, R.N., Jensen, G.L., and Meister, A., Radioprotection by glutathione ester: Transport of glutathione ester into human lymphoid cells and fibroblasts, Proc. Natl. Acad. Sci. (USA), 81 (1984) 4732-4735.

Wendell, P.L., Measurement of oxidized glutathione and total glutathione in the perfused rat heart, Biochem. J., 117 (1970) 661-665.

White, C.W., Mimmack, R.F., and Repine, J.E., Accumulation of lung tissue oxidized glutathione (GSSG) as a marker of oxidant induced lung injury, Chest, 89 suppl. (1986) 111-113.

Whitten, C.F. and Brough, J.A., The pathophysiology of acute iron poisoning, Clin. Toxic., 4 (1971) 585-595.

Yong, V.W., Perry, T.L., and Krisman, A.A., Depletion of glutathione in brainstem of mice caused by N-methyl-4-phenyl-1,2,3,6-tetrahydropyridine is prevented by antioxidant pretreatment, Neurosci. Lett., 63 (1986) 56-60.

Youdim, M.B.H. and Green, A.R., The effects of iron deficiency on brain biogenic monoamine biochemistry and function in rats. In: Porter, R. and Fitzsimons, W. (Eds.), Iron Metabolism, Elsvier, Amsterdam, 1977, pp. 201-226.

Youdim, M.B.H., Green, A.R., Bloofield, M.R., Mitchell, B., Heal, D.J., and Grahame-Smith, D.G., Neuropharm., 19 (1980) 254-267.

Zervas, N.T., Hori, H., Negora, M., Wurtman, R.J., Larin, F., and Lavyne, M.H., Reduction of brain dopamine following experimental cerebral ischemia, Nature, 274 (1974) 283-284.